

SHAKEDOWN AND RATCHETING BEHAVIOR OF
STRUCTURES UNDER THERMAL CYCLING

CENTRE FOR NEWFOUNDLAND STUDIES

**TOTAL OF 10 PAGES ONLY
MAY BE XEROXED**

(Without Author's Permission)

SRIRAM SWAMINATHAN



**SHAKEDOWN AND RATCHETING BEHAVIOR OF
STRUCTURES UNDER THERMAL CYCLING**

By

Sriram Swaminathan

A thesis submitted to the School of Graduate Studies
in partial fulfillment of the requirements for
the Degree of

Master of Engineering

Faculty of Engineering and Applied Science

Memorial University of Newfoundland

August 2005

© 2005 Sriram Swaminathan



Library and
Archives Canada

Bibliothèque et
Archives Canada

Published Heritage
Branch

Direction du
Patrimoine de l'édition

395 Wellington Street
Ottawa ON K1A 0N4
Canada

395, rue Wellington
Ottawa ON K1A 0N4
Canada

Your file *Votre référence*
ISBN: 978-0-494-19402-7
Our file *Notre référence*
ISBN: 978-0-494-19402-7

NOTICE:

The author has granted a non-exclusive license allowing Library and Archives Canada to reproduce, publish, archive, preserve, conserve, communicate to the public by telecommunication or on the Internet, loan, distribute and sell theses worldwide, for commercial or non-commercial purposes, in microform, paper, electronic and/or any other formats.

The author retains copyright ownership and moral rights in this thesis. Neither the thesis nor substantial extracts from it may be printed or otherwise reproduced without the author's permission.

AVIS:

L'auteur a accordé une licence non exclusive permettant à la Bibliothèque et Archives Canada de reproduire, publier, archiver, sauvegarder, conserver, transmettre au public par télécommunication ou par l'Internet, prêter, distribuer et vendre des thèses partout dans le monde, à des fins commerciales ou autres, sur support microforme, papier, électronique et/ou autres formats.

L'auteur conserve la propriété du droit d'auteur et des droits moraux qui protègent cette thèse. Ni la thèse ni des extraits substantiels de celle-ci ne doivent être imprimés ou autrement reproduits sans son autorisation.

In compliance with the Canadian Privacy Act some supporting forms may have been removed from this thesis.

Conformément à la loi canadienne sur la protection de la vie privée, quelques formulaires secondaires ont été enlevés de cette thèse.

While these forms may be included in the document page count, their removal does not represent any loss of content from the thesis.

Bien que ces formulaires aient inclus dans la pagination, il n'y aura aucun contenu manquant.


Canada

Abstract

Analysis of stress generation in pressure vessels during thermal cycling is a difficult complex subject that is receiving increased attention. Cyclic plastic finite element analysis was performed with thermal cycling with a view to quantify the phenomena of ratcheting. The framework of constitutive theory of rate-independent plasticity has been reviewed and the new developments in this field summarized. This thesis also reviews the basic equations, solution methods and important phenomena associated with thermal cycling that require numerical treatment. Stress analysis begins with a heat transfer analysis followed by a thermal stress analysis. Further complicating phenomena including shakedown ratcheting and structure-dependent plasticity is also considered. Computational issues include numerical methods of handling these phenomena, and two-dimensional and three-dimensional stress states.

Table of Contents

List of Tables	viii
List of Figures	x
List of Symbols	xiii
Acknowledgments	xvi
Chapter 1	
Introduction	1
1.1 Background and Motivation	1
1.2 Code Guidelines for Ratcheting Check	2
1.3 Scope of the Current Study	5
1.4 Organization of Thesis	6

Chapter 2

Literature Review	7
2.1 Problem Definition	10
2.2 Fundamental Structural Thermal Behavior	11
2.2.1 Thermal Expansion	12
2.2.2 Thermal Expansion Against Rigid Axial Constraints	12
2.2.3 Thermal Bending	14
2.2.4 Strains and Strain rates	15
2.3 Basics of Plasticity Theory	15
2.3.1 Structural Behaviour	19
2.3.2 Virtual Work Principle	21
2.3.3 General Relations for Elastic-Plastic Structures	21
2.4 Shakedown Theorems	23
2.4.1 Lower Bound Shakedown Theorem	23
2.4.2 Residual Stresses	24
2.5 Solution of Melan's Theorem by Linear Programming	25
2.5.1 Formulation	25
2.6 Upper Bound Shakedown Theorem	27
2.7 Cyclic Incremental Analysis	28
2.7.1 JPVRC Criterion for Ratcheting Check	33

Chapter 3

The Non-Cyclic Method	36
3.1 Formulation	37
3.2 Finite Element Implementation	38
3.2.1 Bree Problem by the Non-Cyclic Method	41

3.2.1.1	Results from Finite Element Analysis	43
3.3	The Elastic-Core Concept	45
3.3.1	Analogy Between the Elastic Core and the Non-Cyclic Methods	46

Chapter 4

	Multi Bar Models	47
4.1	Two-Bar Problem	47
4.2	A Simple Analysis of the Two-Bar Model	49
4.3	Finite Element Analysis And Discussion	51
4.4	Effect of Hardening	54
4.5	Three-Bar Problem	56
4.6	Analytical Solution for the Three-Bar Problem	57
4.7	Finite Element Analysis and Discussion	60
4.7.1	Response at 12% Above Shakedown Temperature T_0	63
4.7.2	Response at 125% Above Shakedown Temperature T_0	64

Chapter 5

	Bree Problem by Plastic FEA	65
5.1	Introduction	65
5.2	Interaction Diagrams	66
5.3	Solution by Cyclic Incremental Analysis	68
5.3.1	Finite Element Results	69
5.3.2	Effect of Change in Material Properties	71
5.4	Proportional Variation of Loads	74
5.4.1	Alternative Loading History	75
5.5	Interaction Diagram for a Tube	77
5.5.1	Parameter Sensitivity of the Ratcheting Boundary	79

5.6	Interaction Diagram using the Non-cyclic method	80
5.6.1	Why Does the Non-cyclic Method give a Lower Bound? . . .	81
5.6.2	The Size Effect	83
5.7	Slow Rates of Convergence	84
5.7.1	Sample Calculation of Strain Increments	86
5.8	Asymptotic Trend Near Shakedown	86
5.9	Shakedown Check using JPVRC Criterion and Comparison with ASME	88
5.10	Tube as Cylinder in Plane Strain Condition	90
5.10.1	Results and Discussion	92
5.10.2	Comparison with the Axisymmetric Model	95
5.10.2.1	Hoop Strain Increments Near the Shakedown Bound- ary	96

Chapter 6

	Conclusions and Future Research	99
6.1	Conclusions	99
6.2	Future research	102

	References	103
--	-------------------	------------

Appendix A

	Sample calculations	107
A.1	Sample Calculation	107
A.2	Material Property Data	109
A.3	Proof of Melan's Theorem	111
A.4	Tables	114

A.5	Macros for the Non-Cyclic method	117
A.6	Input file for the Bree Problem	119
A.7	Input file for the Three-Bar Problem	124
A.8	Input file for the Plane Strain Condition	128
A.9	Input File for the Clamped Beam Problem	136

List of Tables

2.1	Data table of plastic strain increments at $t=0.82$	34
5.1	Data for the Bree problem plane stress model	70
5.2	Load data at shakedown for pressure varying proportionally with temperature	74
5.3	Load data at shakedown for the axisymmetric tube of Radius 100 in	79
5.4	Load data at shakedown for a axisymmetric tube of Radius 20 in .	79
5.5	Table showing the calculation of hoop strain increments for a tube of Radius 20 in	87
5.6	Table showing the calculation of equivalent plastic strain increments for a tube of Radius 20 in	89
5.7	Load data at shakedown for a tube of radius 20in and thickness 1 inch using plane strain approximation	91

5.8	Load data at shakedown for a tube of radius 20in and thickness 5 inch using plane strain approximation	93
A.1	Data table of plastic strain increments for element number 21 node number 54 for the axisymmetric model	114
A.2	Data table of plastic strain increments for element number 240 node number 26 for the axisymmetric model	115
A.3	Data table of plastic strain increments for loads near shakedown boundary for the plane strain model	115
A.4	Data table of plastic strain increments for loads near shakedown boundary for the axisymmetric Model	116

List of Figures

2.1	Simply supported beam subjected to a uniform rise in temperature	12
2.2	Axially restrained beam subjected to a uniform rise in temperature	13
2.3	Simply supported beam subjected to a transverse thermal gradient	14
2.4	General body of domain Ω subjected to surface and body forces . .	19
2.5	General body (domain Ω) with a discontinuity subjected to surface and body forces	20
2.6	Schematic diagram of the beam problem	29
2.7	Equivalent stress in the beam in the end of heat up cycle	30
2.8	Hoop strain increments versus increase in thermal load near the shakedown boundary	31
2.9	Plot of equivalent plastic strains versus number of cycles at $t=0.82$.	35
3.1	Flow chart for the Non-cyclic method	40
3.2	Schematic diagram of the beam problem	41

3.3	Schematic diagram of the beam problem	42
3.4	Post processor plot showing equivalent stress	43
3.5	The Bree diagram by Non-cyclic method and comparison with theory	44
3.6	Elastic Core	45
4.1	Schematic diagram of the two bar problem	48
4.2	Displacement vs number of cycles	52
4.3	Displacement vs number of cycles	53
4.4	Single surface plasticity model	54
4.5	Multi-surface plasticity model	55
4.6	Schematic diagram of the three bar problem	57
4.7	Load displacement diagram at total collapse	60
4.8	Axial displacement vs load cycle number at shakedown	62
4.9	Axial displacement versus load cycle number 12% percent above shakedown temperature	63
4.10	Axial displacement vs load cycle number at 125% shakedown tem- perature	64
5.1	Interaction diagram for the Bree problem	67
5.2	Schematic diagram of the Bree problem	69
5.3	The Bree interaction diagram along with results from theory	70
5.4	Plastic strain versus load cycle number for chaboche model	72
5.5	Equivalent stress plot after 250 cycles	73
5.6	Schematic diagram showing the load variation	74
5.7	Bree diagram with different loading histories	75
5.8	Schematic diagram of the Bree problem with two temperature cycles for one pressure cycle	76

5.9	Schematic diagram of the axisymmetric tube	77
5.10	Comparison between axisymmetric tube of Radius 20 in and plane stress model	78
5.11	Shakedown boundary comparison by cyclic and non-cyclic methods for a tube of Radius 20 in	80
5.12	Equivalent stress plot after the thermal cycle for a tube of Radius 5in	82
5.13	Shakedown boundary for tubes of different radii using the non-cyclic method.	83
5.14	Displacement vs cycles at the shakedown load after 250 cycles for a tube of Radius 20 in	85
5.15	Hoop strain increments vs cycles at the shakedown load after 10 cycles	88
5.16	Schematic diagram of the plane strain condition	90
5.17	Post processor plot of the equivalent stress distribution.	91
5.18	Interaction diagram for the Bree problem in plane strain condition.	92
5.19	Ratcheting boundaries for the tube with t/r ratio of 0.25	94
5.20	Comparison between axisymmetric and plane strain models for the same shakedown load	95
5.21	Hoop strain increments after two cycles	96
5.22	Hoop strain increments after four cycles	97
A.1	Displacement versus load diagram for the Bree problem	108
A.2	Plastic strain versus load diagram for the Bree problem	109

List of Symbols

$\Delta \epsilon_{ij}^C = \int_0^\tau \dot{\epsilon}_{ij}^C$ Accumulated plastic strain over a cycle compatible with displacement increment Δu_i^C .

σ_{ac} Axial Stress.

X_i Body force tensor.

$\sigma_{ij}, \epsilon_{ij}, \dot{\epsilon}_{ij}$ Cartesian components of stress and strain rates,.

α Co-efficient of thermal expansion.

$u, \Delta u$ Displacement, Displacement difference.

d Displacements, Deformations.

$\sigma_{ij}^C, \dot{\epsilon}_{ij}^C$ Elastic component of strain rate in upper bound theorem and corresponding stress.

$\hat{\sigma}_{ij}^P$ Elastic stress field corresponding to primary load P.

F_i External loads.

R Internal radius of the cylinder.

λ_L, P_L Limit load values of λ and P, corresponding to yield stress σ_y

S_m Maximum allowable stress intensity

$\bar{\sigma}_P = \frac{\sigma_P}{\sigma_y}$ Non dimensional primary stress.

n_j Normal vector.

$\epsilon_{ij}^P, \dot{\epsilon}_{ij}^P$ Plastic component of strain and strain rate.

λ_i Plastic strain components.

ν Poisson's ratio.

P Primary load.

σ_{PM} Primary membrane stress

σ_P Primary stress, uniform stress corresponding to load .

σ_{br} Range of bending Stress.

ρ_{ij} Residual stress field; satisfies equilibrium equations within the body and zero surface tractions on the surface.

$\rho, \bar{\rho}$ Residual stress tensor.

$\underline{x} = (x, y, z), t$ Space and time.

μ Scalar temperature parameter

σ_{SM}	Secondary membrane stress
p_i, T_i	Surface traction.
m^0	Scalar load multiplier.
k	Thermal conductivity.
$T, \Delta T$	Temperature, Temperature difference.
σ_t	Thermal stress.
σ, ϵ	Uniaxial stress and strain.
V_F	Volume of the zone of reverse plasticity.
V_S	Volume of the elastic-core.
f, k	Von-Mises yield function.
σ_y	Yield stress

Acknowledgments

I would like to thank my advisor, Dr. R. Seshadri for his generous help and support on this research. I would also like to thank Dr. Wolf Reinhardt of Babcock and Wilcox, Cambridge Ontario for the many helpful suggestions and emails regarding important aspects of my thesis. I thank the several sources which provided financial support during the course of my program. Also, I would like to thank many researchers over the years who have contributed to this thesis in some way.

CHAPTER 1

Introduction

1.1 Background and Motivation

The objective of this paper is to determine the ratcheting boundaries for cylindrical pressure vessels. The effect of thermal cycling on the state of stress in pressure vessel components and constrained systems is investigated using numerical techniques. Due to complexity of developing closed form solutions for system with time, temperature, material properties and boundary conditions all combined, the solutions are obtained numerically using the finite element method. The basic concepts of shakedown, ratcheting and alternating plasticity are defined within the context of pressure vessel design and analysis. Computer based analysis to ensure shakedown loads are described. The FEA results presented in this thesis are obtained using

ANSYS. Discussion of the results obtained focuses on the residual stresses developed and their effect on ratcheting. The effect of plastic cycling under the action of Thermo-mechanical loads is interpreted as per the guidelines specified by ASME (American Society of Mechanical Engineers). The results are compared with the method proposed by Reinhardt [22]. The other issues addressed in this thesis are:

- The difference between ratcheting and collapse at limit state.
- What kind of capabilities are needed to evaluate progressive collapse?
- Comparison of different methods and tools that are available
- Verification of predictive capabilities of different approaches

This work is an attempt to understand thermal and residual stresses that develop during thermal cycling. An understanding of development of residual stress over time when subjected to thermal cycling could contribute to effective design and failure analysis for a variety of applications and is therefore of interest to the pressure vessel industry.

1.2 Code Guidelines for Ratcheting Check

Plastic fatigue analysis has been intensively studied since the 1950's. Earlier designs were based on experimental data collected from tests on polished un-notched specimen subjected to fully reversed loading. The specimens are tested till they fail and the data collected is used in the design of actual components. Elastic stress analysis is then performed and the results are compared with the data from experiments to predict failure. This lead to the development of the so called $3S_m$ rule. As per this requirement if the primary plus secondary stress range is less

than $3S_m$ together with the limitations on the primary stress, favorable distribution of residual stresses will develop in a few cycles of loading and shakedown to elastic action will be achieved. This concept is rigorously correct provided the material behaves elastically through a stress range of twice the yield point. The proof of this concept is demonstrated through Melan's shakedown theorem which in essence states that if a structure shakes down, then it will shakedown after a few load cycles. In practice the application of this shakedown principle used in ASME (American Society of Mechanical Engineers) Section III and USAS B31.7 [1] [2] runs into complications. Wherever there is stress concentration a non-linear distribution of stresses occurs. ASME Section III and USAS B31.7 suggests that the so called peak strains should also be predicted by elastic analysis, but actually it is only an approximation. In many situations involving structural discontinuities in power piping components under service conditions, the peak stresses are usually greater than $3S_m$ ¹. As a result, the area in which the peak strains occur plastifies even though the membrane stresses are within the shakedown limit. However the peak plastic strain concentration at the discontinuity may cause failure by fatigue. Peak plastic strains is not an issue as far as ratcheting is concerned. This is because failure by ratcheting involves the formation of a local plastic mechanism. This fact is demonstrated by several researchers². The deficiencies of methods based on elastic analysis are listed below.

- *No evaluation of the ultimate shakedown load:* An elastic analysis gives no indication of the ultimate loads at which ratcheting commences.
- *Stress peaks at singularities:* A purely elastic solution results in high stress values at the points of singularities which are not representative of the phys-

¹Criteria of the boiler and pressure vessel code for design by analysis, ASME,1969

²Shakedown of Elastic-Plastic structures by Jan.A.Konig

ical structural behavior.

- *Stress analysis as a goal*: Here a precise analysis is a goal.
- *Complex material models*: A solution based on elastic analysis cannot capture the behavior of complex material models.

While considering the effects associated with the exceeding the $3S_m$ rule the following factors are important.

- The effect of peak plastic strains for life assessment under low cycle fatigue.
- The effect of plastic redistribution.
- The effect of ratcheting.

With respect to ratcheting ASME suggests that shakedown state must be achieved where $3S_m$ is exceeded, while B31.7 [2] suggests that either shakedown can be demonstrated by a cyclic elastic-plastic analysis or if the total accumulating strain is accounted for in a fatigue analysis then a shakedown check is not required. To further emphasize the problem with ASME Section III requirement with respect to shakedown, it is extremely difficult to analytically apply an incremental plasticity theory for cyclic loading conditions and track the stress-strain history through several hysteresis loops.

It should also be noted that there are no classical theorems for predicting a stabilized hysteresis loop formation under cyclic loading situations like those that are there for predicting elastic shakedown. In the absence of such a theory problem of evaluating the effect of ratcheting and to determine how much ratcheting is present in a specific loading situation can only be solved through a cyclic incremental finite element analysis.

It is also important to see that condition of ratcheting at load level is specific to a given component, i.e, it depends on the geometry of the component and the loading cycle and it is difficult to generalize or extend one situation to different cases of interest.

Another drawback in applying the $3S_m$ rule is that loads determined by this method are based on elastic analysis and therefore cannot predict the residual stresses nor plastic strains.

A number of methods for handling this condition has been formulated by various researchers. These methods are reviewed in the sections that follow.

1.3 Scope of the Current Study

The previous section demonstrated that the existing design rules are limited to elastic shakedown and are applied and validated only for a few other simple cases involving ratcheting. The actual shakedown or ratcheting behaviour for structures with different shapes and loading histories is unknown. The application of design rules for such problems, may therefore be inefficient or even unsafe. The current study aimed at obtaining an insight into the shakedown and ratcheting behavior for a general class of problems. The other focus of the study is on simplified methods for generating interaction diagrams and applying them for the solution of practical problems. The methodologies were tested against standard benchmark problems to validate the results obtained by comparison with cyclic inelastic finite element analysis. Detailed comparisons between the different approaches, the assumptions involved and the calculations are highlighted in the appropriate sections. Finally, emphasis was also given on proper documentation of the work done including the relevant theoretical background.

1.4 Organization of Thesis

Chapter-2 considers the fundamental problem of structural response when subjected to thermal loads. The relevant governing equations are derived and the basics of theory of plasticity is outlined. The JPVRC criterion for carrying out a ratcheting check is illustrated through a simple example. Chapter 3 describes the Non-cyclic method proposed by Reinhardt [22] and the elastic core method proposed by Kalnins [10]. The two methods are compared and the similarities between them highlighted. Chapter 4 has the numerical and finite element results for the two bar and three bar problems. The basic concepts of residual stress and stress redistribution are explained through examples. Chapter 5 has the results and discussions on the Bree problem. The assumptions made in the simplifications are critically examined. The Bree diagram is generated by different methods and the solutions are compared. Chapter 6 has some general conclusions and directions of future research. The appendices contain the ANSYS macros that are necessary for solving the numerical examples. All plots in this thesis were generated using MATLAB. Each chapter can be reviewed independently of the other chapters.

Literature Review

Over the last thirty years there have been a considerable number of methods described in literature for the direct evaluation of limit and shakedown loads. The mathematical or the analytical approach for solving the problem involves solving a set of differential equations or finding the extremum of a certain functional determined by fundamental shakedown theorems. However applying such techniques to practical problems in pressure vessel design with fluctuating mechanical and thermal loads is extremely difficult as it involves time integrals over applied loadings. Analytical solutions for a restricted class of problems is addressed in [4] [6] [9] and [12]. In reference [4], closed form solution for the Bree problem is given. In reference [8] analytical solution for a circular cylinder that is subjected to a internal pressure and cyclic temperature variation through thickness, based on an exten-

sion of Koiter's theorem to themal problems is presented. In reference [9]&[12] the duality criterion between the static and kinematic shakedown theorems is used to reduce Koiter's equations for a cylindrical shell to coupled partial differential equations that use stress and the curvature as the primary field variables. The numerical solution is then obtained using optimization principles. The numerical approaches generally rely upon the application of linear and non-linear programming methods to upper and lower bound shakedown theorems and the use of finite element approximations. Such methods have remained in the domain of research and have generally not come into general use of engineering design. Finite element simulation codes of great reliability are now available but these methods for assessing shakedown require a whole set of new computer algorithms. For large scale problems, programming techniques are complicated and therefore less preferred than linear elastic solutions. The methods based on linear elastic analysis developed into General Local Stress-Strain Analysis (GLOSS) method by Seshadri [24] and Elastic Compensation Method developed by Mackenzie and Boyle (1993) [14]. The Elastic Compensation Method has been applied to the problem of shakedown by applying the lower and upper bound theorems of plasticity [13] [7]. But these methods are based on the classical lower bound shakedown theorem of Melan [6] [9] and gives a lower bound estimate of the elastic shakedown limit. Recently Preiss [20] [25] used Melan's theorem theorem in conjunction with elastic-plastic FEA to calculate lower bound of shakedown loads. The residual stress fields generated by this method are very close to the exact residual stress. For non-proportional loading cases, the stress history is visualized using a deviatoric map. Gokhfeld and Cherniavsky [6] have applied mathematical programming techniques directly to Koiter's theorem to calculate the upper bounds of the shakedown loads. A similar approach has been adopted by Corradi [5] for structural problems. However

classical shakedown theorems are not able to predict the boundary between stable cycling and ratcheting. Recently Ponter and Chen [19] have developed a minimum theorem to distinguish between shakedown and ratcheting. The check against ratcheting is one of the design checks required in the design by analysis approach of ASME Boiler and Pressure vessel code, Section III, and Section VIII Div. 2 [1] and the code provides the frequently used $3S_m$ criterion for the linearized primary and secondary stress range. But this condition is demonstrated to be overly conservative in some cases and nonconservative in certain other cases by Reinhardt [21]. Further he observes that the code is too conservative for structures with significant thermal loading. In general methods based on Melan's theorem cannot be used to assess whether a state of stable cycling would be attained in structures that are subjected to a combination of cyclic thermal and pressure loads [21]. The direct way to obtain a steady cyclic solution is to actually apply the load cycles. Once the solution has converged sufficiently the absence of progressive plastic deformation can be assessed by observing the strain increments over the load cycles. A decreasing trend suggests that the structure is approaching the shakedown condition. Kalnins [10] suggested the elastic core method to evaluate shakedown under cyclic thermal and pressure loadings. The principle behind this method is that a structure cannot experience incremental collapse as long as a continuous elastic core exists in the structure throughout the load cycles. A Linear Matching Method has been developed by Ponter [17] to evaluate the shakedown boundary for bodies subjected to cyclic loads and temperature and composed of elastic-perfectly plastic material. This method is an extension of the general upper bound method associated with a class of displacement fields as described by a finite element mesh. The method attempts to construct, as a limit of an iterative procedure, a linear strain rate solution for the applied loads by matching the response of the linear material

to that of an elastic-plastic material. A large number of interaction diagrams was produced using this method by Ponter and Carter [18].

2.1 Problem Definition

The problem considered is that of the response and the behavior of elastic-plastic structures under mechanical and thermal cycling. The material is assumed to be elastic-perfectly plastic in most of the cases. The entire system is subjected to cyclic thermal and mechanical loads. Although the principles and theorems that govern the behavior of this type of material behavior are known, determining the complete state of stress over time from the equations given by the classical shakedown theory is no trivial task. A complete stress solution from the classical theory of plasticity will involve five variables; position (x, y, z) , temperature and time. The reader seeking classical solutions to problems of thermal cycling is referred to the work of Gokhfeld [6]. Two methods were used in this thesis to obtain solutions for such problems.

- The problems are solved numerically using Finite Element Analysis. Therefore the results are approximate rather than exact solutions.
- Simplification of the problem geometry by using symmetry to eliminate position dependence. The problems considered are in increasing levels of complexity. In Chapter 4, we consider bar models, to show the concept of stress redistribution. In Chapter 5 we consider biaxial and triaxial effects.

All numerical simulations of physical phenomena require the solutions of relevant governing equations. In the case of static equilibrium of solids as far as this thesis is concerned these are given as *initial value problem's of solid mechanics*. By this

we mean we are interested in finding the state of the body over time satisfying the governing equations and compatibility. This incorporates equilibrium conditions, boundary conditions, and constitutive equations for materials. A particular numerical solution is distinguished by the choice of geometry, initial and boundary conditions used and the material constitutive law. In the following sections the equations relevant to the problem are outlined.

2.2 Fundamental Structural Thermal Behavior

The most fundamental relationship that governs the behavior of structures when subjected to thermal loads is

$$\epsilon_{total} = \epsilon_{thermal} + \epsilon_{mechanical} \quad (2.1)$$

with the total strains governing the deformed shape of the structure, through kinematic or compatibility considerations. The stress state in the structure (elastic or plastic) depends only on the mechanical strains. Where the thermal strains are free to develop in an unrestricted manner and there are no external loads, axial expansion results. By contrast, where the thermal strains are fully restrained without external loads, thermal stresses and plastification results. Thermal gradients causes the beam to curve or bend when it is unrestrained. If the thermal gradients are high, then the curvature can be large, leading to large deformations. Beams whose ends are restrained against expansion produce opposing mechanical strains, caused by forces that appear due to restraints (See equation 2.1). During heating the restraint forces are compressive, and during cooling they are tensile. Similarly if the beam is restrained from bending due to thermal gradients, the thermal

strains appear as mechanical strains caused by bending moments produced at the restraints. These can in turn be tensile or compressive depending on the sign of the bending moment.

2.2.1 Thermal Expansion

Thermal expansion: Heating induces thermal expansion strains ($\epsilon_{thermal}$) in most

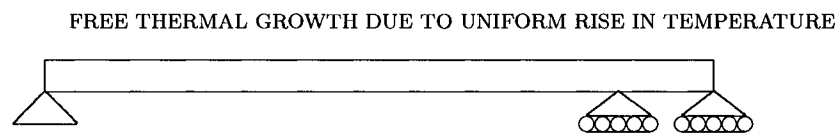


Figure 2.1. Simply supported beam subjected to a uniform rise in temperature

structural materials. These are given by,

$$\epsilon_{thermal} = E\alpha\Delta T \quad (2.2)$$

If a uniform temperature rise, ΔT , is applied to a simply supported beam without axial restraint, the result will simply be an expansion or increase in length of $\alpha\Delta T$ as shown in Figure 2.1. Therefore the total strain (say $\epsilon_{thermal}$) is equal to the thermal strain and there is no mechanical strain (say $\epsilon_{mechanical}$) which means that no stresses develop in the beam.

2.2.2 Thermal Expansion Against Rigid Axial Constraints

Real structures are generally constrained and are not free to elongate. So, a more realistic case is to consider an axially restrained beam subjected to a uniform

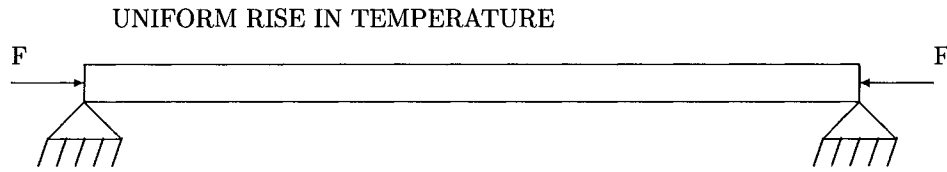


Figure 2.2. Axially restrained beam subjected to a uniform rise in temperature

temperature rise ΔT as shown in Figure 2.2. It is clear to see that in this case the total strain is zero (no displacements). This is because the thermal expansion is canceled out by equal and opposite contraction caused by the restraining force F .

$$F = EA\epsilon_m = -EA\epsilon_T = -EA\alpha\Delta T \quad (2.3)$$

If the temperature is allowed to rise further, there are two basic responses. Depending upon the slenderness of the beam given the beam is constrained axially, the mechanical strain must equal the thermal strain.

- If the beam is sufficiently stocky the axial stress will sooner or later reach the yield stress σ_y of the material and if the material has an elastic-plastic stress-strain relationship, the beam will continue to yield without any further increase in stress, but it will also store an increasing magnitude of plastic strains.
- If the beam is slender then it will buckle before the material reaches its yield stress.

A identical response occurs during unloading i.e cooling. The stresses induced by the restraints are tensile and can reach yield depending upon the temperature and the state of residual stresses in the beam due to prior loading.

2.2.3 Thermal Bending

In the previous section we discussed the effects of uniform temperature rise on axially restrained beams. In pressure vessels and piping under operating conditions, the inner surface of the pipe is at a much higher temperature than the outer surface. This causes the inner surfaces to expand much more than the outer surfaces inducing bending in the member.

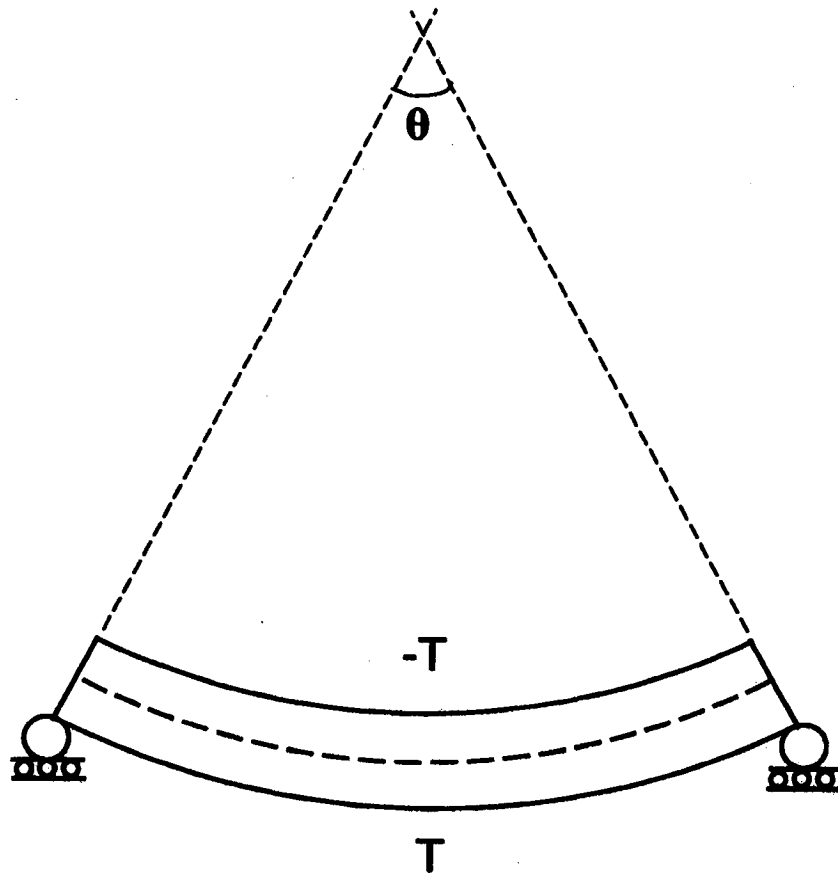


Figure 2.3. Simply supported beam subjected to a transverse thermal gradient

From the discussion it is clear that the effect of boundary restraints is crucial in determining the response of structural members to thermal actions. The important

conclusion to be drawn from the discussion so far is that thermal strains will appear as displacements if they are unrestrained or as stresses if they are restrained through counteracting mechanical strains generated by restraining forces.

2.2.4 Strains and Strain rates

It is useful at this stage to distinguish between strains and strain rates and what “.” the over the generalized stress and strain tensors mean in the context of the problems considered. In strain controlled tests the rate form of the equilibrium equation actually refers to the variation with respect to time.

- Time represents real time for rate dependent problems.
- Time represents response to variation in applied loadings for rate-independent problems.

Prior to any solution being attempted, some basic assumptions were made. Thermal conduction was assumed to be an instantaneous process resulting in uniform distribution of temperatures throughout the body. The coefficient of thermal expansion was assumed to be independent of time. The structure was assumed to be stress free before thermal cycling. Other assumptions that are made in each of the solution methodologies are explained in appropriate chapters.

2.3 Basics of Plasticity Theory

The solution for the problem of structures subjected to thermal cycling involves determining the complete state of stress over time. It also requires determining instantaneous temperature and instantaneous stiffness for the point in time of interest and this requires including the effect of entire thermo-elastic history to

the point. Firstly we define what we mean by a elastic-perfectly plastic material. In contrast to perfectly elastic materials, the elastic energy for such a material is only partially recovered on unloading. The rest of the energy is dissipated into heat. An *elastic perfectly plastic material* is characterized by a elastic modulus E in the elastic range and yield limit σ_y beyond which plastic flow takes place at a constant yield stress. In this section we outline the basic equations of theory of plasticity for such a model. The index notation is used in this thesis. The total strain of the system can be decomposed as

$$\epsilon = \epsilon_m + \epsilon_T \quad (2.4)$$

The total strain field can be decomposed into an elastic part (reversible), a plastic part (irreversible) and thermal part.

$$\epsilon_{ij} = \epsilon_{ij}^E + \epsilon_{ij}^P + \epsilon_{ij}^T \quad (2.5)$$

The elastic strain is given by Hooke's law

$$\epsilon_{ij}^E = E_{ijkl}^{-1} \bar{\sigma}_{kl} \quad (2.6)$$

For an isotropic continuum the elastic modulus is given by

$$E_{ijkl}^{-1} = \frac{1}{E} [(1 + \nu) \delta_{ik} \delta_{jl} - \nu \delta_{ij} \delta_{kl}] \quad (2.7)$$

where ν is the Poisson's ratio

Stress is obtained by inverting the stress-strain relationship

$$\sigma_{ij} = E_{ijkl} \epsilon_{kl}^E \quad (2.8)$$

and the tensor moduli becomes,

$$E_{ijkl} = \frac{E}{1+\nu} [\delta_{ik}\delta_{jl} - \frac{\nu}{1-2\nu} \delta_{ij}\delta_{kl}] \quad (2.9)$$

The stress level at which yielding begins is defined by a yield condition given by

$$f(\sigma_{ij}, \mathbf{x}) - k(\mathbf{x}, T) \leq 0 \quad (2.10)$$

The yield condition provides a potential for plastic strain rates. The associated flow rates are given by,

$$\dot{\epsilon}_{ij}^P = \dot{\lambda} \frac{\partial f(\sigma_{ij})}{\partial \sigma_{ij}} \quad (2.11)$$

and

$$\begin{cases} \dot{\lambda} \geq 0 & \text{if } f = k \text{ and } \dot{f} = 0 \\ \dot{\lambda} = 0 & \text{if } f < k \text{ or } f = k \text{ and } \dot{f} \leq 0 \end{cases} \quad (2.12)$$

If the yield surface is piecewise-linear then the equation can be written as,

$$\dot{\epsilon}_{ij}^P = \sigma_s \dot{\lambda}_s \frac{(\partial f_s)(\sigma_{ij})}{\partial \sigma_{ij}} \quad (2.13)$$

Convexity and the associated flow rule implies that

$$(\sigma_{ij} - \sigma_{ij}^0) \dot{\epsilon}_{ij}^P \geq 0. \quad (2.14)$$

Convexity and normality are just mathematical concepts and they have indirect

physical meaning. The actual idea behind the principle of maximum plastic work is that a real material would dissipate heat when plastic flow occurs. In other words, the work done by the external forces when plastic flow occurs is always positive. Drucker [8] called these materials as stable plastic materials. Here $\dot{\epsilon}_{ij}^P$ is the strain rate associated with the stress state σ_{ij} and σ_{ij}^0 is a stress state such that does not violate yield. If the yield surface is bounded or is a hypercylinder with a axis defined by vector n then there exists two constants such that the following inequality is satisfied [8]:

$$\nu(\dot{\epsilon}_{ij}^P \dot{\epsilon}_{ij}^P)^{\frac{1}{2}} \leq \sigma_{ij} \dot{\epsilon}_{ij}^P \leq \mu(\dot{\epsilon}_{ij}^P \dot{\epsilon}_{ij}^P)^{\frac{1}{2}} \quad (2.15)$$

The inequality allows us to estimate the dissipation from the plastic strain rate. This means that the work done by the external forces is bounded. It also implies that

$$\int_{t_1}^{t_2} D(\dot{\epsilon}_{ij}^P) dt \geq D(\Delta \dot{\epsilon}_{ij}^P) \quad (2.16)$$

where,

$$\Delta \dot{\epsilon}_{ij}^P = \dot{\epsilon}_{ij}^P(t_2) - \dot{\epsilon}_{ij}^P(t_1) \quad (2.17)$$

We can also write the inequality as,

$$D(\dot{\epsilon}_{ij}^1 + \dot{\epsilon}_{ij}^2) \leq D(\dot{\epsilon}_{ij}^1) + D(\dot{\epsilon}_{ij}^2) \quad (2.18)$$

with equality only if there exists scalars α_1 and α_2 such that $\alpha_1 \dot{\epsilon}_{ij}^1 = \alpha_2 \dot{\epsilon}_{ij}^2$.

2.3.1 Structural Behaviour

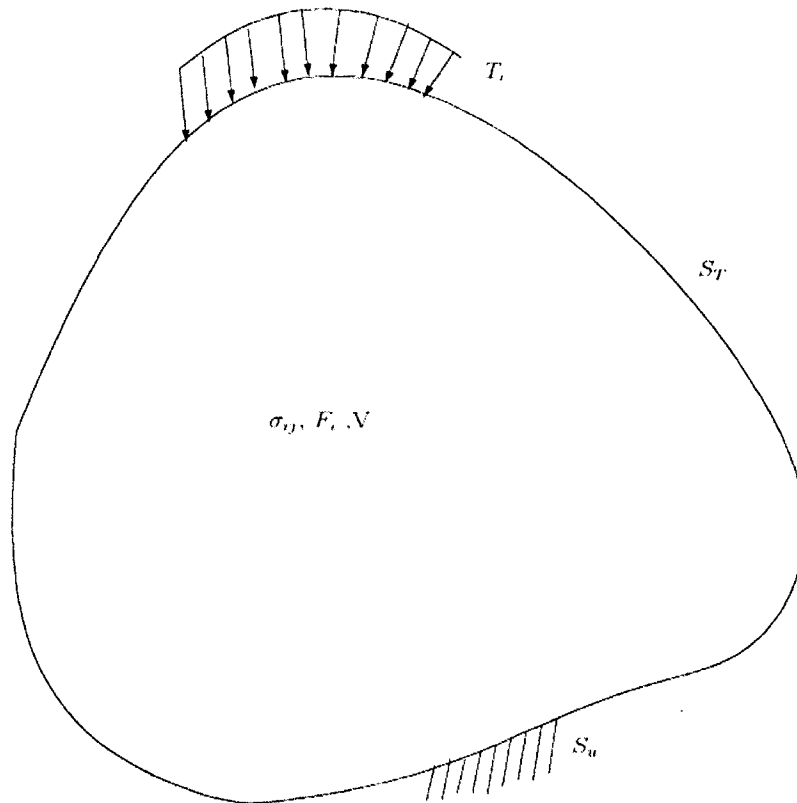


Figure 2.4. General body of domain Ω subjected to surface and body forces

The internal equations of equilibrium are

$$\sigma_{ij,j} + F_i = 0 \quad (2.19)$$

The statical boundary condition is of the form

$$\sigma_{ij}n_j = T_i \quad (2.20)$$

In these formulae F_i are body forces, T_i denote surface traction's and n_j is the

unit outward normal vector (See fig 2.4). The strain-displacement relationship for small strains is given by,

$$\epsilon_{ij} = \frac{1}{2}(u_{i,j} + u_{j,i}) \quad (2.21)$$

If there are discontinuities (see fig.2.5) then equilibrium conditions require that,

$$\sigma_{ij}^- n_j = \sigma_{ij}^+ n_j \quad (2.22)$$

where σ_{ij}^- and σ_{ij}^+ are the stress in both sides of the discontinuity surface and n_j is its normal.

If the strain field is discontinuous then material continuity requires that

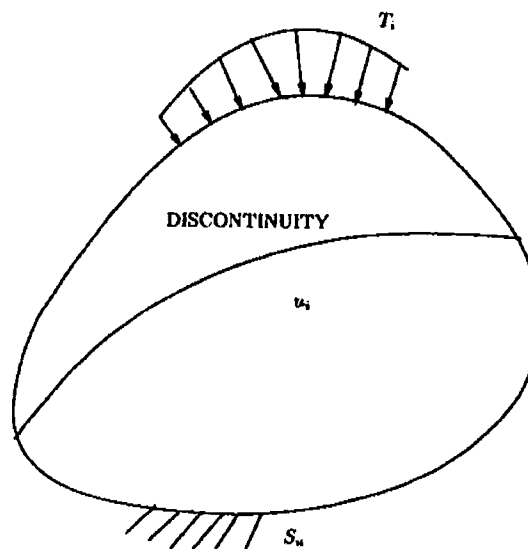


Figure 2.5. General body (domain Ω) with a discontinuity subjected to surface and body forces

$$[\epsilon_{ij}]n_j = 0 \quad (2.23)$$

where $[\]$ indicates a jump and n_j is as above. An example of a discontinuous strain field would be a notched bar subjected to inplane bending loads. The strains on either side of the notch will not be equal, for this component. Discontinuous strain fields also arise on the interface between elastic and plastic regions.

2.3.2 Virtual Work Principle

The virtual work equation is given as,

$$\int_V \sigma_{ij}\epsilon_{ij}dV = \int_S T_i u_i dS + \int_V F_i u_i dV \quad (2.24)$$

where σ_{ij} is in equilibrium with T_i and F_i and ϵ_{ij} is the strain corresponding to virtual displacement u_i . The formula is valid irrespective of any causal relationship between the static and kinematic quantities, and also if the stress and deformation fields contain admissible discontinuities.

2.3.3 General Relations for Elastic-Plastic Structures

The actual stress-field can be decomposed in the following way

$$\sigma_{ij} = \sigma_{ij}^E + \rho_{ij} \quad (2.25)$$

ρ_{ij} satisfies equilibrium and statical boundary conditions. Therefore ρ_{ij} is called residual stress or instantaneous residual stress. On substituting the above expres-

sion into the equation for strain field(2.21), we obtain the strain field as

$$\epsilon_{ij} = E_{ijkl}^{-1}\sigma_{kl}^E + \epsilon_{ij}^T + \epsilon_{ij}^P + E_{ijkl}^{-1}\rho_{kl} \quad (2.26)$$

The strain field is composed of two fields. One corresponding to the perfectly elastic structure and other is the field of residual displacements.

$$\epsilon_{ij}^T + E_{ijkl}^{-1}\sigma_{kl}^E = \frac{1}{2}(u_{i,j}^E + u_{j,i}^E) \quad (2.27)$$

$$\epsilon_{ij}^E + E_{ijkl}^{-1}\rho_{kl}^E = \frac{1}{2}(u_{i,j}^R + u_{j,i}^R) \quad (2.28)$$

From these two equations, residual stress and the displacement fields are uniquely defined by the plastic strain field at every instant. The residual stress can be calculated in principle by inverting the above formulation to get ρ_{ij} explicitly.

$$\rho_{ij} = \frac{1}{2}E_{ijkl}(u_{k,l}^R + u_{l,k}^R) - E_{ijkl}\epsilon_{kl}^P \quad (2.29)$$

Substituting this into the equilibrium equations (2.19) and the strain displacement equations (2.21) we get,

$$E_{ijkl}(u_{k,l}^R + u_{l,k}^R) = 2E_{ijkl}\epsilon_{kl}^P \quad (2.30)$$

with the boundary conditions,

$$[E_{ijkl}(u_{k,l}^R + u_{l,k}^R) - 2E_{ijkl}\epsilon_{kl}^P]n_j = 0 \quad (2.31)$$

from this we can solve for u_i^R . In principle these equations can be used to express stress at any time given any arbitrary loading history. The difficulty in applying

these equations to our problem lies in including the loading history through a correct expression of applied strain. The applied strain along the boundary is difficult to derive.

2.4 Shakedown Theorems

2.4.1 Lower Bound Shakedown Theorem

The static theorem due to Melan gives a sufficient condition for elastic shakedown for a structure made of elastic perfectly plastic material. It can be stated as follows Melan's shakedown theorem is also known as the static shakedown theorem. It states that the necessary and sufficient condition for the occurrence of shakedown to elastic action is the following,

1. There should be a time independent stress field satisfying equilibrium, i.e ,

$$\sigma_{ij,j}^0 + X_i = 0 \quad (2.32)$$

$$\sigma_{ij}^0 n_j = p_i \quad \text{on the surface} \quad (2.33)$$

2. The stress field should be bounded by the yield surface. Then shakedown to elastic action will be attained.

A stress field satisfying these conditions is termed statically admissible stress fields. To apply Melan's theorem we need to identify elastic and residual stress fields. If one assumes that elastic shakedown occurs before fatigue failure, then local plastic deformation and residual stress field become independent of time after a certain number of loading cycles, whereas the local stress as well as the macroscopic stress

varies cyclically with respect to time. Nguyen et al. [15] have extended the Melan's theorem to include the effect of hardening.

2.4.2 Residual Stresses

What is a residual stress?

Residual stress is a type of stress which is present in a material even when no external forces or moments are being applied to it. The residual stress is a function of plastic strain (see Eqn.2.29). The residual stresses must satisfy,

$$\begin{cases} \operatorname{div} \bar{\rho} = 0 & \text{on the volume } \Omega \\ \rho \cdot n = 0 & \text{on the surface } \partial\Omega \\ \bar{\rho} = \frac{\partial \rho}{\partial t} = 0 & \forall t > 0 \end{cases} \quad (2.34)$$

Residual stresses can be either tensile or compressive, and are locked into the material as a result of its previous history of loading. They are very important in components because they can be large in magnitude and will add to (or subtract from) the stresses caused by applied forces. Residual stresses arise when the material is subjected to heating-cooling cycles in the presence of constraints. Residual stresses also occur due to constrained plastic deformation. A practical application of this type of residual stress is autofrettage. In this case the effect of the compressive residual stress is beneficial.

ASME definitions of Secondary and Self-limiting stresses are given below:

A Self-limiting stress, including secondary stress and peak stress, is a kind of stress which is necessary to satisfy the continuity conditions in the structure or with the external constraint. It may also be called deformation-controlled stress (ASME

Code Case N-47-28) or continuity-controlled stress. The main function of self-limiting stress is to satisfy the structural discontinuity. Secondary stress is a stress developed by the self-constraint of a structure. It must satisfy an imposed strain pattern rather than being in equilibrium with an external load. The basic characteristic of secondary stress is that it is self-limiting. Although thermal stresses are self-limiting, they cannot be strictly classified as residual stresses.

2.5 Solution of Melan's Theorem by Linear Programming

2.5.1 Formulation

Linear programming consists of the task of minimizing a linear cost function for a linear profit function under a set of constraints. Linear programming has been used successfully to estimate lower bounds of shakedown loads. Melan's theorem can be posed as a linear programming problem in the following way, let m^0 and m^τ be the parameters describing the external load actions. Then Melan's theorem can be recast as follows,

$$\max m_i^0 =? \quad (2.35)$$

under the constraints,

$$\sigma_{ij,j}^0 + m_k^0 X_{ik}^0 = 0, \quad (2.36)$$

$$\sigma_{ij}^0 n_j = m_k^0 p_{ik} \quad (2.37)$$

and

$$f(\sigma_{ij}^0) \leq 0 \quad (2.38)$$

If the von-Mises yield criterion is used, the constraint becomes non-linear and the problem becomes a non-linear programming problem. A big array of *optimization methods* or *search methods* are available each with its own limits of applicability and computational and convergence requirements. The most general classification is into *deterministic* and *stochastic* methods. Stochastic methods use random elements in their search for global minimum. Examples of this method include *Monte Carlo methods*, *Neural Network methods*, and *Evolutionary Algorithms like Genetic Algorithms*. These methods can handle noisy non-linear problems with hundreds of variables in the objective function. But the yield condition can be linearized and the problem can be converted into a linear programming problem. The *simplex algorithm* is a well established procedure or tackling linear programming problems. It is based on the fundamental theorem of linear programming which states that *if an optimum solution exists, then there exists a feasible basic solution that is optimum*. The optimization procedure consists of a series of pivot transformations until the optimum is found. Since the constraint is *convex*, the first feasible solution found by this method is also the optimum solution. Another advantage of using Melan's theorem as a optimization problem is that multiple load cases are easily handled. Instead of using every load case in the optimum equation, one can establish extreme cases of the load case and superimpose self-equilibrating stresses on these load cases. Although the optimum load parameters obtained will differ from the exact ones, considerable simplification can be achieved by this method.

2.6 Upper Bound Shakedown Theorem

The upper bound theorem is discussed in a paper of Koiter [12]. Koiter's dual, upper bound, theorem states that if any kinematically acceptable mechanism of plastic deformation can be found, in which the total virtual rate of working of the elastic stresses $\lambda\sigma_{ij}^E$ with the assumed plastic rate of deformation $\dot{\epsilon}_{ij}^p$ is greater than the total rate of plastic energy dissipation $D(\dot{\epsilon}_{ij}^p)$ per unit volume, in the assumed mechanism, then shakedown cannot occur. The estimate of the load factor λ obtained by equating these two energy rates is hence an overestimate of λ_{sd} . Mathematically, the relation can be expressed as,

$$\int_0^T \int X_i \dot{u}_i dv + \int_S p_i \dot{u}_i dt \geq \int_0^T dt \int D(\dot{\epsilon}_{ij}^p) dv \quad (2.39)$$

Using the principle of virtual work the inequality (2.39) can be expressed as,

$$\int_0^T \int_{\Omega} \sigma_{ij}^e : \dot{\epsilon}_{ij}^p dt \geq \int_0^T \int_{\Omega} \sigma_{ij} : \dot{\epsilon}_{ij}^p dt \quad (2.40)$$

In this paper [12], it is pointed out that this theorem and its proof do not say anything about the magnitude of plastic deformation which may occur before the structure reaches its shakedown state. It is clear that large plastic deformation that satisfies the inequality (2.39) will also give a acceptable solution. What we mean by this is that we can guess any possible kinematically acceptable mechanism that satisfies the inequality (2.39). But such a solution will have no physical meaning. This leads to the natural question regarding the acceptable value of the plastic strains. Valid expressions of the plastic strains should lead to convergent values

for the total plastic work i.e,

$$\lim_{T \rightarrow \infty} \int_0^T \int_{\Omega} \sigma_{ij}^e : \dot{\epsilon}_{ij}^p dt < \infty \quad (2.41)$$

Only such solutions are acceptable. The upper bound theorem can also be formulated as extrema problem, by minimizing the dissipation function for a given work input to the system.

2.7 Cyclic Incremental Analysis

To show how a ratcheting check can be performed by a cyclic incremental analysis, we consider a clamped beam subjected to a uniformly distributed load (P) and a temperature variation across the thickness. By this we mean that the upper surface of the beam is heated to a temperature (T) and the temperature decreases uniformly and reaches a temperature (-T) at the bottom surface. This problem is similar to piping or nozzle problems where a moment and a secondary load act simultaneously.

During thermal cycling the cumulative change in thermal stress over an entire cycle will always be zero. Here we actually track response through cyclic stress-strain curves and see if ratcheting occurs for a prescribed history of loading.

1. Elastic Plastic FEA can be used to establish shakedown by simulating the structural response and monitoring the resulting plastic strains. This method allows the investigation of any type of loading history and gives a complete (stress-strain) solution for a loading history.
2. This method does not predict specific values of the shakedown loads. It simply demonstrates the response at a given load level.

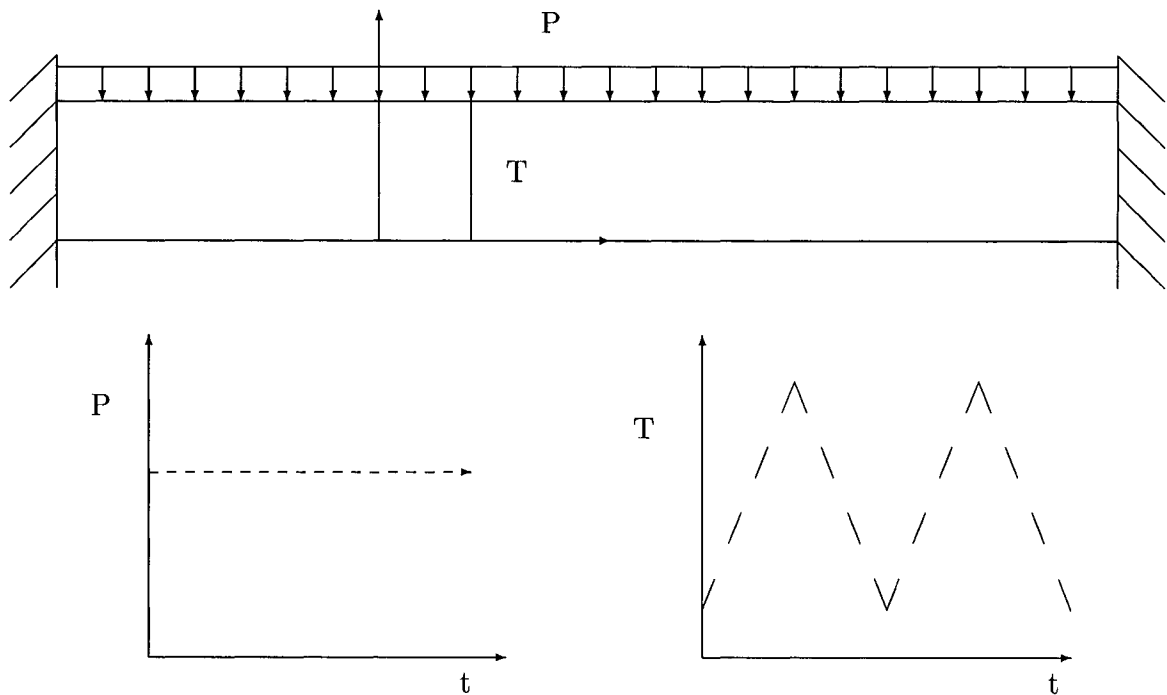


Figure 2.6. Schematic diagram of the beam problem

3. A number of simulations at different load levels have to be performed before the boundary between ratcheting and reverse plasticity can be identified.
4. A lot of different material models have been developed and incorporated in the ANSYS library. An clever choice of material models can accurately capture the true material behavior.

The bending of the beam due to constant distributed load, prestresses the top fibers in tension and the bottom fibers in compression. These stresses are maximum at the center because the maximum bending moment due to the primary load occurs at the center of the beam. When the thermal membrane stress fluctuates with an amplitude of σ_y , the maximum combined stress occur at the top and the bottom of the beam at the start and the end of the heat up cycle (see fig 2.7).

Increase in strain increments means that ratcheting can be rapid. The basic idea

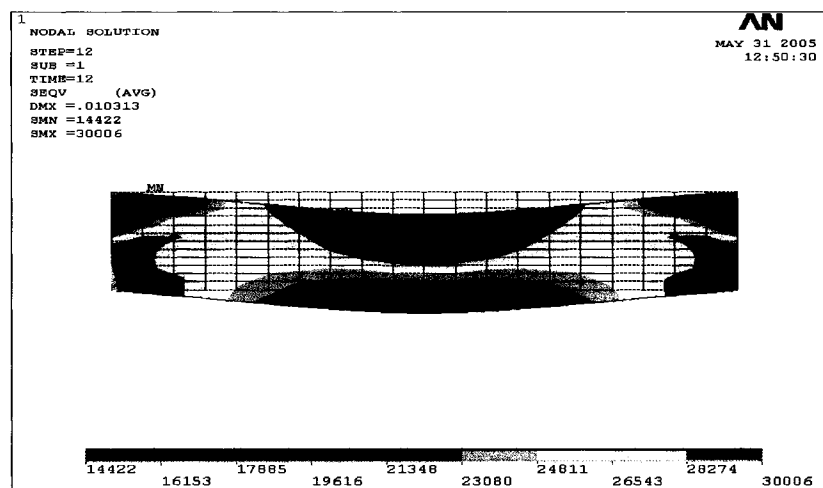


Figure 2.7. Equivalent stress in the beam in the end of heat up cycle

is to predict whether the displacements are going to be acceptable by just cycling or 20 or 40 cycles and evaluating the strain increments. In reality the component may be subjected to well over 5000 cycles of loads and a practical simulation of 5000 cycles would be infeasible. The data in Appendix-A represents the increments per cycle of the plastic strains in the x direction for element near the surface of the beam. We would like to observe the variations in strain by increasing thermal loads keeping the mechanical load fixed. The difference in strain values for successive cycles is given for a pressure of 1000 lbs and differing temperature values. In each cycle there is a steady phase in which the strain in the zone cycles elastically.

These correspond to the zeros in the table. This is followed by a redistribution phase that causes plastic strain increments. This trend suggests a pattern. If the temperature is reduced starting from a value of 0.9 gradually in steps of 0.02, the transition from ratcheting to steady state will involve higher number of thermal cycles. The scenario is shown fig 2.8.

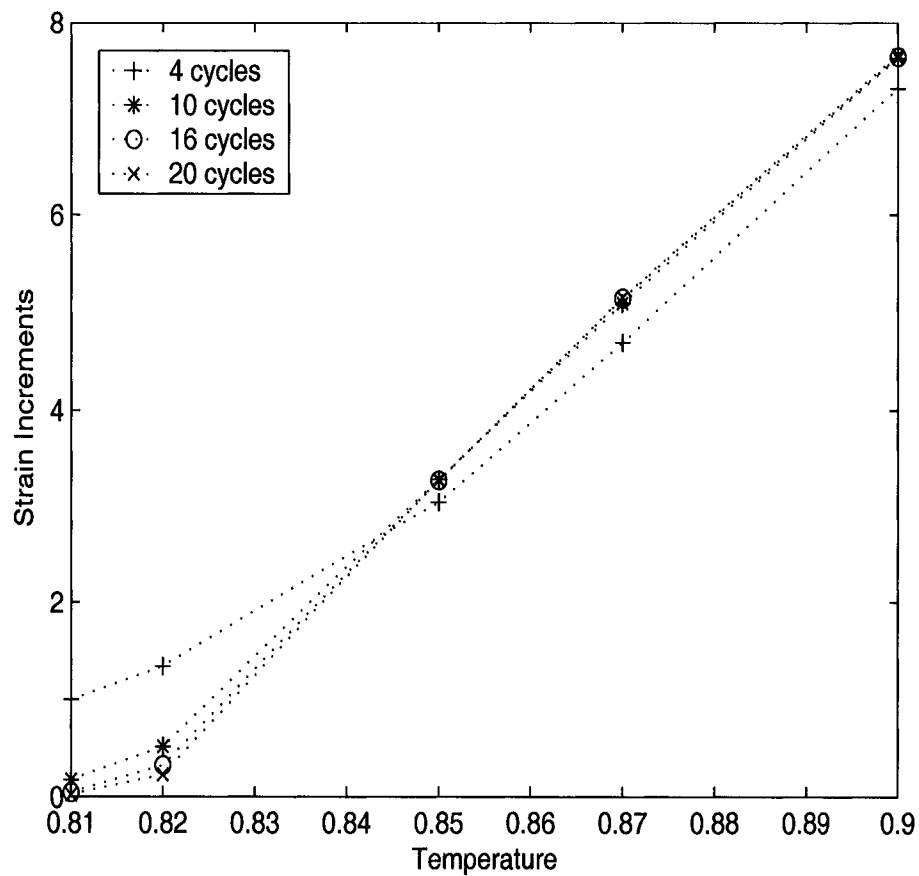


Figure 2.8. Hoop strain increments versus increase in thermal load near the shakedown boundary

Even though the increments appear to be approaching zero for temperatures in the range of $t = 0.8$, there would be no way of confirming if it is actually zero. Code recommends 250 cycles [1] [2] to observe strain growth but this number appears

to be arbitrary. From the difference table we can also estimate sensitivity of the ratcheting boundary to applied loading. For instance for the sixth loading cycle, the difference in the strain increments for a temperature of 0.81 and 0.82 is given by,

$$\text{Increase in ratcheting strain} = (8.94E - 05) - (5.23E - 05) \quad (2.42)$$

$$= 3.71E - 05 \quad (2.43)$$

$$\text{Percentage increase in ratcheting strain} = \frac{3.71E - 05}{5.23E - 05} * 100 \quad (2.44)$$

$$= 70.91\% \quad (2.45)$$

$$\text{Percentage increase in thermal load} = \frac{0.82 - 0.81}{0.81} * 100 \quad (2.46)$$

$$= 1.23\% \quad (2.47)$$

For a 1.2 percent increase in applied load the ratcheting strain jumps by 70 percent, and the magnitude keeps increasing as we go from left to right across the table. This observation is significant because in actual service the component may be subjected to a large number of cycles (say over 5000 cycles). In such a case the growth in ratcheting strain can cause loss of structural integrity and render the component unfit for service. The question is what is the acceptable value of strain increments that can be regarded as safe? If we can agree on a value of the strain increments after say N cycles then we will have a hard specification for the rate of ratcheting. The other questions that need to be addressed are:

- How much strain growth can be permitted in the structure?
- What rate of ratcheting is acceptable for the component to remain service-

able.

JPVRC criterion can be used to evaluate ratcheting. The application of this criterion is demonstrated in the following section.

2.7.1 JPVRC Criterion for Ratcheting Check

The method of analysis that was outlined in the section above is one of the ways of carrying out a ratcheting check. However, it involves quite a large number of runs and a lot of numerical analysis. Such a procedure can quickly get cumbersome and, from a design perspective, simpler methods are required to check for ratcheting. The criterion proposed by JPVRC (Japanese Pressure Vessel Research Council) is simple. This criterion uses the equivalent plastic strain as the ratcheting measure. According to this criterion, if the increments of plastic strain is less than 0.0001 in all plastically cycled points then we can say that ratcheting will not occur [10]. To demonstrate the application of this criterion, we list the von-Mises equivalent plastic strain for an element in the zone of reverse plasticity at a load slightly above the shakedown load ($t = 0.82$).

The maximum equivalent plastic strain in this case is $7.67E-04$ (row 8, column 3, table:2.1) which is greater than 0.0001, so JPVRC criterion predicts ratcheting at $t = 0.82$. A finite element analysis was performed for 250 cycles and the plastic strain continued to increase indicating ratcheting at this load value. This confirms the prediction by the JPVRC criterion. Shakedown occurs at a load of $t = 0.80$. The plastic strain increment converges to zero after 250 cycles for this value of temperature. It is also interesting to note that we could have also come to the same conclusion in just ten cycles. This specification is important because in service the structures may cycle plastically for over 5000 cycles. It makes sense to allow plastic

No.cycles	Equivalent plastic strains	Increments
1	0.0	0.0
2	2.40E-04	3.0
3	2.49E-04	0.00E+00
4	9.80E-04	7.31E-04
5	9.80E-04	0.00E+00
6	1.74E-03	7.57E-04
7	1.74E-03	0.00E+00
8	2.50E-03	7.67E-04
9	2.50E-03	0.00E+00
10	3.26E-03	7.63E-04
11	3.26E-03	0.00E+00
12	4.03E-03	7.63E-04
13	4.03E-03	0.00E+00
14	4.79E-03	7.63E-04
15	4.79E-03	0.00E+00
16	5.55E-03	7.65E-04
17	5.55E-03	0.00E+00
18	6.32E-03	7.66E-04
19	6.32E-03	0.00E+00
20	7.09E-03	7.66E-04

Table 2.1. Data table of plastic strain increments at $t=0.82$

cycling because failure due to low-cycle fatigue will take a large number of cycles of load application (in excess of 50000 cycles). This can be deduced from the table of strain increments. It is obvious that the rate of increase is exponential. Restricting the stress range to $3S_m$ will lead to overly conservative designs. A plot of equivalent plastic strains is given in figure (2.9). We can observe the steady increase in the strain values after each cycle and this continues indefinitely.

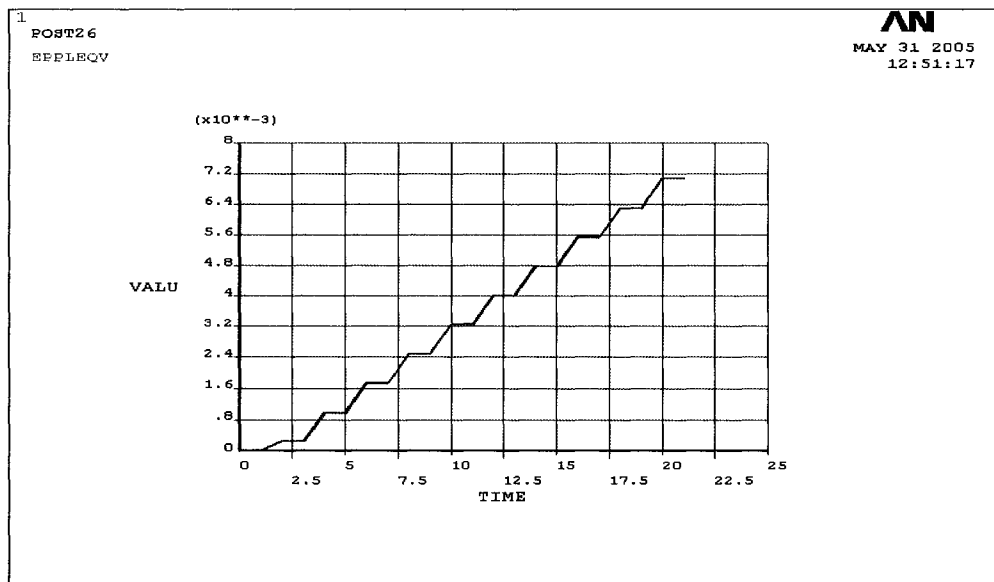


Figure 2.9. Plot of equivalent plastic strains versus number of cycles at t=0.82

The Non-Cyclic Method

A non cyclic lower-bound method for the analysis of plastic shakedown has been proposed by Reinhardt [22]. In this section the method is outlined and it's application demonstrated to some simple problems. The fundamental idea is that whether it is possible to arrive at the plastic shakedown boundary without having to evaluate the cyclic history. In this approach the problem of shakedown analysis is reduced to one of limit analysis, and it is an extension of the one adopted by Gokhfeld [6] for problems of elastic shakedown. This idea is also related to the concept of pseudo yield surfaces.

3.1 Formulation

The material is assumed to be elastic-perfectly plastic. The yield surface is defined by the von-Mises yield criterion.

$$f(\sigma_{ij}) = \sqrt{\frac{3}{2}\sigma'_{ij}\sigma'_{ij}} \quad (3.1)$$

where $f()$ is the yield function and σ'_{ij} is the deviatoric stress. The associated flow rule is

$$\epsilon_{ij} = \lambda\sigma'_{ij}. \quad (3.2)$$

for a periodic loading with a time period Δt ; the stress and the displacements are also periodic as well, with the same period once the steady state is reached. The idea now is to extend the lower bound shakedown theorem of Melan to the range of plastic shakedown. Melan's theorem states that a time-invariant residual stress when added to a purely elastic response due to cyclic loads such that the sum lies within the yield surface, then shakedown to elastic action is assured. In the plastic shakedown range, the plastic strains are no longer constant with respect time, and therefore a constant residual stress is no longer sufficient to keep the stress history within the yield surface. Therefore, we can infer that a time dependent residual stress is now required to satisfy yield condition. This can be written as

$$f(\sigma_{ij}^e(t) + \sigma_{rij} + \sigma_{vij}(t)) \leq \sigma_y \quad (3.3)$$

In this formula $\sigma_{ij}^e(t)$ is the elastic stress and σ_{rij} and $\sigma_{vij}(t)$ are the constant and variable residual stresses. The equation does not determine the constant residual stress and the variable residual stress uniquely. A unique determination of the

variable residual stress is given by the following equation

$$\begin{cases} f(\sigma_{ij}^e(t) + \sigma_{rij} + \sigma_{vij}(t)) = \sigma_y & \text{if } \dot{\epsilon}_{ij} \neq 0 \\ f(\sigma_{ij}^e(t) + \sigma_{rij} + \sigma_{vij}(t)) \leq \sigma_y & \text{if } \dot{\epsilon}_{ij} = 0 \end{cases} \quad (3.4)$$

An additional constraint on the stress state, when plastic flow occurs, is derived from the condition of plastic shakedown. For plastic shakedown,

$$\int_t^{t+\Delta t} \dot{\epsilon}_{ij}^P dt = 0 \quad (3.5)$$

Using the flow rules from the theory of plasticity this equation can be rewritten as,

$$\int_t^{t+\Delta t} \lambda \sigma'_{ij} dt = 0 \quad (3.6)$$

where $\sigma'_{ij} = \sigma_{ij}^e(t) + \sigma_{rij} + \sigma_{vij}(t)$ and λ the plastic multiplier. This means that the total change in stress for a full cycle after stabilization should be zero. We can also infer that the stress should change sign in equation (3.6) for the integral to equal zero.

3.2 Finite Element Implementation

The outline or the implementation of the theory described earlier is listed below.

- Decompose the loading into constant and fully reversed proportional components.
- Create the finite element model. Use elastic-perfectly plastic yield properties with a cyclic yield stress of σ_y .

- Apply the load range of the cyclic load components successively. For example if there is a loading history, which is split into one constant load and two cyclic loads, apply the load range of each cycle successively to the model.
- For each location of the element subtract one half of the von-Mises stress from the current yield stress and the difference is current yield stress of the element.
- Repeat the same procedure for the second cyclic load range.
- Using the current distribution of the yield stress perform a limit analysis. The limit load is lower bound to the shakedown load.

What we actually achieve by this procedure is that, we are physically cutting out the zones of reverse plasticity. Now if the remaining part of the structure is able to support the constant loads, then shakedown will be achieved. The constant load takes the structure to the ratchet boundary. One of the advantages of this method is that it is applicable to a wide range of cyclic reversed loading. A corresponding incremental analysis would be extremely difficult in situations with multiple cyclic loads. But the method is likely to be overly conservative in such situations because it fails to account for all possible interactions of the cyclic load histories, but might still yield a acceptable lower bound estimate of the ratcheting load. For example in multi axial situations when primary and the secondary loads interact i.e the primary load contributes to bending (secondary actions) treating them as if they don't interact will lead to conservative answers. Another possible shortcoming is problem of incorporating cyclic hardening.

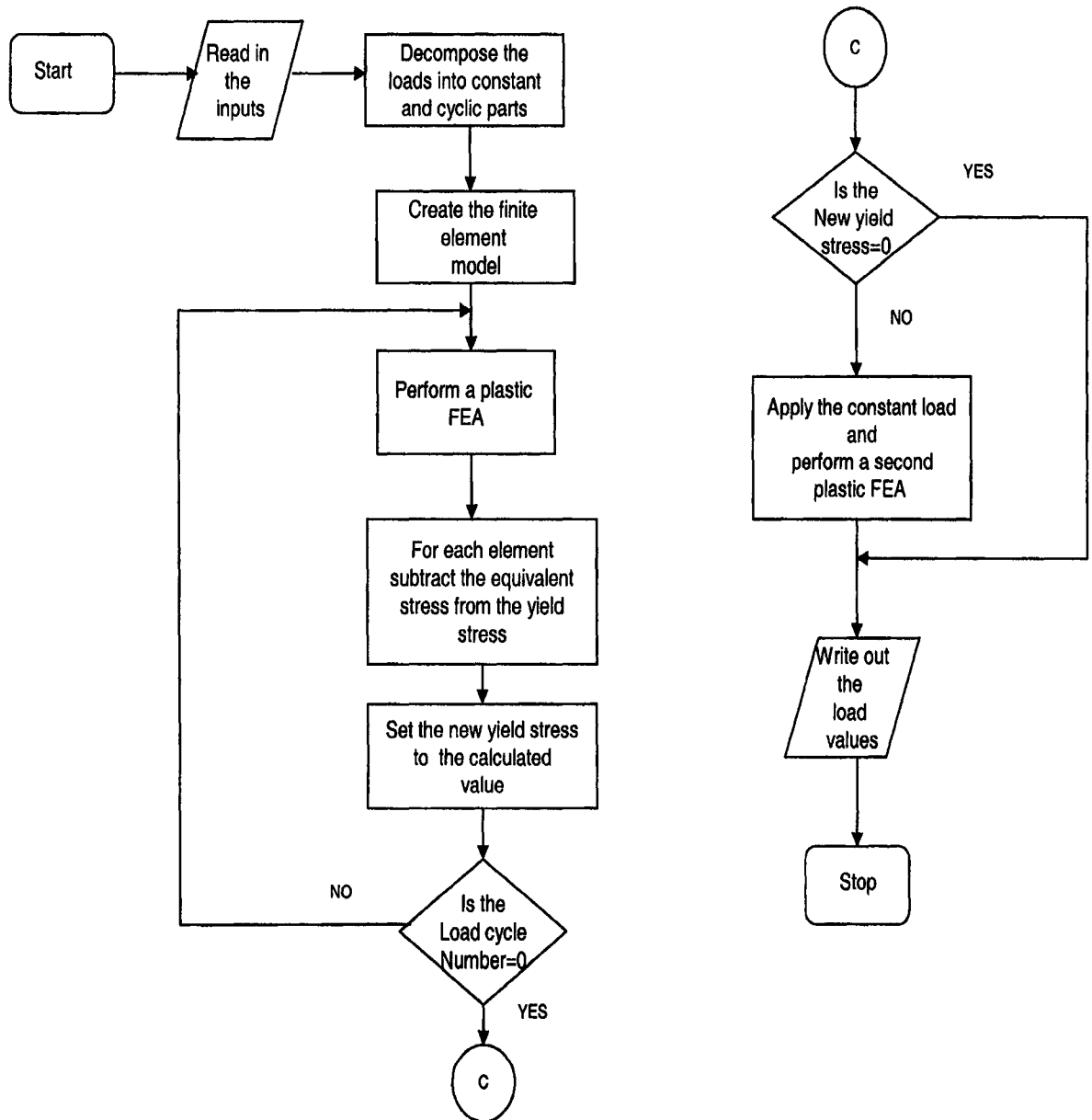


Figure 3.1. Flow chart for the Non-cyclic method

3.2.1 Bree Problem by the Non-Cyclic Method

The problem is simplified as a beam in a state of plane stress subjected to a cyclic variation of temperature through the thickness and a constant axial load. As described in the previous section, the loading is decomposed into a cyclic load (secondary) due to temperature and a constant load (primary) due to pressure. The cyclic load gives a linear distribution of stresses and causes the stress in the extreme fibers to fluctuate between σ_{br} and $-\sigma_{br}$.

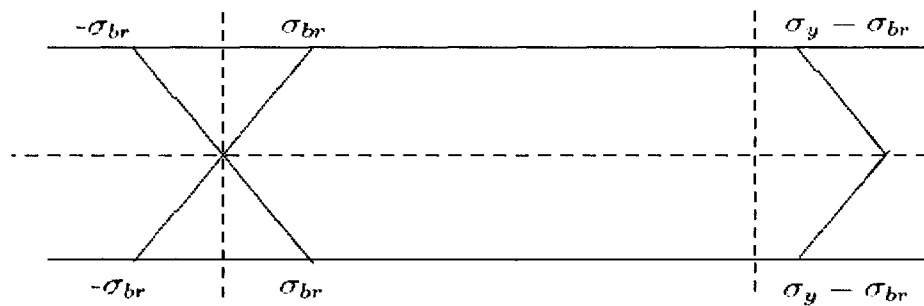


Figure 3.2. Schematic diagram of the beam problem

Half the calculated von-Mises stress range is subtracted from the yield stress. Now there are two possibilities.

If the cyclic load range causes the fibers to reach a value less than yield, the axial stress at collapse can be written as

$$\sigma_{ac} = \frac{(\sigma_y - \frac{\sigma_{br}}{2})h + \frac{\sigma_{br}h}{4}}{h} = \sigma_y - \frac{\sigma_{br}}{4} \quad (3.7)$$

In the case when the outer fibers reach yield, the axial stress at collapse stress

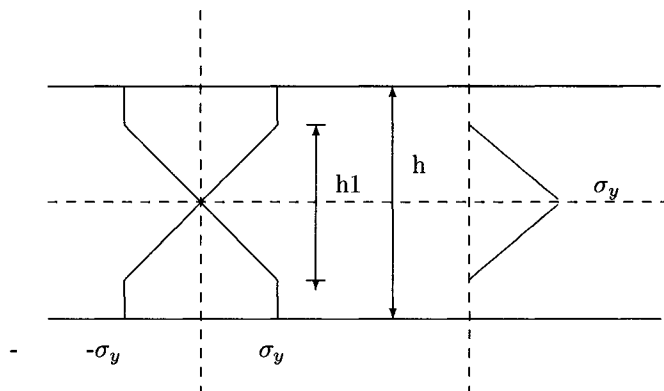


Figure 3.3. Schematic diagram of the beam problem

becomes (using similar triangles see fig 3.3)

$$\sigma_{ac} = \frac{\sigma_y h_1}{2h} = \frac{\sigma_y^2}{\sigma_{br}} \quad (3.8)$$

This result matches exactly with that obtained by Bree [4]. The Bree problem is a special case of symmetric cyclic loading. For this loading history, both elastic and plastic stresses cycle symmetrically with respect to time. Therefore, the stress evolution is periodic over time and the stress in the beam after a period of $\Delta(t_0)$ is given by equation 3.9.

$$\sigma'_{ij}(t_0 + \Delta(t_0)) = -\sigma'_{ij}(t_0) \quad (3.9)$$

What this equation means is that at every part of the structure the combined stress at a time t_0 is reversed after a period of Δt_0 . This equation has to be true for (3.6) to hold. The bending stress fluctuates between σ_b and $-\sigma_b$ and the maximum and the minimum elastic stresses are equal. That is

$$\sigma_{ij}^e = -\sigma_{ij}^e \quad (3.10)$$

and the actual stress history at any point of time in the cycle can be replaced by that happening at a half cycle preceding or succeeding it. That is,

$$\sigma_{ij}(t_0) = -\sigma_{ij}(t_0 + \Delta t_0/2) = -\sigma_{ij}(t_0 - \Delta t_0/2) \quad (3.11)$$

If this transformation holds true for the entire stress history at every point in the structure then we can conclude that ratcheting will not occur.

3.2.1.1 Results from Finite Element Analysis

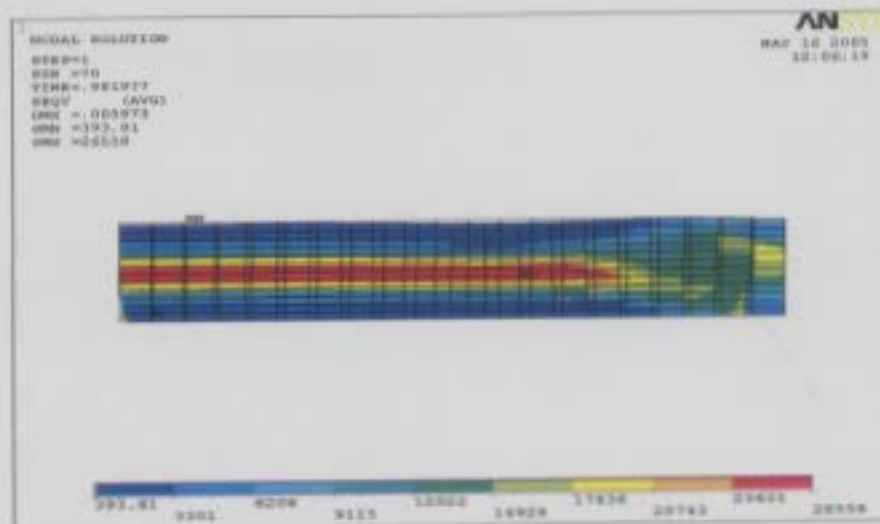


Figure 3.4. Post processor plot showing equivalent stress

The red zone is the elastic core, the blue zone at the top and bottom is where maximum bending stresses occur and these are the zones of reverse plasticity. The primary load is carried by the elastic-core (Fig.3.4) at the state of collapse. From

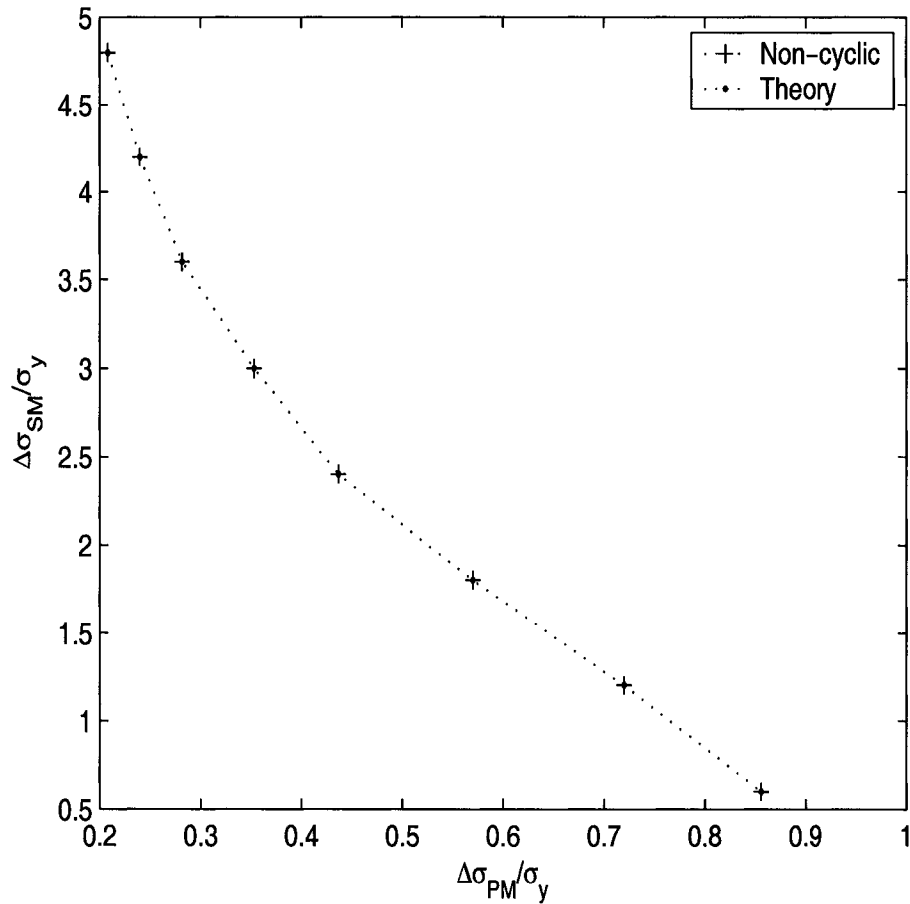


Figure 3.5. The Bree diagram by Non-cyclic method and comparison with theory

Fig.3.5) we can observe that Bree diagram is exactly recovered by the non-cyclic method. The finite element results are in exact agreement with theory. This analysis confirms the results obtained by Reinhardt[22].

3.3 The Elastic-Core Concept

Kalnins [10] has proposed a method for establishing shakedown. The idea behind this method is that if a part of the structure is always elastic under the action of cyclic loads, then ratcheting will not occur (See figure 3.6). Plastic FEA is carried out over one load cycle and the equivalent plastic strain is plotted across the thickness. The presence of a elastic core indicates shakedown, and its absence may indicate ratcheting. The key question that has to be examined here is whether

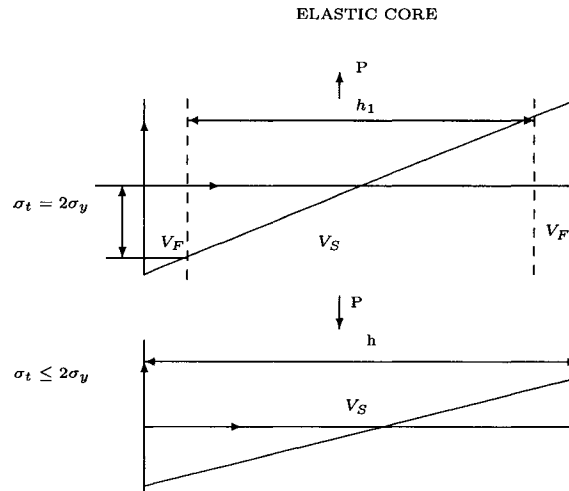


Figure 3.6. Elastic Core

the presence of an elastic core will always lead to shakedown? A counter example of system in which through thickness yielding occurs at shakedown is given in [21]. For situations where a region of material cycling plastically is surrounded by a large region that cycles elastically, it is easy to see that ratcheting will not occur because the strain growth in the plastic zone is limited by the surrounding elastic zone. On the other hand when we have an elastic-core, and the plastic-zone is *not* surrounded by a elastic region, it is not easy to visualize how ratcheting is

prevented by the elastic core. Ponter [19] has given a proof equivalence between this method and his minimum theorem for determining the ratcheting boundary. In multiaxial loading situations the transient phase may extend for large number of cycles before it stabilizes. In such situations check by Elastic-Core method appears to be a easier option.

3.3.1 Analogy Between the Elastic Core and the Non-Cyclic Methods

From the discussions in the previous sections there appears to be a direct relationship between the Non-cyclic and the elastic core methods. The analogy is that the elastic core is required to support the primary load after the regions of reverse plasticity caused by secondary loads are cut out. This is obvious because regions cycling plastically cannot carry more load. It is also interesting to note that its is the *constant primary load that causes ratcheting*. The advantage of the elastic core method is that the check for ratcheting can be made by just looking at the post processor plot without actually having to calculate the strain increments. For this reason it's very attractive from a designer's perspective as it does away with lengthy numerical computations.

Multi Bar Models

4.1 Two-Bar Problem

The two-bar problem is one of the problems that has been studied extensively. The aim here is to describe as precisely as possible the effect of variable repeated thermal loading of elastic plastic structures. In order to introduce the necessary notions and ideas that are involved it is best to start with bar systems. The two bar system illustrates the ability of the system to redistribute stresses caused by external loadings generating and superimposing certain *self equilibrating* stress fields that are usually termed as *residual* or internal stresses. The geometry and the thermal loading history of the structure is shown in the figure 4.1. Both the bars are coupled to undergo the same displacements. One bar is twice as thick

as the other bar and the thin bar is subjected to thermal cycling. The basic

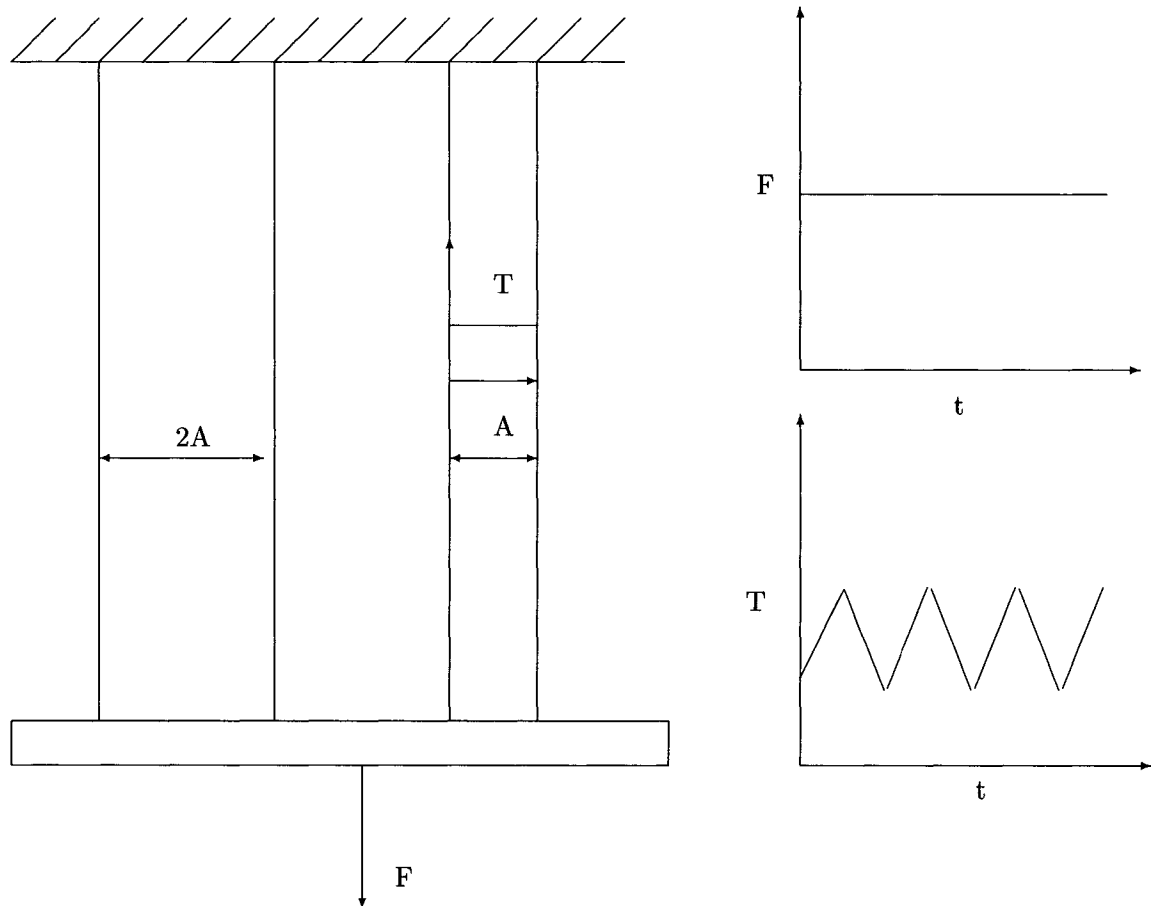


Figure 4.1. Schematic diagram of the two bar problem

structural response of the two bar system when subjected to thermal cycling is shrinking and expanding. This structure can be compared to a structure in which the bulk of the material operates in the elastic range while the small portions of the structures cycles plastically.

4.2 A Simple Analysis of the Two-Bar Model

The problem is to find the thermal and residual stresses in the bars during a heating-cooling cycle. The bars are attached to two fixed plates of which one is fixed and the other may translate but not rotate. In the discussion that follows the subscript 1 denotes the thin bar and subscript 2 denotes the thick bar. Since both the bars are of the same material, the Young's modulus and the co-efficient of expansion are the same for both the bars. When the thin bar is heated by a temperature T , the deformation and thermal stresses in the bars are

$$d_1 = \alpha Tl + \frac{\sigma_1}{E}l \quad (4.1)$$

$$d_2 = \frac{\sigma_2}{E}l \quad (4.2)$$

Since the final length of both bars after heating is the same, the following equality holds.

$$\alpha Tl + \frac{\sigma_1}{E}l = \frac{\sigma_2}{E}l \quad (4.3)$$

Equation of equilibrium of forces is

$$\sigma_1 A + \sigma_2 2A = F \quad (4.4)$$

Re-arranging this equation we get

$$\sigma_1 = \frac{F - \sigma_2 2A}{A} \quad (4.5)$$

Substituting in Eq.4.3, we get

$$\sigma_1 = \frac{F - 2A\alpha ET}{3A} \quad (4.6)$$

$$\sigma_2 = \frac{F + \alpha ET}{3A} \quad (4.7)$$

Depending upon the values of F , α and T , the thermal stress σ_1 is positive and thermal stress is tensile while σ_2 is negative that is the stress in the thick bar is compressive. During heating-cooling cycle one bar undergoes tensile stress while the other undergoes a compressive stress.

The corresponding deformations is given by

$$d_1 = d_2 = \frac{(F + A\alpha ET)l}{3AE} \quad (4.8)$$

When T is positive i.e during heating the deformations d_1 and d_2 is positive and the bars elongate. It is interesting to note that a two-bar system with a positive T that is during heating undergoes elongation irrespective of the state of stress in the bars. For instance the thick bar may have compressive stress and still elongate!. From this discussion we can make a general conclusion for thermal stress problems. The fact that the bars elongate does not produce a sufficient basis to conclude which bar is under tension and which bar is under compression.

By subtracting the free thermal expansion from the final deformation the following expressions result for the thick bar and the thin bar respectively,

$$d_1 - \alpha ET = \frac{\sigma_1 l}{E} \quad (4.9)$$

$$d_2 = \frac{\sigma_2 l}{E} \quad (4.10)$$

The deformation minus the free thermal expansion is proportional to the thermal stresses in the bars. If this quantity is positive, the bar is under tension and vice-versa. As already mentioned one of the bars is in tension while the other is in compression. A complete tracking of the stresses and the resulting deformations during loading-unloading-reloading sequence can be done graphically¹.

4.3 Finite Element Analysis And Discussion

When the thin bar cycles plastically (it can carry no load) the resulting load is equilibrated by a like section of the thick bar, and the primary load is safely carried. As long as the thick bar does not yield the primary load is safely carried and the deformation of the system is limited by the deformation of the thick bar. Finite elements results confirm this observation. If the bars are made of isotropically hardening materials then on unloading a much stiffer response occurs as the load state is now entirely within the yield surface. This increases the force on the thick bar and may cause it to yield. Although the system reaches an elastic state finally due to an expanding yield surface, the amount of deformation during the transient would be much higher than the isotropic case due to yielding of the thick bar. Finite element results verify this conclusion. The displacement during the transient phase is twice the displacement in the bars, if they were made of elastic perfectly plastic material. This is important while assessing adaptation in the transient phase, because in this case the assumption of an elastic-perfectly plastic model will lead to nonconservative estimates of the shakedown load. The effect of

¹Refer to Limit analysis of structures at thermal cycling, by Gokhfeld and Cherniavsky, 1980

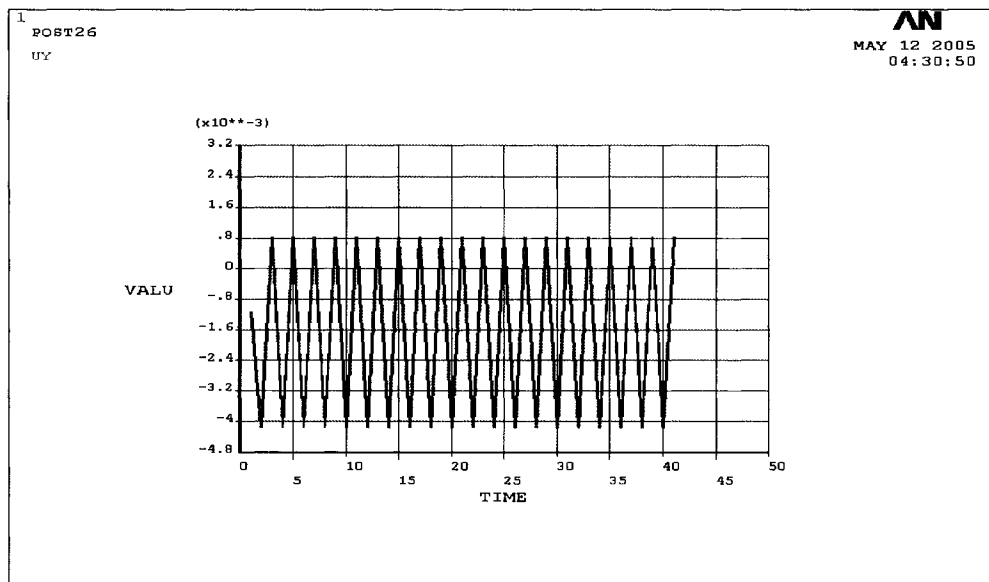


Figure 4.2. Displacement vs number of cycles

hardening is important while evaluating the response of the system in the transient phase during thermal cycling. The assumption of bi-isotropic hardening material with a high tangent modulus will significantly overestimate the value of displacements during the *transient phase*. The assumption of the model being perfectly elastic-perfectly plastic will lead to conservative estimates of the deformation if the system were to harden. Therefore in conclusion, we have to choose the material

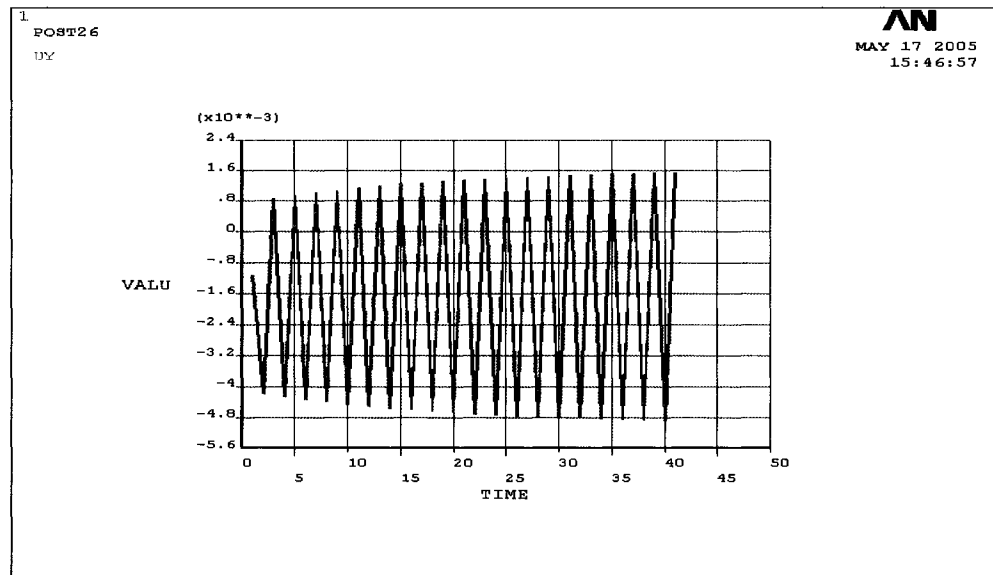


Figure 4.3. Displacement vs number of cycles

model cleverly so that real material behavior is captured. If experimental data is available then it can serve as a guideline in choosing the proper material model.

4.4 Effect of Hardening

A single surface plasticity model would model a test where increasing cycles of stress are applied to the structure. When a force is applied to the structure, whose

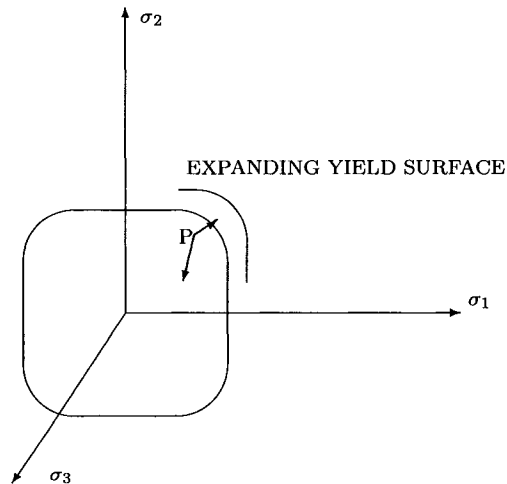


Figure 4.4. Single surface plasticity model

state of loading is on the yield surface, the yield surface expands as plasticity occurs. On unloading the load state is within the yield surface. On reloading, a stiffer response occurs (a effect similar to strain hardening), plasticity occurs only if the load state again reaches the yield surface. This clearly does not represent true material response to cyclic loads because during cyclic loading both plastic hardening and softening (For example Bauschinger effect) have been observed experimentally. So an extension of classical theory of plasticity should incorporate both effects. This is done by including multiple yield surfaces to represent cyclic plasticity. Each surface should have a plastic potential (to calculate plastic strains) and to describe the direction of plastic flow, and they should satisfy the convexity and normality concepts. This type of theory has been developed for constitutive modeling of materials, after extensive experimental investigations (see for exam-

ple Lemaitre, 1999). The rules of constitutive material models developed through

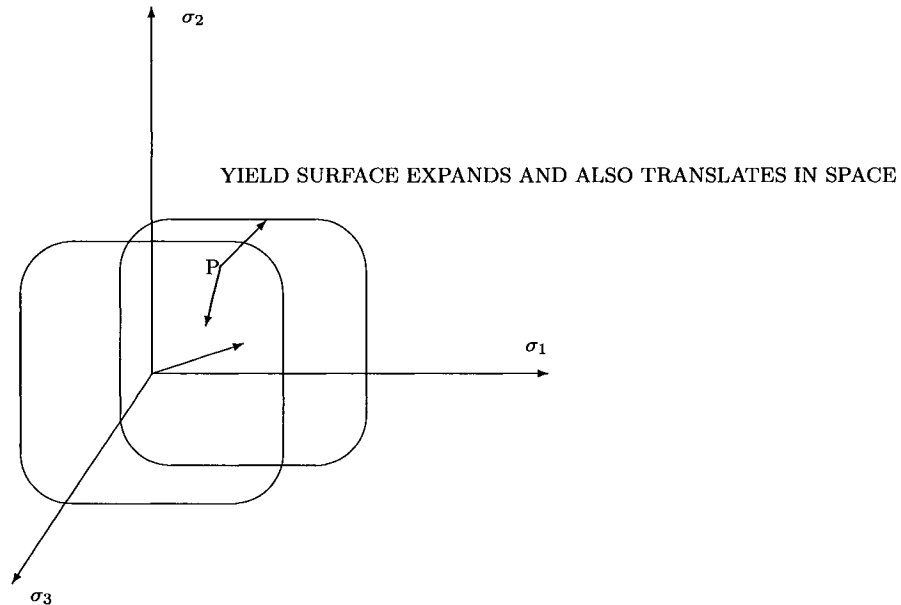


Figure 4.5. Multi-surface plasticity model

experiments are empirical and the equations have a number of constants. Therefore a number of parameters must be specified for each yield surface. For accurate modeling of material behavior this can lead eventually to a rather unwieldy theory. A theory of plasticity based on thermodynamic principles has been developed by Lemaitre and Chaboche (1991). Readers interested in a complete description of theory can refer [8]. In the phenomenological description of plasticity, the plastic strain field has a number of components each associated with a corresponding yield surface. The effective yield surface is obtained by superposing the constituent yield surfaces. The mathematical description involves formulating a potential for plastic flow consisting of two potentials. The first potential is the free energy of the system and the second potential is the dissipation function. For the case of the infinite field of plastic strains these potentials are functionals of the plastic strain and its

rate. One of the advantages of the functional representation is that it generalizes the classical theory of plasticity for rate independent materials. This theory can be used to describe rate dependent effects such as viscoplasticity, and inelastic effects like creep. The parameters corresponding to such effects are simply added to the functional. For instance Zarka's back stress can be included as a vector expression in the potential function. The numerical algorithms to calculate the plastic strains based on this theory has been implemented in most commercial FEA packages. Conventional plasticity theory is a special case of the new approach. The result is that theories can be constructed in which response of the material to different loading combinations can be modeled accurately and with computational efficiency.

4.5 Three-Bar Problem

The three bar problem is representative of strain accumulation due to pure thermal cycling. This phenomenon is frequently encountered in industries with high temperature working environments. Strain accumulation in the absence of mechanical loads can be observed in gas turbine engines in combustion chambers and fuselages, aircraft brakes etc. The schematic diagram of three bar system is shown below. The end displacement of the bars is coupled. The bars are heated one by one to a temperature T . The heating cooling cycle is such that when one particular bar reaches a temperature of t , the other bars cool down to their initial temperatures so that only one bar is hot at any particular instance of time.

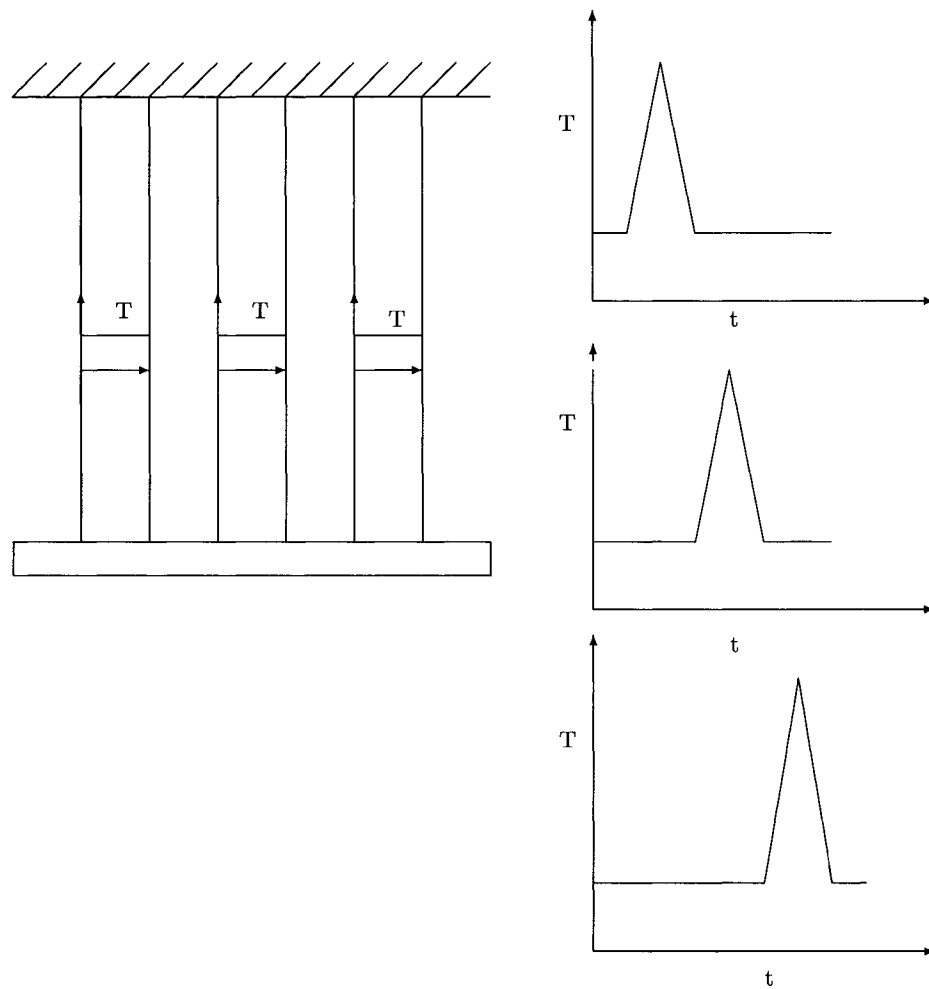


Figure 4.6. Schematic diagram of the three bar problem

4.6 Analytical Solution for the Three-Bar Problem

The setup of the three bar model resembles the two-bar model. All three bars are attached to a fixed plate on end and a plate that can move but not rotate on the other end. The subscripts 1, 2 and 3 refers to the bars in the Fig.4.6 in that order. All three bars are identical, therefore the material properties and the

cross-sectional areas are the same for all three bars. When bar 1 is heated by a temperature T , it elongates. Since the end displacement of all three bars are coupled, they elongate by the same amount. Therefore we have

$$\alpha Tl + \frac{\sigma_1}{E}l = \frac{\sigma_2}{E}l = \frac{\sigma_3}{E}l = K(\text{say}) \quad (4.11)$$

rearranging this equation we get

$$\sigma_2 = \sigma_3 = \frac{KE}{l} \quad (4.12)$$

$$\sigma_1 = \frac{E}{l}(K - \alpha Tl) \quad (4.13)$$

Since there is no external force on the system, equilibrium implies

$$\sigma_1 A + \sigma_2 A + \sigma_3 A = 0 \quad (4.14)$$

Substituting Eq.4.13 into Eq.4.14 we get,

$$\frac{E}{l}(K - \alpha Tl) + \frac{2KE}{l} = 0 \quad (4.15)$$

Solving for K we get

$$K = \frac{\alpha Tl}{3} \quad (4.16)$$

Substituting the value of K into equation 4.11 and solving for σ_1 we get,

$$\sigma_1 = \alpha ET \frac{2}{3} \quad (4.17)$$

This is the expression for the thermoelastic stress in bar 1 after the heating cycle. According to upper bound theorem the sufficient condition for strain accumulation

is that thermo-elastic stress should be less than the yield stress. If it exceeds yield then ratcheting will take place. By equating this stress to the yield stress we can calculate the maximum temperature of the limiting cycle as

$$T_0 = \frac{3\sigma_y}{2E\alpha} \quad (4.18)$$

It is interesting to see what will happen when this temperature is exceeded. Let us assume that the bar 1 is heated to a temperature $T_1 > T_0$. During heating the contraction of bar1 is given by

$$d_1 = -\alpha Tl + \frac{3\sigma_y l}{2E} \quad (4.19)$$

The other bars will be stretched by similar amounts. During cooling bar 1 will be stretched with the stress,

$$\sigma^0 = -\sigma_y + \frac{2E\alpha T_1}{3} \quad (4.20)$$

and the remaining bars will undergo a compression. During the next heating cycle the second bar will start yielding at a lower temperature since it is already in state of compressive stress. So the system of residual compressive stresses set up in bars in this example is clearly unfavorable. Two important conclusions can be drawn from this discussion.

- Although thermal stresses are self-equilibrating, they are clearly not *self-limiting* as per the definitions of ASME code. Ratcheting happens due to pure secondary cyclic load.
- The calculated thermo-elastic stress range is $1.5\sigma_y$. Code limit of $3S_m$ or $2\sigma_y$ is clearly nonconservative in this case.

The finite element analysis confirms these observations.

4.7 Finite Element Analysis and Discussion

During the heating-cooling cycle different elements reach yield at different times. This is in stark contrast with total collapse where all the elements reach yield at the same time (figure 4.7). As each bar is heated in succession the bar elongates

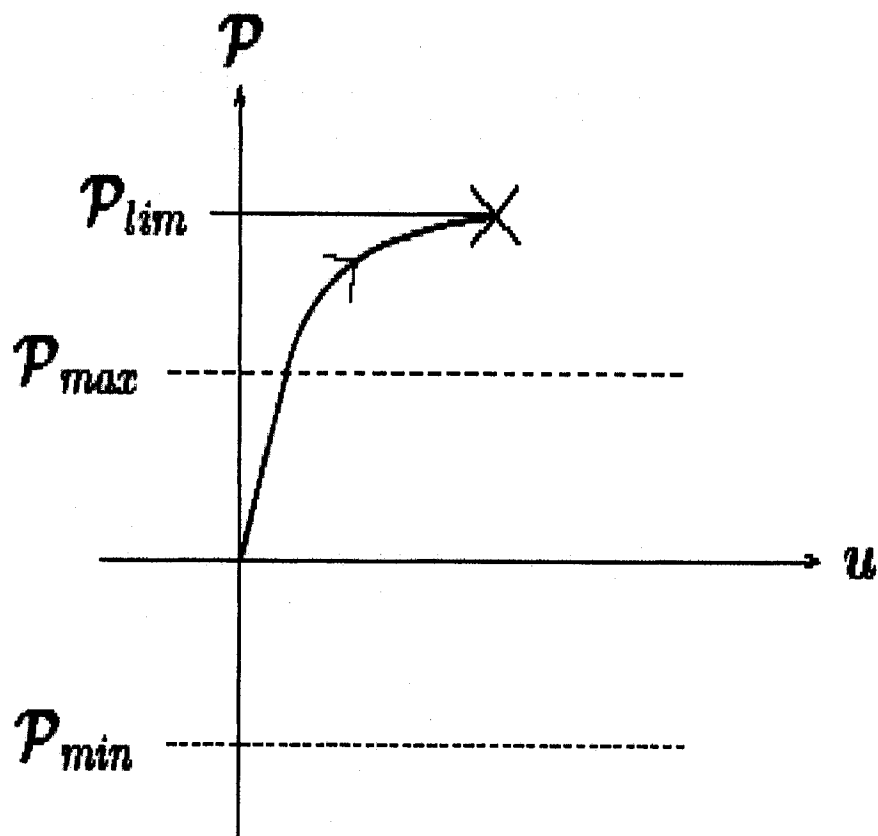


Figure 4.7. Load displacement diagram at total collapse

while the other two bars contract. This means that a rise in temperature in one part of the system produces stresses in other parts and changes the overall stress

distribution in the system. Ratcheting begins as soon as the compressive stress in one bar reaches yield. This example is important because in this case the ASME $3S_m$ rule is nonconservative. The same pattern of residual stresses repeat in the bars during heating cooling cycle. In this case the system of stresses built up is extremely unfavorable. According to the lower bound shakedown theorem, superposition of self equilibrating stresses does not affect the load carrying capacity of the structure.

The success of shakedown concept depends on a system of beneficial self equilibrating stresses induced by plastic deformation. But in this case the stresses induced by constraints are not self equilibrating.

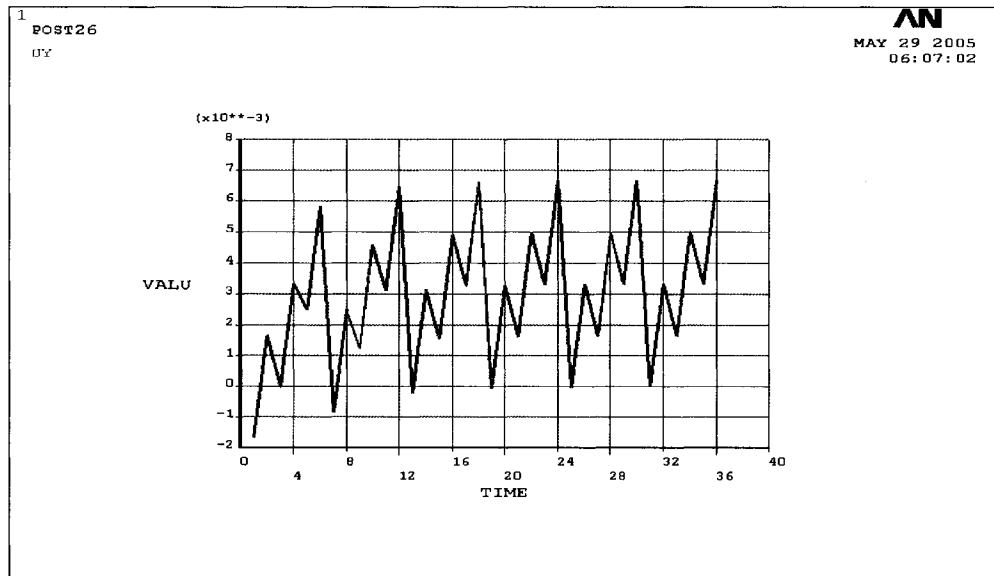


Figure 4.8. Axial displacement vs load cycle number at shakedown

4.7.1 Response at 12% Above Shakedown Temperature T_0

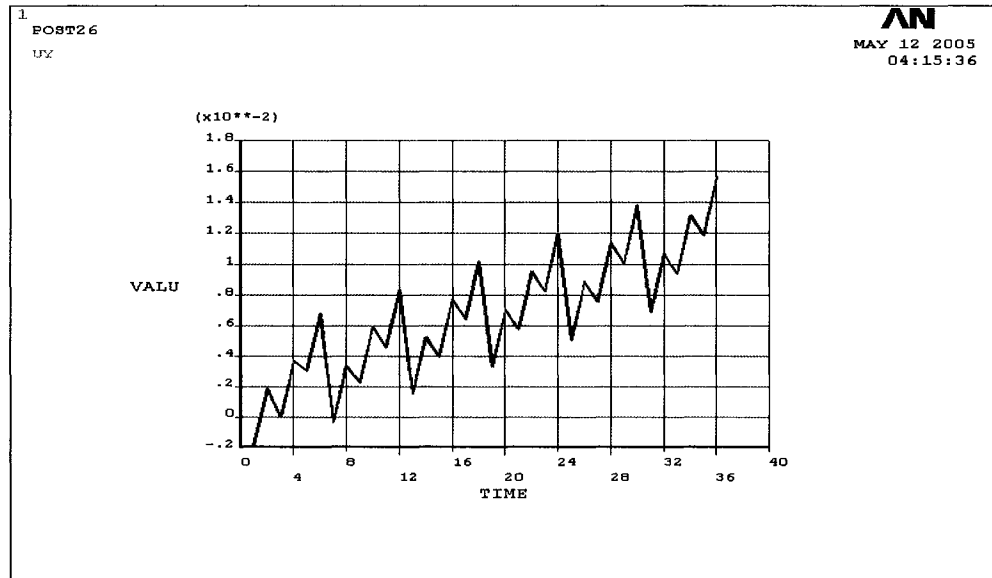


Figure 4.9. Axial displacement versus load cycle number 12% percent above shakedown temperature

This (Fig.4.9) is the displacement profile when the temperature is increased marginally (by 12%) above the temperature for which shakedown occurs. In this case the compressive residual stress pattern in the system exceeds $1.5 \sigma_y$ and this causes ratchetting. This verifies the analytical predictions.

4.7.2 Response at 125% Above Shakedown Temperature

T_0

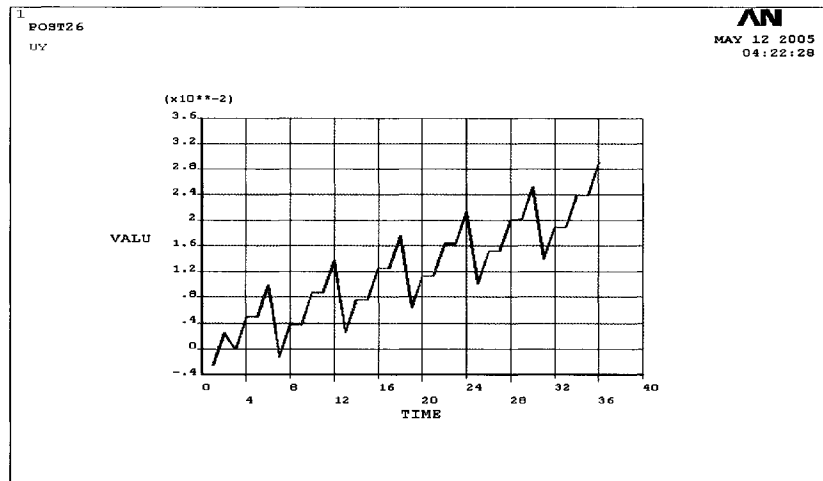


Figure 4.10. Axial displacement vs load cycle number at 125% shakedown temperature

The same effect is more pronounced by cycling the system at a higher temperature. The corresponding displacement at the end of each cycle is higher than the previous case. Prolonged cycling at this temperature would lead to rapid accumulation of displacements and failure due to ratchetting.

Bree Problem by Plastic FEA

5.1 Introduction

Thermal and stress fields encountered in the pressure vessel industry will be exceedingly complex. Thermal fields in vessels arise from volumetric heating rates with complex temporal and spatial variations due to processes in the vessel. Similarly stress fields arise from material non-linearities and temperature dependent material properties. However analytical models of simplified systems can still be used for testing numerical models ultimately used for design. In this section we present analytical models of several cases relevant to pressure vessels starting from the simple plane stress model followed by numerical results and then we move on to certain slightly complicated situations. The general problem consists of a struc-

tural component which is subjected to two separate loading systems. A constant load, which may be pressure loading or a localized loading given by λP where λ is scalar loading parameter. In addition, the structure is subjected to a cyclic temperature $\mu(x, t)$, where μ is a second scalar parameter and T is a distribution of temperature that varies in space and time. The behavior of such a system is quite complex but we can summarize the behavior of the structure in the form of a general Bree diagram shown below 5.1. For ease of interpretation the scalars λ and μ are not used as axes but two equivalent non-dimensional quantities $\frac{p}{p_i}$ where p_i is the limit load parameter of yield stress σ_y at some reference temperature T_r . The basic idea is to extend the thermal loads in excess of yield stress and the possibility of occurrence of plastic shakedown under the influence of high thermal loads and low mechanical ones is to be emphasized.

5.2 Interaction Diagrams

The interaction diagram has three separate regions, E, P and R.

- For load intensities in the region E plastic flow occurs during the initial few cycles, but ceases to develop further and the structure responds elastically. This is the classical definition of shakedown. This also implies that the total accumulated dissipation is bounded.
- For load intensities in the region P, the strain increments change sign in every cycle and they cancel each other. The total deformation remains small. This is called alternating plasticity or elastic shakedown. After a number of cycles the structure will fail by low cycle fatigue.
- In the region R the plastic sign in each load cycle are of the same sign. After

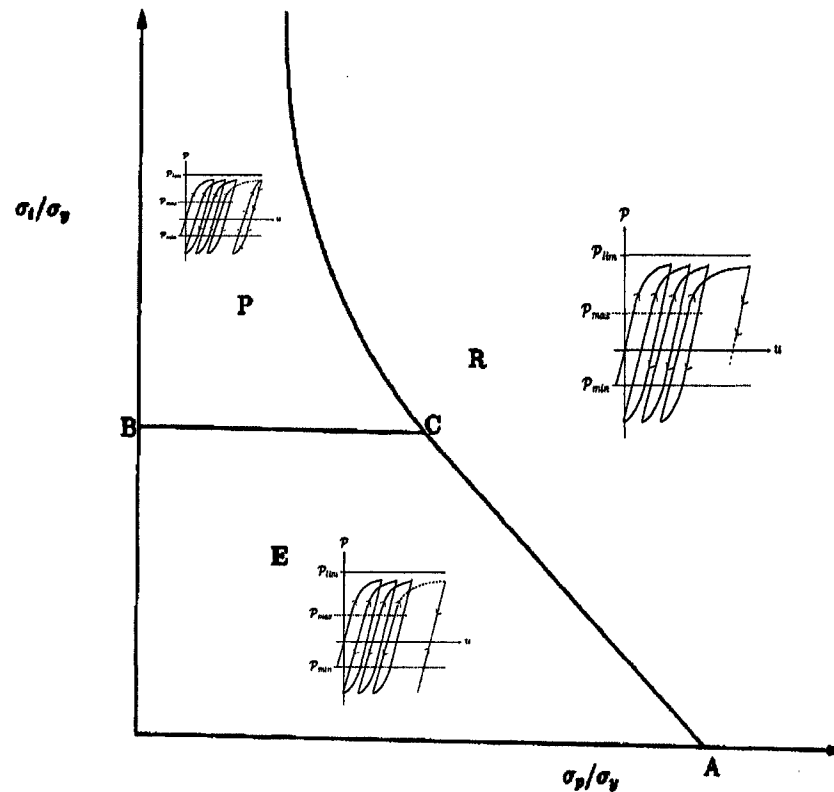


Figure 5.1. Interaction diagram for the Bree problem

a sufficient number of cycles the total accumulated displacements become so large that the body loses its fitness for service. This phenomenon is called *incremental collapse* or *Ratcheting*.

The ratchet boundary asymptotes to the $\frac{\sigma_y}{\sigma_t}$ boundary as σ_p reduces to zero. This means that for low values of σ_p a large value of σ_i can be tolerated before ratcheting occurs. The rate at which ratcheting will occur for a load points in excess of line BC in 5.1 depends on the details of the material behavior. It can be seen that Bree diagram for just one load will be a point in either the x axis or y axis. For thermo-mechanical loadings the regions of the Bree diagram show possible responses of

the structure to a combination of mechanical and thermal loads. At this point it is interesting note that for pure thermal cycling the Bree diagram reduces to a line. For a thermal and mechanical load, the Bree diagram lies on a plane. In multi-parameter loading situations, the dimension of the Bree diagram increases by one for each independent load and it will lie in a n-dimensional space.

5.3 Solution by Cyclic Incremental Analysis

The Bree problem can be solved by considering the tube as a beam in plane stress subjected to linear temperature gradients through the thickness. We can use a beam instead of a cylinder for the Bree problem since it was solved originally as a beam [4]. The only difference is with a beam model we get a linear distribution across the thickness whereas in a cylinder, it's not exactly linear. The model is constructed using plane stress elements (PLANE 82 in ANSYS). Here the curvature of the beam due to thermal expansion is restrained.

Some basic assumptions

- A linear-elastic ideal plastic material
- Mises yield criterion and associated flow rule.

Without any loss of generality we can choose the temperature to vary between zero and a maximum value. The allocation of the loading direction as “+ve” and “-ve” in figure (5.2) is purely arbitrary but indicates that the load is applied in the opposite directions. The reader is reminded here that this example and the examples that follow, the exact values of temperatures and material properties are not important. The trends are important. Different material will have different material properties and therefore different stress values. However regardless of

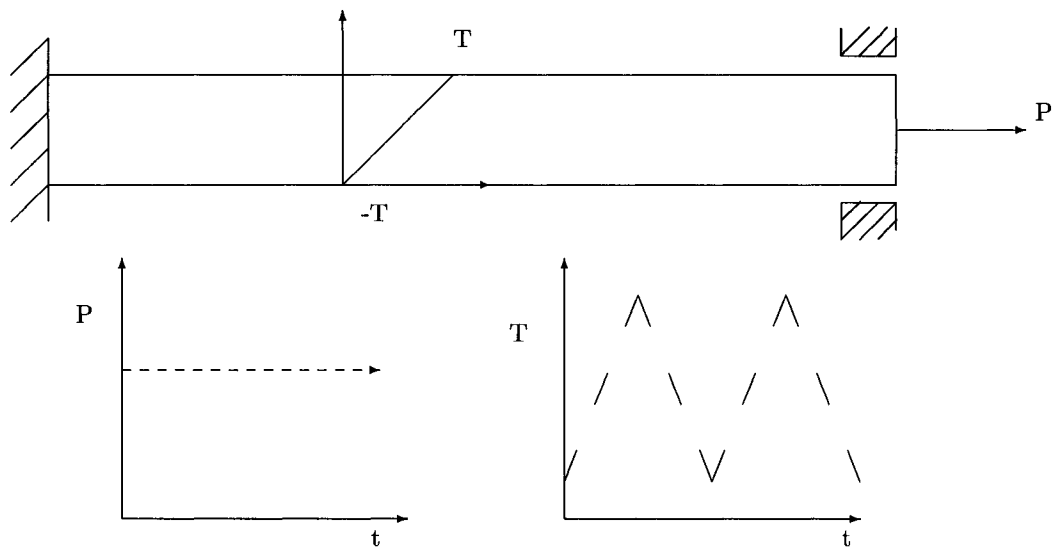


Figure 5.2. Schematic diagram of the Bree problem

the temperatures or the amount of time cycled the trends of stress development is universal. The finite elements model achieves shakedown to elastic or cyclic plastic action within a few load cycles. The results are in good agreement with theory. The cyclic analysis is iterative and incremental in nature. Using such an analysis, the deformation characteristics can be evaluated at each load increment until failure. The results of analysis showing the load values at shakedown is given in table 5.1.

5.3.1 Finite Element Results

The Bree problem converges to a steady state solution within 5 cycles. This can be seen from the deflection profile (Appendix A A.1) and the plastic strain plot (A.2) after 10 cycles. Figure (5.3) shows the interaction diagram obtained from cyclic FEA and its comparison with theory. The results from cyclic analysis are in exact agreement with the theoretical solution. The results are summarized in

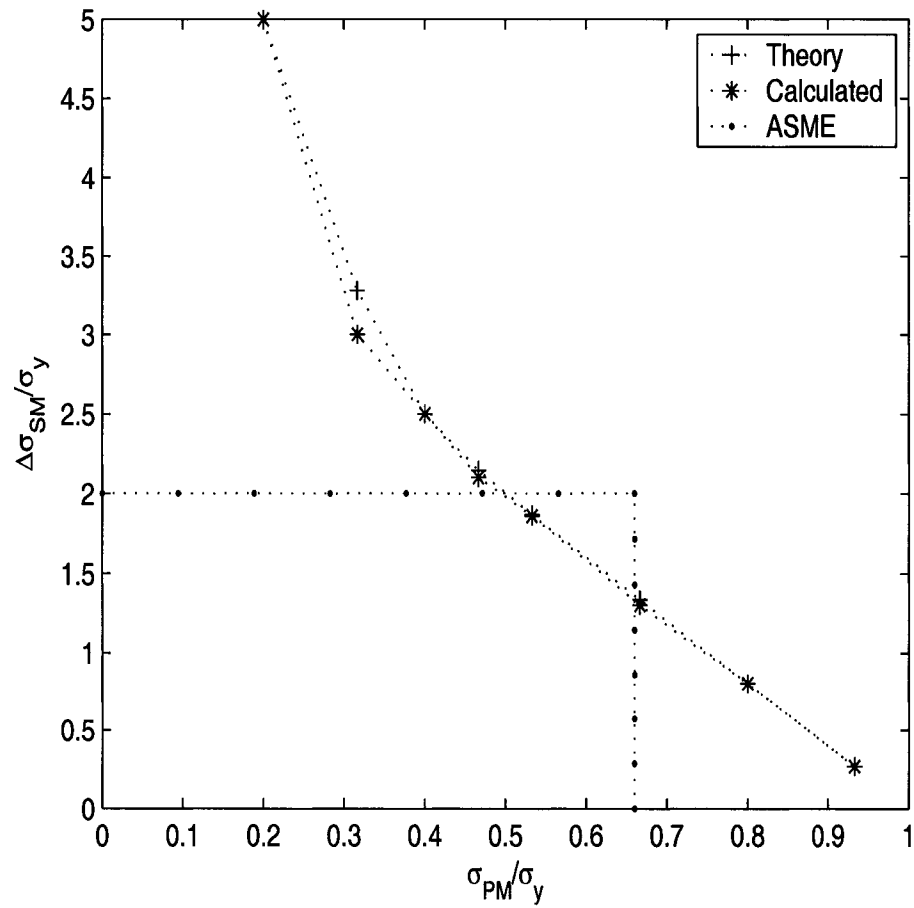


Figure 5.3. The Bree interaction diagram along with results from theory

P, lbs	Theory	Calculated
6000	5.0	5.0
9500	3.16	3.0
12000	2.5	2.5
14000	2.14	2.10
16000	1.86	1.86
20000	1.33	1.32
24000	0.80	0.80
28000	0.26	0.26

Table 5.1. Data for the Bree problem plane stress model

table 5.1. Sample calculations of the theoretical value's is shown in Appendix A.

5.3.2 Effect of Change in Material Properties

It is well known that materials harden and soften when they are subjected to load cycling. A detailed study of the various kinematically hardening models has been done by Ohno et.al [21] for a cylinder loaded by thermal front moving in axial direction. The models used in the study are

- Elastic perfectly plastic model
- Linear Kinematic hardening model
- Armstrong and Fredrick hardening model
- Ohno-Wang model

the general conclusion was the loads that caused thermal ratcheting for elastic-plastic model caused the plastic strains to diminish for other hardening rules. Extensive investigations on hardening and softening of materials when subjected to cyclic loads were carried out by Lemaitre and Chaboche [8]. The material model proposed by Chaboche based on their investigations is available in the ANSYS library. The chaboche model incorporates the effect of hardening and softening of the material with loading un-loading cycles. The idea is to compare the redistribution of stresses due to hardening with the case where hardening is absent.

The results from the finite element analysis confirm their conclusion. The effect of hardening and softening during loading-unloading also causes different distribution of residual stresses.

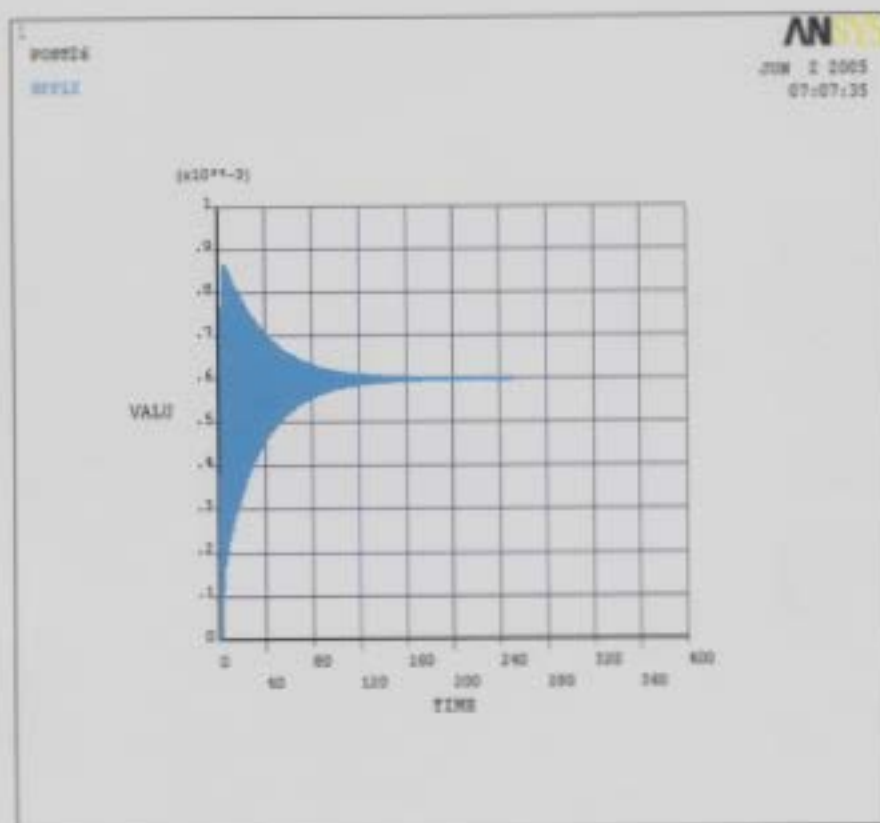


Figure 5.4. Plastic strain versus load cycle number for chaboche model

Comparing the stress plot of the elastic-perfectly plastic model (see section 3.4) with figure 5.5 we can see that the zone of reverse plasticity vanishes and plastic strain increments asymptotes to zero (See figure 5.4). It is also interesting to observe the change in the size of the elastic-core due to expansion of the yield surface with applied loading. For the same temperature range we find that the strains become zero after 250 cycles. Cyclic hardening seems to be beneficial as shakedown is eventually attained after a number of cycles of load application.

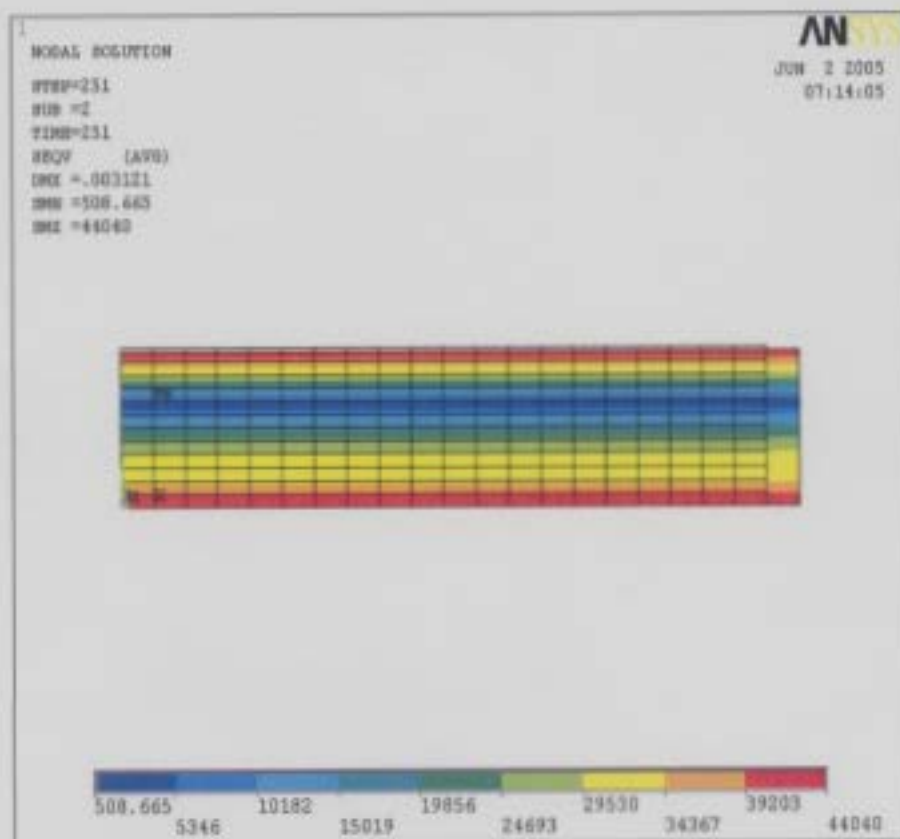


Figure 5.5. Equivalent stress plot after 250 cycles

5.4 Proportional Variation of Loads

In this section we consider a loading history where the pressure ramps up proportionally with temperature. This is situation representative of operating conditions. Proportional variation is defined as the situation where the stresses are independent of the load parameter¹. The pressure and temperature load data at shakedown is

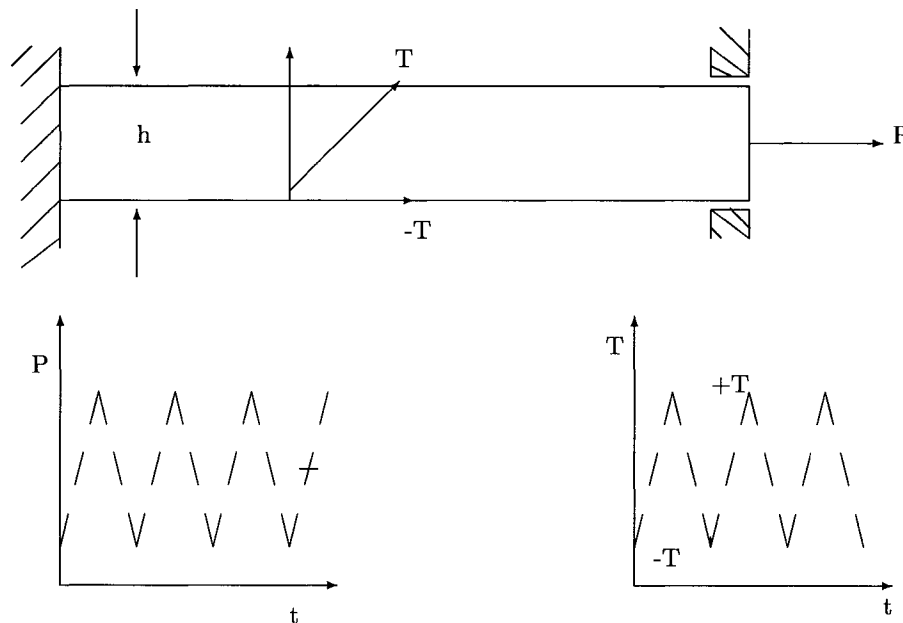


Figure 5.6. Schematic diagram showing the load variation

presented in the table 5.2. We can compare this data with the data obtained

P, lbs	6000	9500	12000	14000	16000	30000	30000	30000
T	4.8	4.2	3.6	3.0	2.4	1.8	1.2	0.6

Table 5.2. Load data at shakedown for pressure varying proportionally with temperature

with a constant pressure load (5.1). We see that the values of pressure load is

¹Mechanics of Solid Materials, Lemaitre and Chaboche, Cambridge University Press, 1991

almost doubled for the same values of thermal loads. For this case the shakedown boundary lies sufficiently above the boundary prescribed by the ASME code [1] (See figure 5.7). Another variation of the load considered is that the pressure

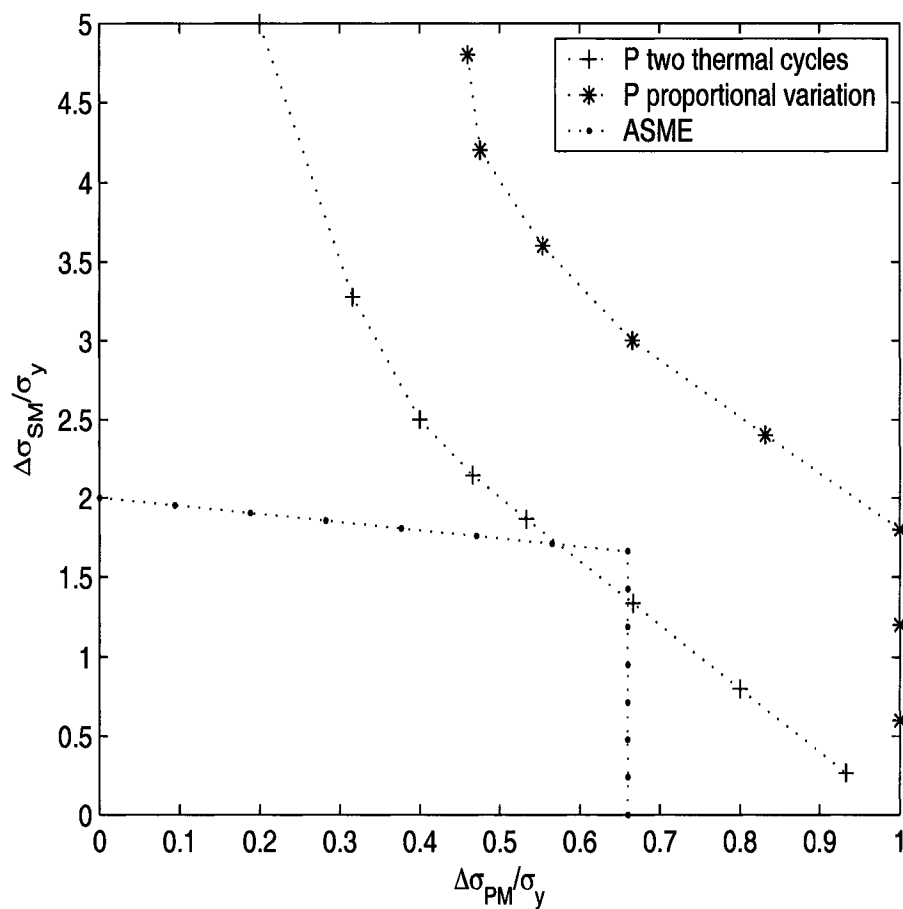


Figure 5.7. Bree diagram with different loading histories

ramps up and two thermal cycles occur for a one pressure cycle. In this case the Bree diagram is recovered exactly.

5.4.1 Alternative Loading History

A loading history in which the pressure cycling in proportion with temperature was considered in the previous section. Here we consider a history wherein we

have two temperature cycles for every pressure cycle. This situation is shown in figure 5.16. For case where we have two thermal cycles for one pressure cycle the

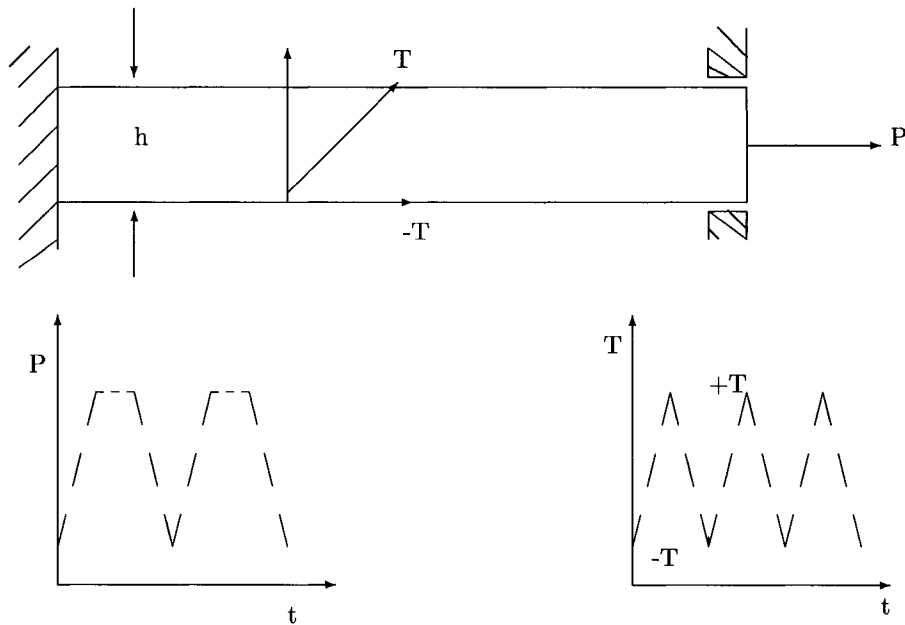


Figure 5.8. Schematic diagram of the Bree problem with two temperature cycles for one pressure cycle

original Bree diagram is recovered exactly. See figure 5.7. For this loading history the code allowable region in the diagram changes. Limiting the primary stress range to $2/3\sigma_y$ reduces the secondary stress range from $2\sigma_y$ to $2/3\sigma_y$. From the two cases considered it can be concluded that the code criterion is conservative for Bree type situations.

5.5 Interaction Diagram for a Tube

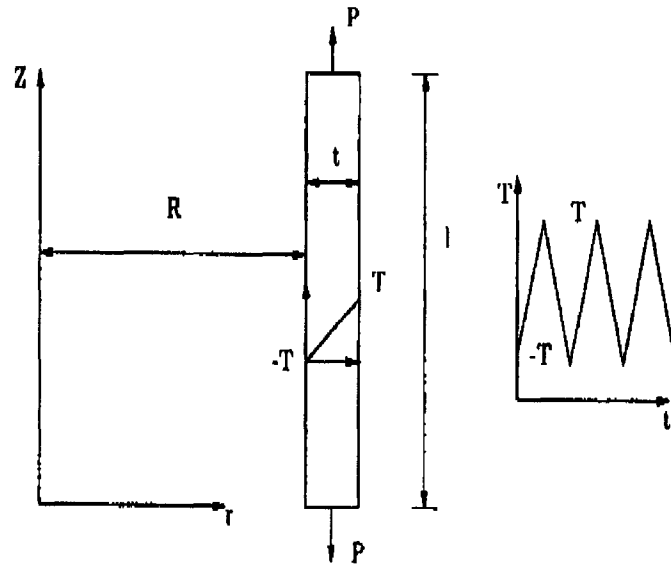


Figure 5.9. Schematic diagram of the axisymmetric tube

In this section we study the results from a triaxial-stress model for the Bree problem. Both models were subjected to same history of loading shown in figure (5.2). A axisymmetric finite element model is used to investigate the growth in plastic strain in the hoop direction of a pressurized tube. The Bree problem can viewed as a axisymmetric cylinder subjected to a axial tension and through thickness temperature cycling. The axial direction is defined as the z direction in figure (5.9). Here we are interested in observing the strain growth in the hoop direction and comparing the results with the from the plane stress condition. The Bree simplification and the simplifications connected with the Bree problem will

lead us to ignore the components σ_z, τ_{zr} and $\tau_{z\theta}$, and will lead to uniform stress distribution through the thickness. By considering the problem as a axisymmetric problem we account for these stresses. The evolution of these stresses with thermal cycling could be important because in combination with the axial stress they might initiate cracks at regions of high thermal gradient. The difference in load values at shakedown is shown in figure (5.10). From the figure (5.10) we can observe that

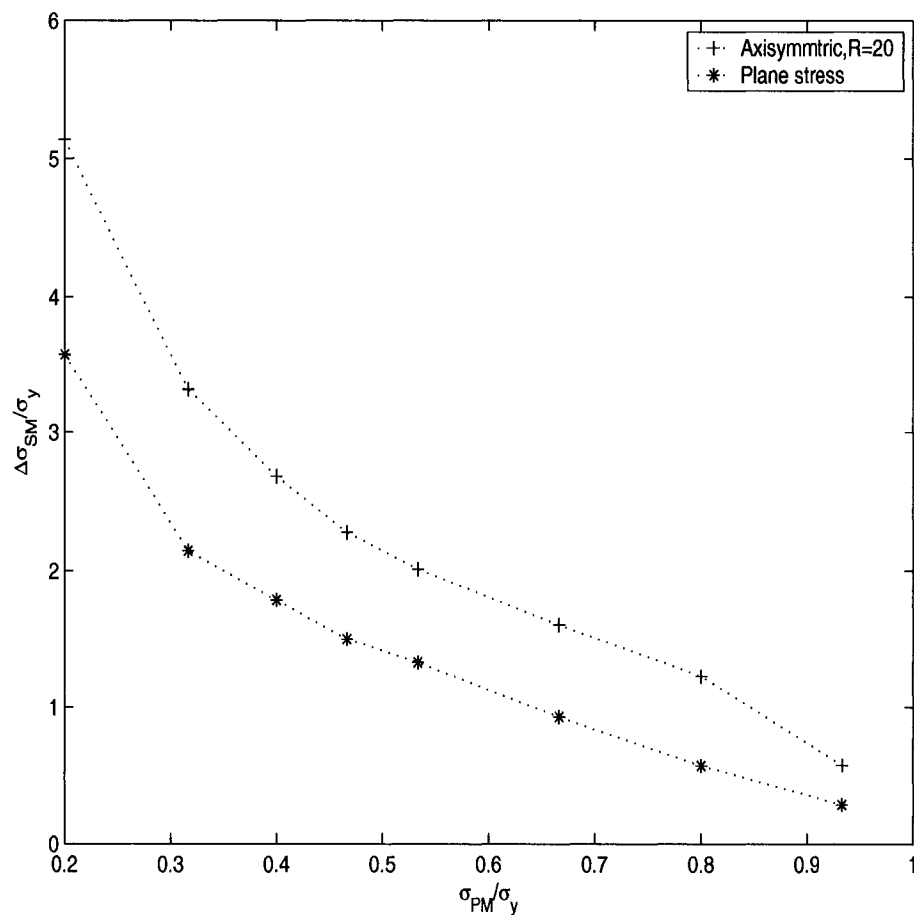


Figure 5.10. Comparison between axisymmetric tube of Radius 20 in and plane stress model

the ratchet limit increased by about 10% (value of the thermal load) for the tube in comparison with the plane stress model. The difference in assumptions in the

two cases suggests that the reverse plasticity mechanism is affected by the relative stiffness of the elements in the respective finite element models. The simplification of geometry and the assumptions associated with it also simplifies the analytical solution. The Bree simplification leads to a system of ordinary differential equations. In this case we get partial differential equations of equilibrium².

5.5.1 Parameter Sensitivity of the Ratcheting Boundary

It is interesting to study the sensitivity of the ratcheting boundary by varying the parameters of the finite element models. Tables showing the variation in the load values at shakedown with size of the tube. The shakedown boundary for the two cases is obtained after 250 cycles of finite element analysis.

P,lbs	6000	9500	12000	14000	16000	20000	24000	28000
T	3.5	2.32	1.875	1.42	1.22	1.123	0.86	0.403

Table 5.3. Load data at shakedown for the axisymmetric tube of Radius 100 in

P,lbs	6000	9500	12000	14000	16000	20000	24000	28000
T	3.58	2.30	1.874	1.59	1.40	1.12	0.87	0.40

Table 5.4. Load data at shakedown for a axisymmetric tube of Radius 20 in

Comparing the values of the temperature for the two cases, we find a small but definite decrease in the value of temperature at shakedown with an increase in the radius of the tube.

²For analytical treatment of cylinders subjected to axisymmetric loading see for example, Theory of Elasticity, by Timoshenko and Goodier

5.6 Interaction Diagram using the Non-cyclic method

In the following the results of the finite element analysis of the axisymmetric tube by the cyclic and the non-cyclic methods is discussed. In this section we generate

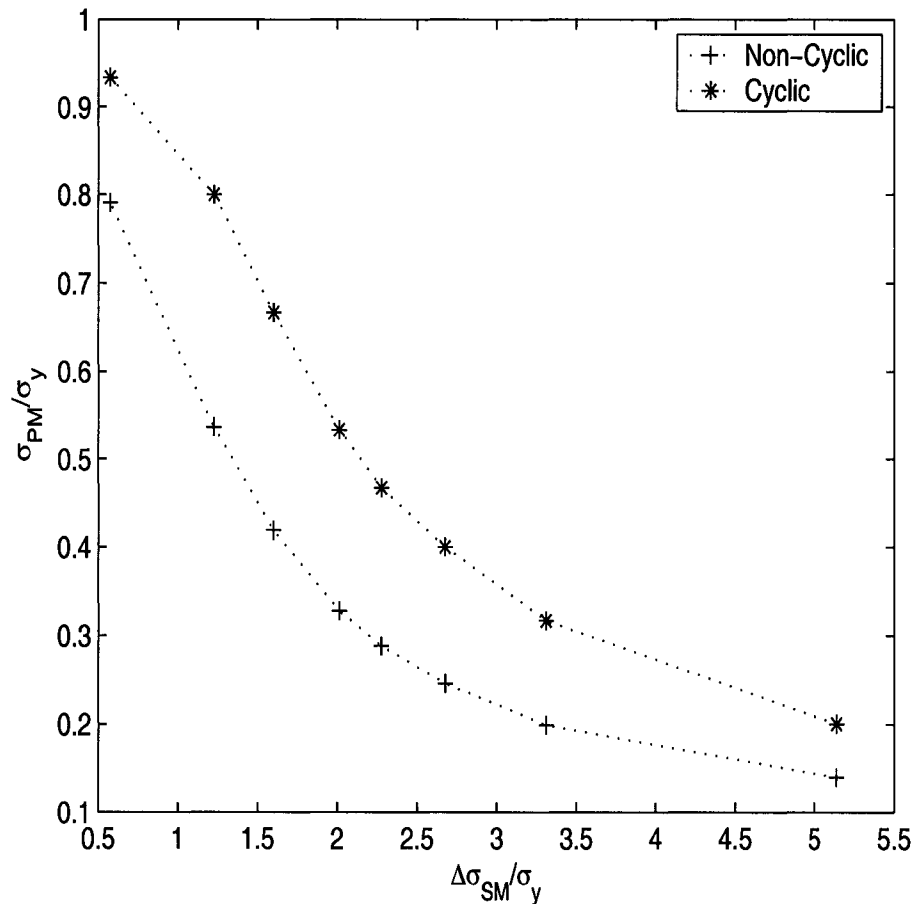


Figure 5.11. Shakedown boundary comparison by cyclic and non-cyclic methods for a tube of Radius 20 in

the interaction diagrams for the same tube using the non-cyclic method. The thermal loading is symmetric so one cycle of thermal load is applied first and a plastic FEA is carried out. The yield stress of each element at which reverse plasticity occurs is adjusted. Then a second FEA is carried out applying the axial load to estimate the limit load of the tube. In this case we find that the non-

cyclic method gives a lower bound solution to the exact shakedown boundary as expected.

5.6.1 Why Does the Non-cyclic Method give a Lower Bound?

The Non-cyclic method separates the loading into a constant and a variable part. Effect of the each load is considered individually. As a result the interaction between the axial load and the thermal loads gets disregarded in the case of the Bree problem, and the problem is basically simplified to a 1-D condition. In real situations the axial pressure affects the hoop strain and the vice-versa.

- The plane stress assumption reduces the problem to one dimension.
- The axisymmetric model is a better representation of the tube. Here we account for the interaction between the axial forces and the thermal loads.
- The same problem can be analyzed using the plane strain assumption.

The post processor plot of the von-Mises equivalent stress shows a displaced elastic core. The blue region is the region of reverse plasticity where the yield stress is close to zero (figure 5.12). Due to the curvature of the shell, the temperature distribution across the thickness is logarithmic as opposed to a linear distribution obtained in the plane stress model. As a result the elastic core gets shifted to the right towards the outer edge of the cylinder. This further introduces errors in the estimation of the primary limit load capacity of the cylinder (The second step of the non-cyclic method). The red region is zone of reversed plasticity and the blue region is the elastic core. It should be noted that the elastic core is displaced from the center due to the curvature of the cylindrical shell.

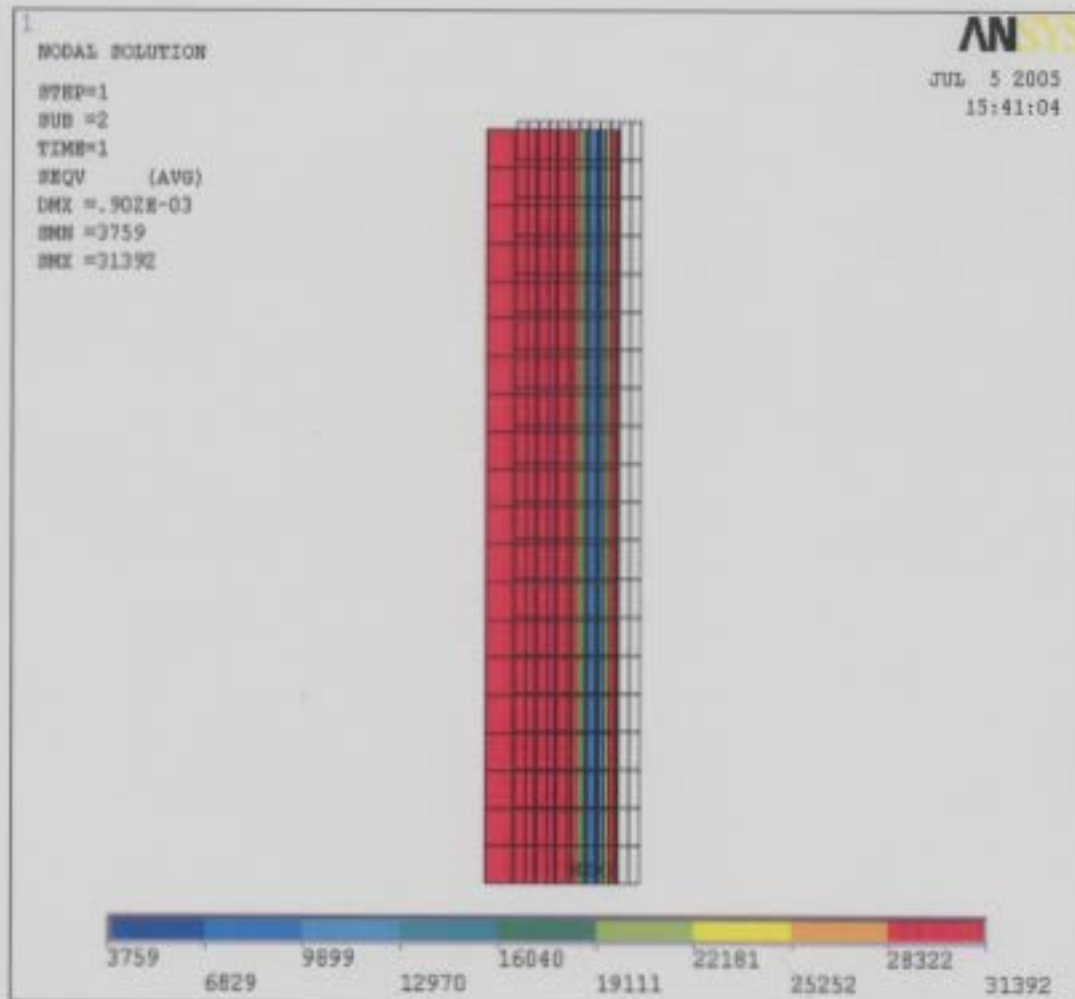


Figure 5.12. Equivalent stress plot after the thermal cycle for a tube of Radius 5in

5.6.2 The Size Effect

In the parametric study stage, we are interested we interested in studying the variation of the shakedown boundary with radius keeping all other parameters fixed. It is interesting to see how much the non-cyclic solution differs from the cyclic solution for tubes of different radii subjected to the same set of thermal and mechanical loads. The shakedown boundary is calculated for tubes of three different radii using the non-cyclic method. See figure 5.13. As the radius of the

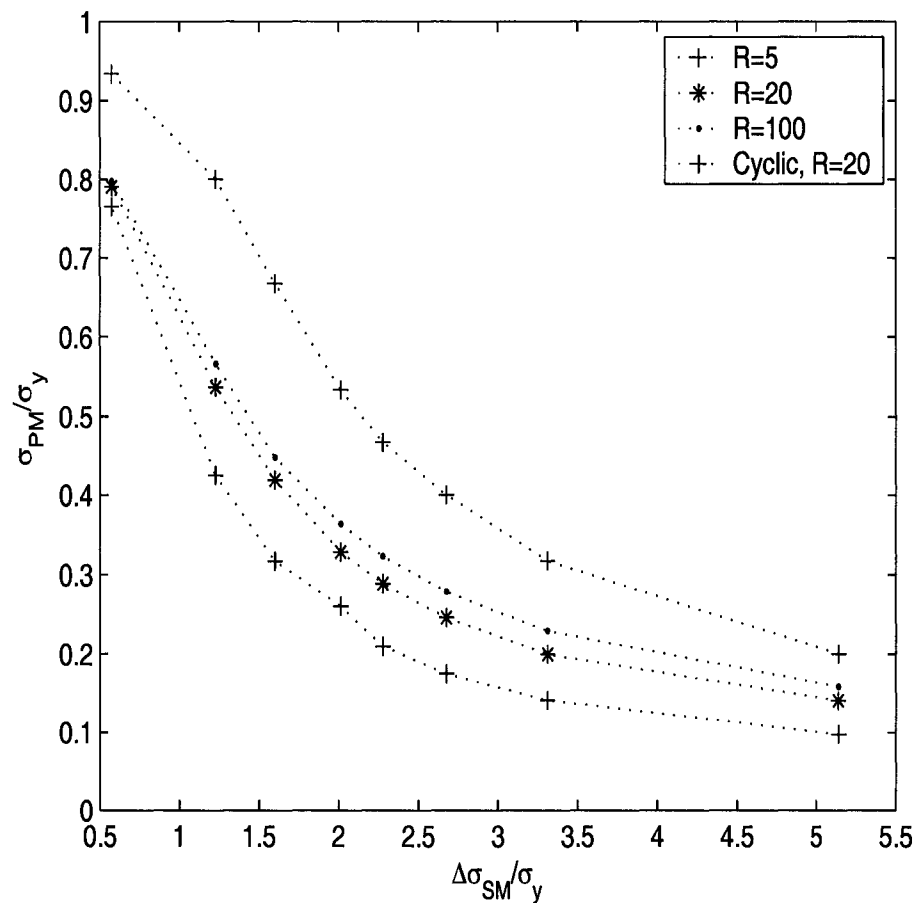


Figure 5.13. Shakedown boundary for tubes of different radii using the non-cyclic method.

tube keeps increasing the non-cyclic solution approaches the cyclic solution and

this can be observed from figure (5.13). This is because the elastic core shifts towards the center as we increase in radius of the tube and the load is uniformly supported by the elastic core. The figure also gives us an idea of the size effect. As the internal radius increases the curvature of the cylinder keeps decreasing and the cylinder resembles a plate subjected to axial load and a through thickness temperature difference. This also shows how a shakedown problem can be viewed in a different way. Traditionally, we are interested in finding the largest load factor (factors in case of multi-parameter loading) for which shakedown is attained. Alternatively, we can also determine the dimensions of the structure for which there is no ratcheting for a given load parameter and loading history.

5.7 Slow Rates of Convergence

For a 3-D state of stress the stabilization of displacements is slow. This is unlike the 2-D (Plane stress) situation wherein shakedown is attained in just 20 cycles. Here the mechanism of reverse plasticity is easy to visualize as it only involves extension and compression of the extreme fibers during the heating cooling cycle. The figure (5.14) shows stabilization of displacements after 250 cycles for the axisymmetric model. Even after 250 cycles, there is a small increment in plastic strains near shakedown loads. This can be seen in the table of plastic strains available in the ANSYS post-processor. However, this strain increment occurs in the 5th or 6th significant digit of the value of plastic strain. This phenomenon is known as *Transient Ratcheting*. Slow rates of stabilization can be attributed to the reverse plasticity mechanism that operates in zones of reverse plasticity. In three dimensions this is difficult to visualize because an extension in the axial direction will cause shortening in the hoop direction and so on. Also this involves evalu-

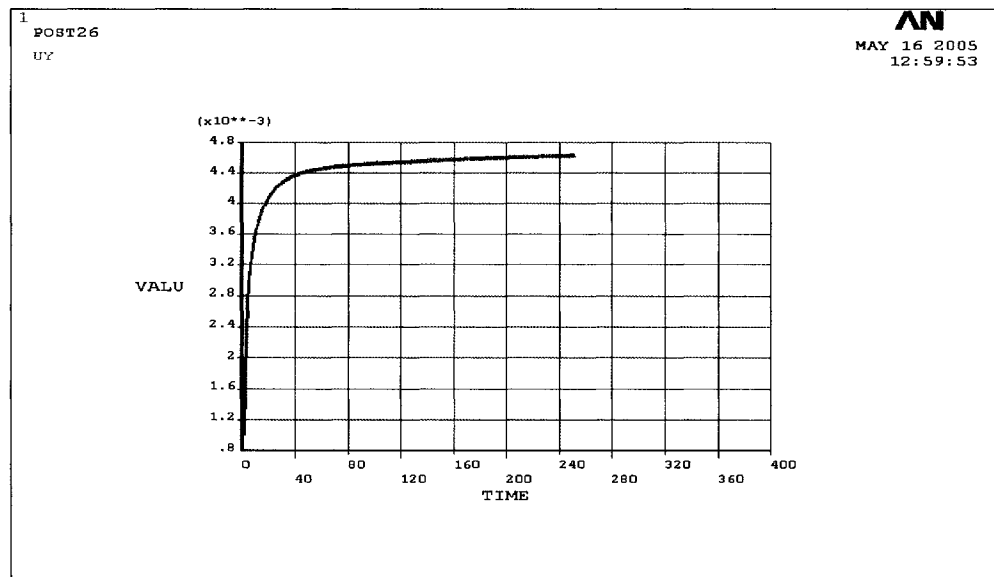


Figure 5.14. Displacement vs cycles at the shakedown load after 250 cycles for a tube of Radius 20 in

ating the full 3-D stress solution for the mesh for hundreds or thousands of time steps per cycle. The mesh was therefore chosen to be relatively coarse to reduce the process load on the computer. To minimize computer execution time, Pre-Conditioned Conjugate gradient solver is used for the models with a large number of degrees of freedom. The PCG solver is a robust solver that approximates the

solution within a specified tolerance value. Because of non-linear nature of plasticity, auto-matic time stepping is used to control convergence. Automatic time stepping is used when convergence is not occurring in a given number of equilibrium iterations, and errors like “Small pivot” etc can be overcome by adjusting the tolerance. Good selection of tolerance limits and good mesh will lead considerable savings in the analysis time.

5.7.1 Sample Calculation of Strain Increments

The rate of load application can be carefully controlled in ANSYS by specifying the number of load steps and sub-steps manually. The table (5.5) lists the hoop strain increments over a number of cycles at shakedown. We can choose the radial displacement to be the ratcheting measure that addresses the failure mode of incremental growth in the dimensions of a vessel because permanent changes in dimension are measured by permanent changes in the radius. Table (5.5) shows a sample calculation of the increments in hoop strain for a given history of loading.

From the data of strain increments from the regions cycling plastically, we can extract useful information about the whole system from which a mathematical model can be developed. Experiments can be performed to validate the model. Having such a model will be useful in predicting the life of components.

5.8 Asymptotic Trend Near Shakedown

Constructing a difference table of the equivalent plastic strains is useful because it allows us to plot and follow the trends of growth in the vessel for a prescribed history of loading. From figure (5.15) we can observe that the trend of strain increments becomes asymptotic near the shakedown boundary. At this point the

Number of cycles	Plastic hoop strains	Increments Calculated
1	0.0	
2	-1.36E-03	
3	1.20E-03	
4	-1.44E-03	7.42E-05
5	9.61E-04	
6	-1.48E-03	3.90E-05
7	9.33E-04	
8	-1.50E-03	2.20E-05
9	9.19E-04	
10	-1.51E-03	1.40E-05
11	9.05E-04	
12	-1.53E-03	1.23E-05
13	8.93E-04	
14	-1.54E-03	1.00E-03
15	8.85E-04	
16	-1.54E-03	7.65E-04
17	8.78E-04	
18	-1.55E-03	5.42E-06
19	8.73E-04	
20	-1.55E-03	4.85E-06

Table 5.5. Table showing the calculation of hoop strain increments for a tube of Radius 20 in

reader might ask after how many cycles does the hoop strain increments reduce to zero? Zero strain growth implies shakedown. This question can be answered by extrapolating the curve to touch the X axis. But even then the value that is obtained is not a definitive measure for zero strain growth. This is because small fluctuations appear in the the plastic strain values near the shakedown boundary.

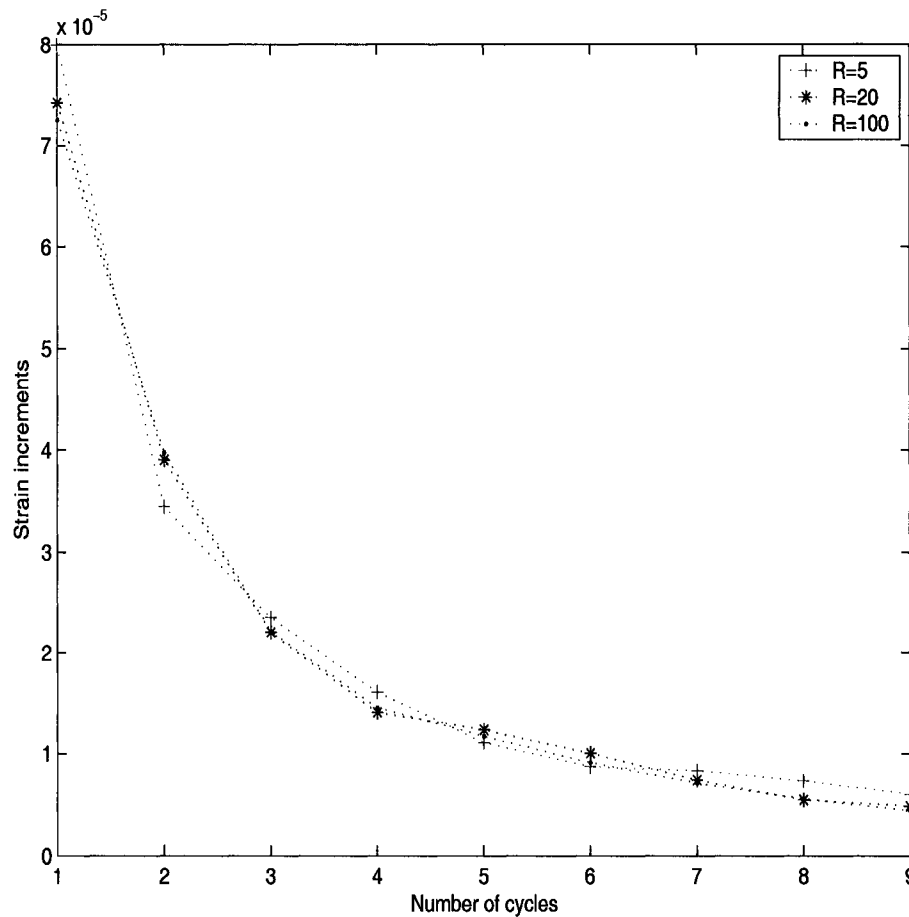


Figure 5.15. Hoop strain increments vs cycles at the shakedown load after 10 cycles

5.9 Shakedown Check using JPVRC Criterion and Comparison with ASME

The JPVRC recommendation can be used a *PASS/FAIL* check of ratcheting. The table (5.6) gives the values of the equivalent plastic strains and its difference. The maximum strain increment for twenty cycles of the prescribed loading history is 5.12×10^{-05} (row 4 column 3 table 5.6) which is less than 10^{-04} . Therefore the conclusion of shakedown for this case agrees with the result obtained after 250 cycles. It is also interesting to observe the rate of decay of the strain increments.

Number of cycles	Equivalent plastic strains	Increments Calculated
1	0.0	0.0
2	1.41E-03	0.0
3	1.39E-03	-1.76E-05
4	1.44E-03	5.12E-05
5	1.47E-03	2.62E-05
6	1.48E-03	1.42E-05
7	1.50E-03	2.07E-05
8	1.50E-03	4.63E-06
9	1.52E-03	1.90E-05
10	1.52E-03	-2.09E-06
11	1.54E-03	1.53E-05
12	1.54E-03	-6.50E-07
13	1.55E-03	9.97E-06
14	1.55E-03	2.06E-06
15	1.55E-03	5.16E-06
16	1.56E-03	3.85E-06
17	1.56E-03	2.27E-06
18	1.56E-03	4.56E-06
19	1.57E-03	7.80E-07
20	1.57E-03	5.25E-06

Table 5.6. Table showing the calculation of equivalent plastic strain increments for a tube of Radius 20 in

In this case the decay level of the order of 10^{-05} is attained within 10 cycles and from then onwards the magnitude fluctuates between 10^{-06} and 10^{-07} . After that the rate of decay is really slow. So from the results, it appears as if one can get a fairly good estimate of the shakedown load using the JPVRC criterion for a small number of cycles say between 5-10 cycles.

5.10 Tube as Cylinder in Plane Strain Condition

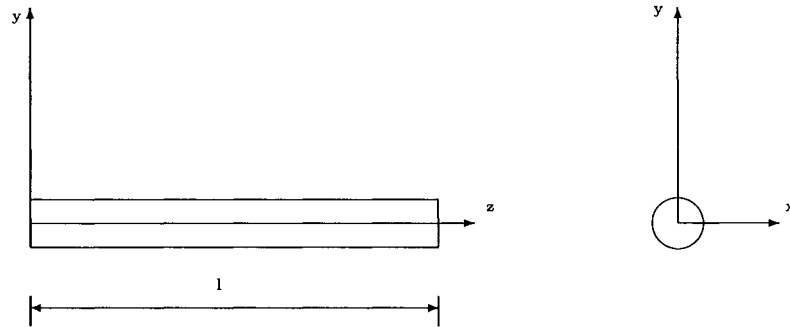


Figure 5.16. Schematic diagram of the plane strain condition

Thick cylinder in plane strain is one of the well studied problems in the theory of plasticity. In this section we analyze the same tube problem using the plane strain assumption. We can do so because the mechanical and thermal loads are distributed along the longitudinal axis of the body. It should be noted that there is no variation in temperature or pressure along the length of the cylinder. Therefore the strains in the longitudinal direction is zero ($\epsilon_{zz} = 0$). Then, the long body with possible exception of end regions undergoes displacements that consists of three components. One component is along the axis of the body which we take as the z axis. The other two components are functions of x and y only. For the ease of comparison between the two models, the same thermal load is applied to both models. The aim here is to study the interaction effect between the mechanical and the thermal load in a different way by considering the tube to be very long.

P, lbs	187.2	295.2	370.2	425.4	497.8	630.3	800.2	1330.8
T	3.5	2.32	1.875	1.42	1.22	1.123	0.86	0.403

Table 5.7. Load data at shakedown for a tube of radius 20in and thickness 1 inch using plane strain approximation

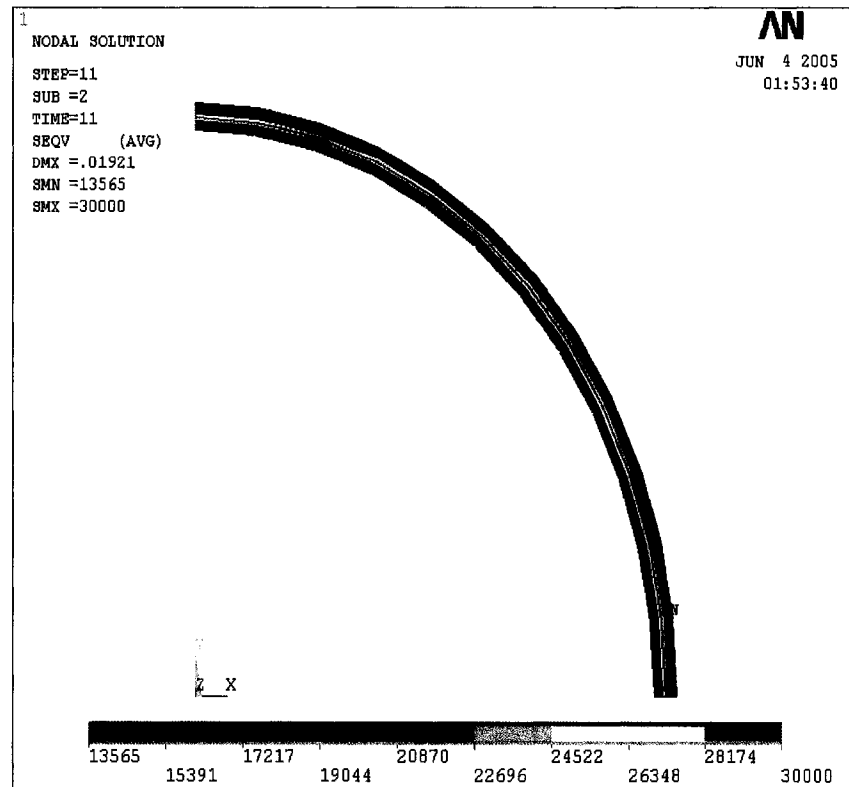


Figure 5.17. Post processor plot of the equivalent stress distribution.

For the purpose of comparison with the axisymmetric model, a quarter cylindrical section with an internal radius of 20 inches and a thickness of 1 inch is modeled (Fig.(5.17)) and it is subjected to the same thermal load values as the axisymmetric model. A mapped graded mesh was generated keeping in mind the temperature distribution across the thickness is logarithmic, as opposed to a linear distribution

that is obtained in the case of the plane stress model. Symmetry constraints are applied to the elements at the symmetry plane locations. The problem is similar to the axisymmetric problem, except that in this case the mechanical load is applied as a constant internal pressure, i.e in the radial direction as opposed to the axial direction in the former problem.

5.10.1 Results and Discussion

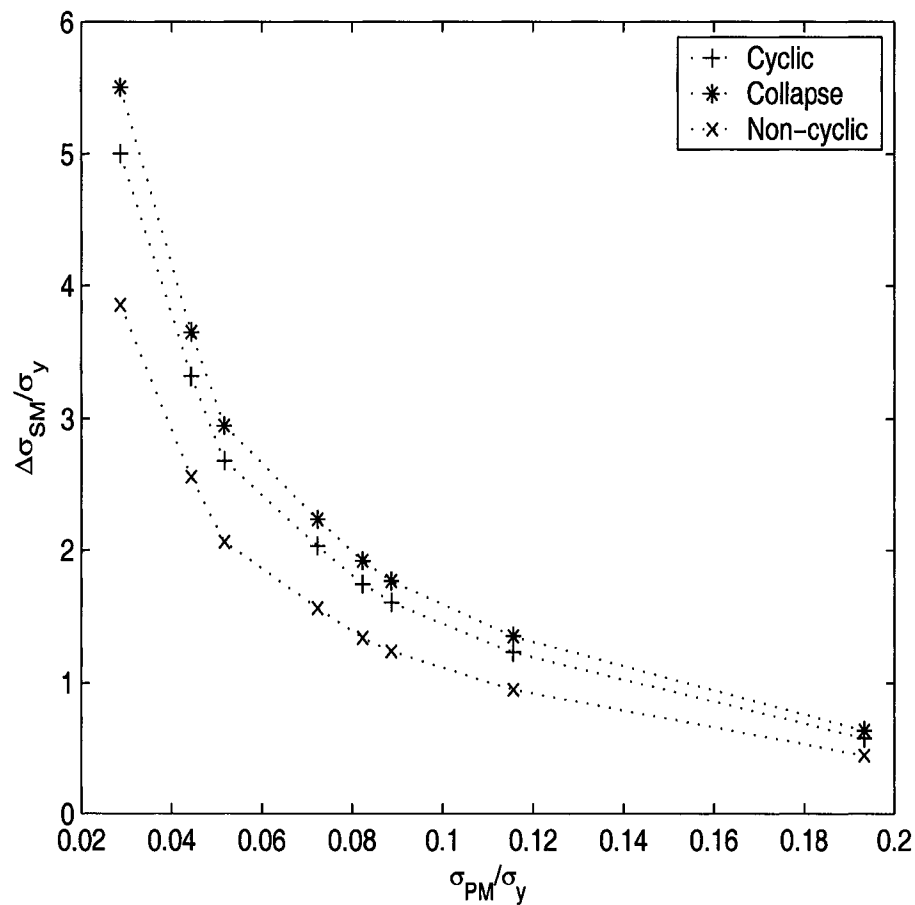


Figure 5.18. Interaction diagram for the Bree problem in plane strain condition.

In this case, the plot of $\frac{\sigma_{PM}}{\sigma_y}$ versus $\frac{\Delta\sigma_{SM}}{\sigma_y}$ yields a Bree like diagram as it is to be expected. Figure (5.18) shows the ratchet boundary for the tube problem obtained

using the plane strain approximation. The analytical solution for this problem is given in [9]. As we can see from the figure, the ratchet boundary lies very close to the collapse boundary. This can also be inferred from the post-processor plot of the von-Mises stress (Fig.(5.17)). The elastic core is very thin and section on either side of it has reached the yield limit. The collapse load is only about 1% higher than the shakedown load. The value of the collapse load and the trend of the result obtained for the assumed thickness to radius ratio (0.05) has close similarities with theoretical investigations [9]. While using the non-cyclic method since the inner elements (elements to the left of the elastic core) have reached yield, it is desirable to leave some stiffness in the inner ring of elements so as to transfer the internal pressure to the elastic core. The accuracy of the results obtained will depend on the amount of stiffness left in the inner ring of failed elements. The ratchet limit computed by the non-cyclic method differs from the cyclic solution by about 15% on an average. Again we observe that the non-cyclic method gives a lower bound to the exact ratchet boundary.

P,lbs	860.2	1330.4	1550.2	2170.4	2470.8	2660.3	3470.2	5820.8
T	3.5	2.32	1.875	1.42	1.22	1.123	0.86	0.403

Table 5.8. Load data at shakedown for a tube of radius 20in and thickness 5 inch using plane strain approximation

The ratchet boundary for a thickness to radius ratio of (0.25) is shown in Fig.(5.19). The load data is presented in table (5.8).

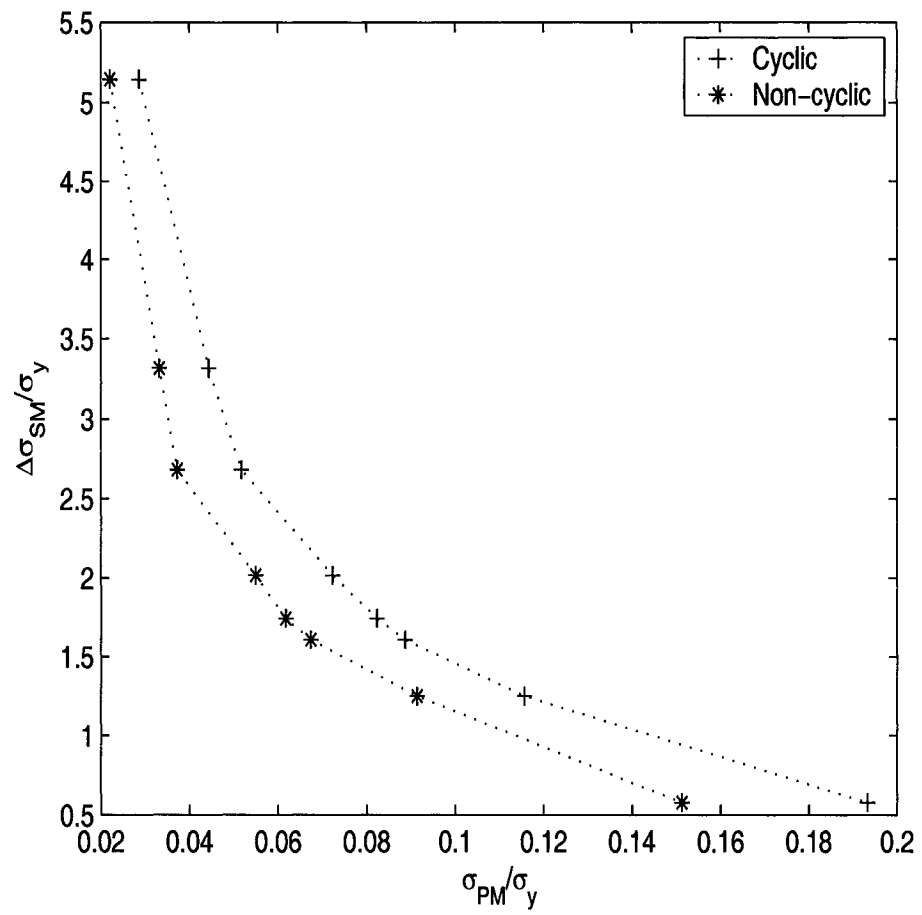


Figure 5.19. Ratcheting boundaries for the tube with t/r ratio of 0.25

5.10.2 Comparison with the Axisymmetric Model

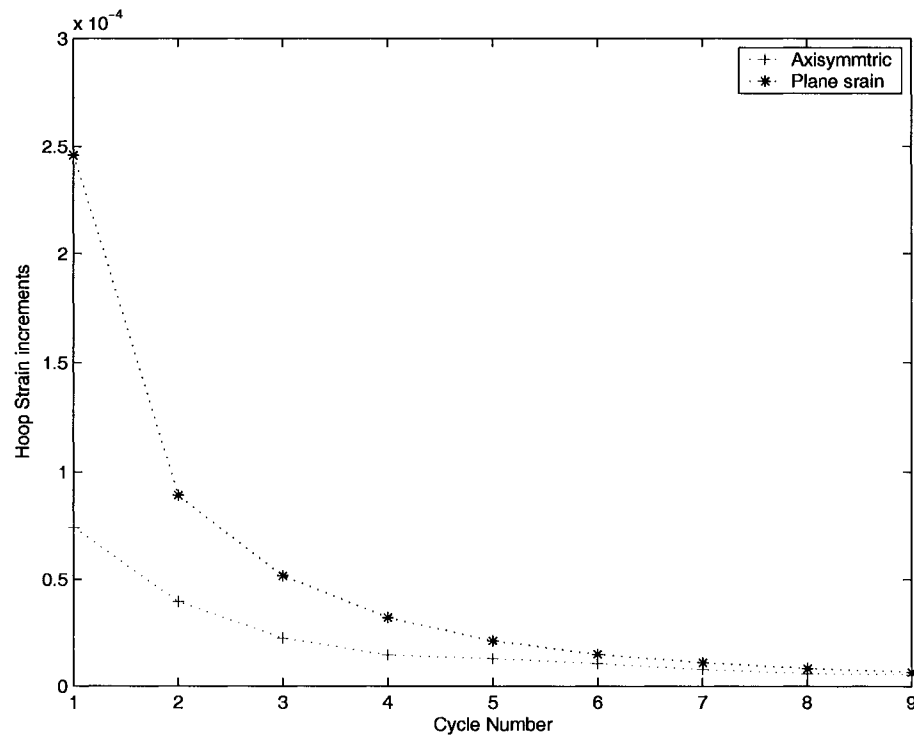


Figure 5.20. Comparison between axisymmetric and plane strain models for the same shakedown load

In the discussion that follows, the results from the finite element analysis of the axisymmetric model (section 5.5) is compared with the plane strain model. We are interested in studying the rate of increase of hoop strains near the ratchet boundary. For the purpose of comparison we have to identify the same location (radius) in cylinder and then get data for the plastic strains in the hoop direction for both models. For the values of strain increments see tables A.1 and A.2 Appendix A. The figure suggests that the increments in the axisymmetric model decrease at a slower rate in comparison with the plane strain model. That is the rate of decay of plastic strains is higher for the plane strain model. It is also interesting to observe that the strain increments appear to converge after 10 cycles for both

cases.

5.10.2.1 Hoop Strain Increments Near the Shakedown Boundary

In this section we compare the hoop strain increments in near the shakedown boundary for the plane strain (section 5.10) and the axisymmetric models (section 5.5). It is interesting to observe how the ratcheting strain increments as we approach the shakedown boundary for the plane strain and the axisymmetric models. This is depicted in the figure (5.21). The strain increments are computed for 10, 20 and 40 percent increase in the value of the mechanical load for both cases.

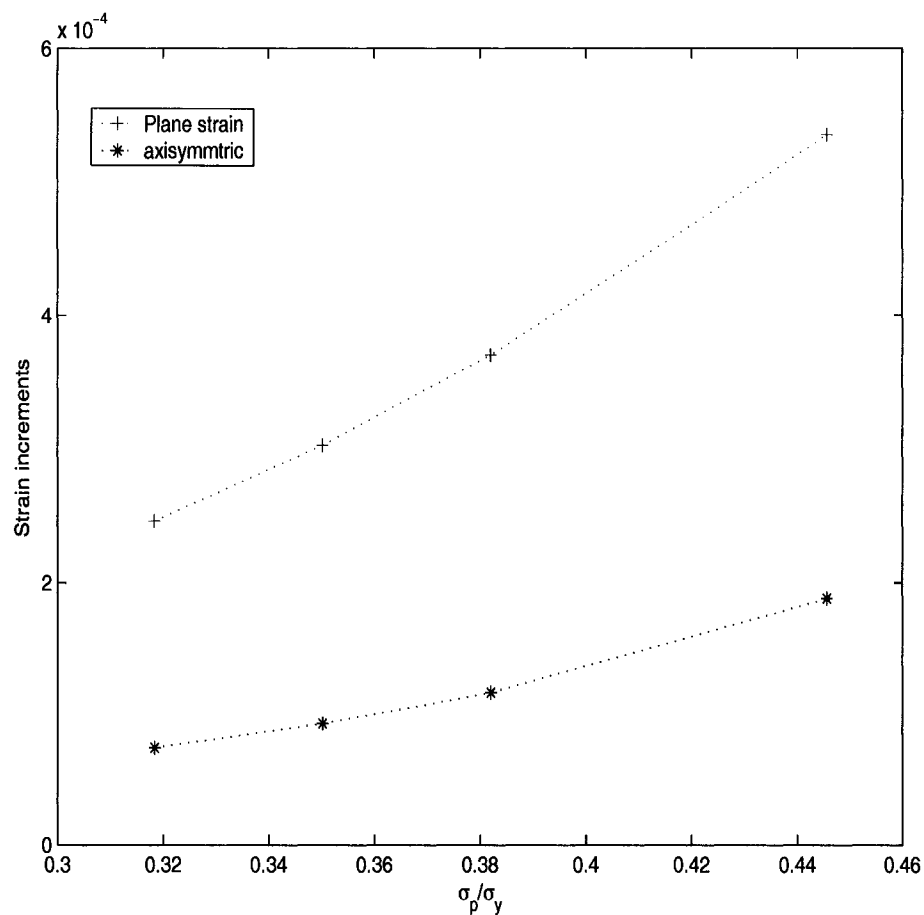


Figure 5.21. Hoop strain increments after two cycles

The trend shown in the figure suggests that the strain increments approach zero at a faster rate for the plane strain model as compared to the axisymmetric model.

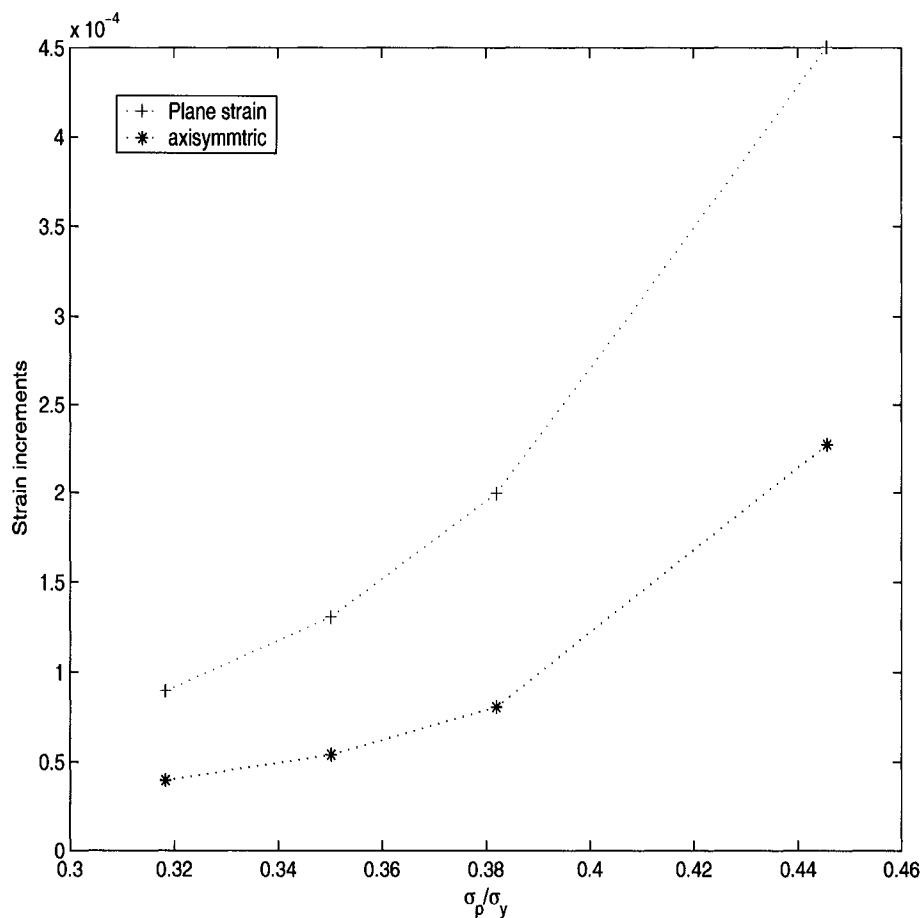


Figure 5.22. Hoop strain increments after four cycles

One direct observation when we compare figure (5.21) and (5.22) is that after 4 cycles the strain growth in the plane strain model is much larger than axisymmetric model for a corresponding increase in the shakedown load. The difference in behavior suggests that plane strain model predicts a faster incremental collapse than the axisymmetric model. The figures also indicate the sensitivity of the ratcheting boundary with variations in loading under different assumptions. A possible

explanation for this could be the initial state of stress. Axial pressure creates a uniform stress across the thickness before the thermal cycling. On the other hand the hoop stress variation with thickness is not uniform. This changes the residual stress distribution. This creates a tensile residual stress on the cold side of the cylinder before thermal cycling. Thermal cycling ratchets up the tensile stress on the cold side. This could be a possible reason for faster strain growth in the plane strain model.

Conclusions and Future Research

6.1 Conclusions

A comprehensive theoretical and finite element study on the phenomenon of shake-down and ratcheting is presented. The theoretical work included a through survey of the current literature on the subject and a brief review of the ASME code criterion. The finite element analysis included application of the non-cyclic method to 2-D and 3-D stress states. On the basis of the analysis done and the examples discussed the following general comments can be made.

- For the Bree problem, a plane stress analysis (simplification) *does not* approximate a plane strain analysis.

- The non-cyclic method gives exact ratcheting boundary in simple Bree like situations. For triaxial situations it gives a lower bound to the exact boundary between shakedown and ratcheting. The method is conservative and will lead to safer designs.
- The non-cyclic method uses a procedure in which the yield stress of the material is altered in the zones of reverse plasticity. This requires that the yield stress of the model be kept constant and therefore hardening behavior that is expansion and translation of the yield surface during actual loading cannot be represented.
- The separation of the loading history into constant and cyclic parts and the application of the cyclic component successively will disregard the interaction effects between the constant and the cyclic loads.
- The advantage of the non-cyclic method is that it has a lower computational cost and leads to faster designs.
- Ratcheting check through cyclic plastic FEA gives exact results for the Bree problem and the solutions obtained are fairly reliable. The effect of hardening and other inelastic effects can be simulated by a clever choice of material models.
- Drawback of the cyclic analysis is that it involves heavy computation which is expensive and the time involved in the analysis and convergence is heavily mesh dependent.
- Another drawback of the cyclic analysis is that convergence in problems involving geometrical non-linearities can be really slow.

- The use of the cyclic analysis accounting for all non-linear effects can produce the most accurate predictions of ratcheting.
- Cyclic analysis will lead to longer design times. But this can be justified by the accuracy of the results obtained.
- There are no proper guidelines for the levels of ratcheting that can be tolerated in components.
- The JPVRC specification accurately predicts ratcheting for the problems discussed.
- The Elastic-Core method is accurate in bi-axial situations. In triaxial models a small amount of ratcheting may still persist even when an elastic core is present.
- An advantage of these methods is that shakedown or ratcheting can be demonstrated directly in terms of strain increments and without relying on the restrictions on Code allowable values for the primary and secondary stresses. Thus issues involving stress classification can be disregarded.

It can be seen that simplified methods can be used effectively to solve a wider variety of problems, more effectively than most other procedures. The implementation of the procedures and calculations using different design tools available can help future researchers in this field to get acquainted with the working of the design of structures under a general class of cyclic thermo-mechanical loading, as well as to use them for solving practical problems.

6.2 Future research

- The heating cooling cycles are assumed to be quasi-static in the problems discussed. In real situations, the heating is usually non-uniform. So transient stresses during startup and shutdown should be taken into consideration.
- In the problems discussed, the thermal profiles were assumed to be fully reversed. In practical problems however the stress amplitudes often vary from cycle to cycle and cycles are not fully reversed. This will lead to a non-zero mean stress and its effect needs to be accounted for.
- The addition of temperature dependence of coefficient of expansion and thermal conductivity could be a additional contribution.
- Thermal profiles are seldom exactly predictable curves. More often a plot of temperature over time reveals a random distribution. Statistical methods should be combined with current analysis to model realistic temperature profiles.
- Physical ageing of the material and inelastic time dependent phenomena such as creep and the corresponding residual stresses should be another consideration that should be accounted for.
- The possibility of ratcheting due to thermal shock effects could be an important problem in the nuclear industry.

References

- [1] ASME. *Boiler and pressure Vessel code*. American Society of Mechanical Engineers, New York, 1998.
- [2] ASME. *B31.1 Power Piping Code*. American Society of Mechanical Engineers, New York, 2001.
- [3] S. Bari and T. Hassan. Anatomy of coupled constitutive models for ratcheting simulation. *International Journal of Plasticity*, 16:381–409, 2000.
- [4] J. Bree. Elastic plastic analysis of thin tubes subjected to internal pressure and intermittent high heat fluxes with applications to fast-nuclear reactor fuel elements. *Journal of strain Analysis*, 2(3):226–238, 1967.
- [5] L. Corradi and A. Zavaleni. A linear programming approach to shakedown

- analysis of structures. *Computer Methods in applied mechanics and engineering*, pages 37–53, 1974.
- [6] D.A Gokhfeld and O.F Cherniavsky. *Limit Analysis of structures at Thermal cycling*. Suthoff Nordhoff, 1980.
- [7] R. Hamilton, D. Mackenzie, J. Shi, and J.T. Boyle. A simple upper bound method for calculating shakedown loads. *Journal of Pressure Vessel Technology*, 120:195–199, 1998.
- [8] Lemaitre J. and Chaboche J.L. *Mechanics of Solid Materials*. Cambridge University Press, 1990.
- [9] Konig J.A. *Shakedown of Elastic-Plastic Structures*. Elsevier, 1987.
- [10] A. Kalnins. Shakedown check for pressure vessels using plastic fea. *ASME Bound Vol, Pressure Vessel and Piping Codes and Standards*, 419:9–16, 2001.
- [11] A. Kalnins. Shakedown and ratcheting directives of asme bpv code and their execution. *PVP, ASME PVP Conference, Vancouver, BC, Canada*, 439:9–16, 2002.
- [12] W.T Koiter. General theorems for elastic-plastic solids. *Sneddon, J. N. and Hill, R., 1, North-Holland, Amsterdam*, pages 165–221, 1960.
- [13] D. Mackenzie and J. T. Boyle. A simple method of estimating shakedown loads for complex structures. *In proceedings of ASME Pressure Vessels and Piping Conference Denver, Colorado*, 265(3):89–94, 1990.
- [14] D. Mackenzie and J.T. Boyle. A simple method of estimaing shakedown loads of complex structures. *In proceedings of ASME Pressure Vessels and Piping Conference*, 265:89–94, 1993.

- [15] D.H Nguyen and L. Palgen. Shakedown analysis by displacement methods and equilibrium finite elements. *Transactions of the Canadian Society of Mechanical Engineers*, pages 37–53, 1980-81.
- [16] American Society of Mechanical Engineers. Criteria of the boiler and pressure vessel code for design by analysis in sections-iii and viii div2. *THE ASME New york*, pages 37–53, 1969.
- [17] A.R.S. Ponter and K.F. Carter. Limit state solutions based on linearly based elastic solutions based spatially varying elastic modulus. *Computer Methods in Applied Mechanics*, pages 237–258, 1997.
- [18] A.R.S. Ponter and K.F. Carter. Shakedown state simulation techniques based on linear elastic solutions. *Computer Methods in Applied Mechanics*, pages 259–279, 1997.
- [19] A.R.S. Ponter and H. Chen. A minimum theorem for cyclic load in excess of shakedown with application to evaluation of a ratchet limit. *Eur.J.Mech.A/Solids*, 20:259–279, 1997.
- [20] R. Preiss. Ratcheting and shakedown analysis of pressure equipment using elasto-plastic finite element analysis. *International Journal of Pressure Vessel and Piping*, 76(3):421–434, 1999.
- [21] W.D. Reinhardt. Distinguishing ratcheting and shakedown conditions in pressure vessels. *ASME PVP Conference, Cleveland, OH*, 2003.
- [22] W.D. Reinhardt. A non-cyclic method for plastic shakedown analysis. *ASME PVP Conference, Cleveland, OH*, 2003.

- [23] W.D. Reinhardt, R. Kizhatil, and G.H. McClellan. Design and analysis of a tube sheet for extreme thermal loading. *In proceedings of ASME Pressure Vessels and Piping Conference*, 360(3):143–150, 1998.
- [24] R. Seshadri. Generalized local stress-strain analysis (gloss)-theory and applications. *Journal of Pressure Vessel Technology*, 113:219–227, 1991.
- [25] Z.L. Zeman and R. Priess. The deviatoric map-a simple tool in design and analysis. *International Journal of Pressure Vessel and Piping*, 76(3):339–334, 1999.

APPENDIX A

Sample calculations

A.1 Sample Calculation

The theoretical solution to the Bree problem is given by

$$\begin{cases} \Delta\sigma_t = \frac{\sigma_y^2}{\sigma_P} & \text{iff } |\sigma_P| \leq \frac{1}{2}\sigma_y \\ \Delta\sigma_t = 4(\sigma_y - \sigma_P) & \text{iff } |\sigma_P| \geq \frac{1}{2}\sigma_y \end{cases} \quad (\text{A.1})$$

These are the limits given by NB-3222.5 of Section-III [1] [2]. Given the values of the yield stress (σ_y) and the value of the primary membrane stress we can calculate the temperate range from the equations given above. For the problems considered the values are $\sigma_y = 30000$ applied primary membrane stress is 6000 i.e

$\sigma_P = 6000$. Therefore $\Delta\sigma_t = \frac{30000^2}{6000} = 150000$. In nondimensional form can be obtained by dividing σ_t by the yield stress and this gives 5. Now the maximum thermal stress in the beam is given by the formula $E\alpha\Delta T$, where E is the Young's modulus and α is the coefficient of thermal expansion. The values are $30e06$ and 0.001 respectively. This implies that, $\frac{E\alpha}{\sigma_y} = \Delta T = 5$. This calculation shows how the temperature can be calculated theoretically. The calculated values are given in the table 5.1 below.

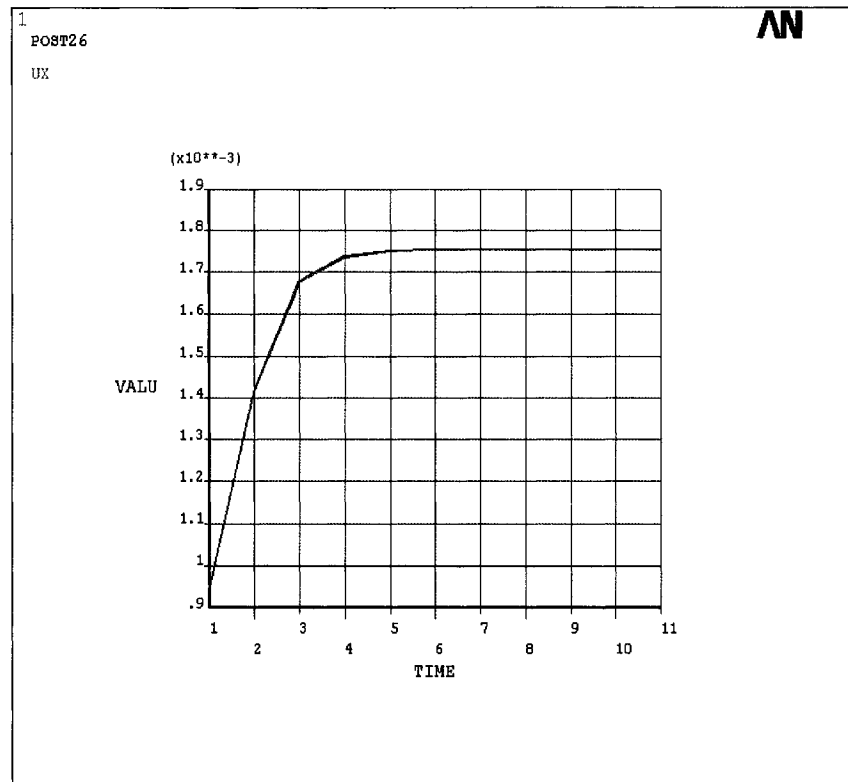


Figure A.1. Displacement versus load diagram for the Bree problem

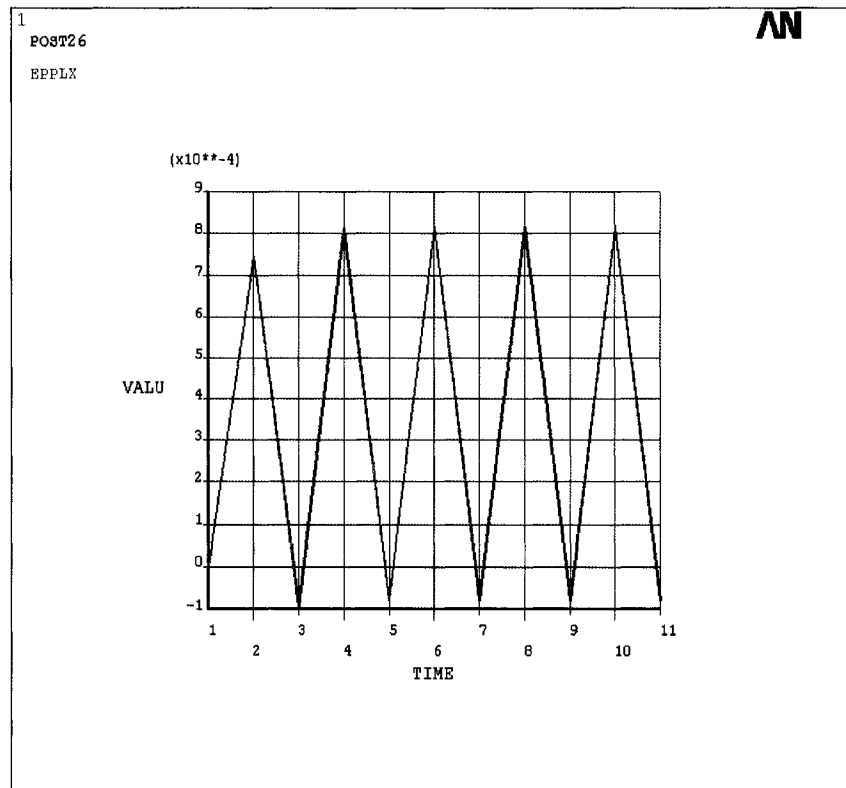


Figure A.2. Plastic strain versus load diagram for the Bree problem

A.2 Material Property Data

The material property data for FEA is listed below.

Young's Modulus= $30e6$

Coefficient of thermal expansion= 0.001

Thermal conductivity= 0.01

Poisson's ratio= 0.3

For the Chaboche Model

The three constants for a single surface hardening model are [8]:

C1=30000

C2=4351132.1402165

C3=60

The element PLANE82 is selected from the ANSYS library for the analysis. It is a higher order element of Plane42 with mid-side nodes. It has two degrees of freedom per node (translations in the x and y directions). It can also be used to do a coupled field thermal analysis. It can tolerate relatively coarse meshes and give results of high accuracy.

A.3 Proof of Melan's Theorem

A solution for stress from the theory of elastoplasticity σ , can be expressed as a sum of two components,

$$\sigma = \sigma^e + \rho \quad (\text{A.2})$$

Let σ^s be a the stress solution for shakedown. Then by Melan's theorem it can be expressed as,

$$\sigma = \sigma^s + \bar{\rho} \quad (\text{A.3})$$

Here $\bar{\rho}$ is a constant stress. If we consider the energy of deformation associated with the residual stresses, it can be expressed as,

$$J(t) = \frac{1}{2} \int_{\Omega} (\rho - \bar{\rho}) : E^{-1} : (\rho - \bar{\rho}) dV \quad (\text{A.4})$$

Since the constant residual stress $\bar{\rho}$ is independent of time, the derivative of the energy $J(t)$, with respect to time becomes,

$$\dot{J}(t) = \frac{1}{2} \int_{\Omega} (\rho - \bar{\rho}) : E^{-1} : \dot{\rho} dV \quad (\text{A.5})$$

Using the relationship between the residual stress and strain (see previous section), this expression can be simplified to,

$$\dot{J}(t) = \frac{1}{2} \int_{\Omega} (\rho - \bar{\rho}) : (\dot{\epsilon} - \dot{\epsilon}^e - \dot{\epsilon}^p) dV \quad (\text{A.6})$$

Since the residual stresses (ρ) and $(\bar{\rho})$ satisfy the equilibrium conditions, their difference $(\rho - \bar{\rho})$ also satisfies equilibrium. Similarly the strains (ϵ) and (ϵ^e) satisfies compatibility conditions, therefore the difference of their derivatives should also be compatible. By applying the principle of virtual work we can conclude,

$$\int_{\Omega} (\rho - \bar{\rho}) : (\dot{\epsilon} - \dot{\epsilon}^e) dV = 0 \quad (\text{A.7})$$

Therefore equation (A.6) becomes,

$$\dot{J}(t) = - \int_{\Omega} (\rho - \bar{\rho}) : \dot{\epsilon}^p dV \quad (\text{A.8})$$

and using equations (A.2) and (A.3) equation (A.8) can be written as,

$$\dot{J}(t) = - \int_{\Omega} (\sigma - \sigma^s) : \dot{\epsilon}^p dV \quad (\text{A.9})$$

now we also know that energy is always positive i.e

$$J(t) \geq 0 \quad \forall t > 0 \quad (\text{A.10})$$

and since the first derivative of the energy functional is negative everywhere in the interval $[0,t]$ it means that the function is decreasing in that interval. Therefore

we can conclude that,

$$J(0) \geq J(t) \quad \forall t > 0 \quad (\text{A.11})$$

or we can also say,

$$0 \leq J(t) \leq J(0) \quad \forall t > 0 \quad (\text{A.12})$$

This means that function $J(t)$ is bounded. But the function $\dot{J}(t)$ is the product of $(\sigma - \sigma^s)$ and the derivative of the plastic stain tensor $\dot{\epsilon}$. Therefore intuitively we can see that area under the stress strain diagram tends to a constant. This can happen only if

$$\lim_{t \rightarrow \infty} \dot{\epsilon}^p = 0 \quad (\text{A.13})$$

or we can say that,

$$t \rightarrow \infty \quad \epsilon^p \rightarrow c \quad (\text{A.14})$$

Hence we prove Melan's theorem.

A.4 Tables

Table of increments for the plane strain condition.

Number of cycles	Plastic strains in the hoop direction	Increments Calculated
1	0.0	
2	1.85E-03	
3	-9.37E-04	
4	2.09E-03	2.46E-04
5	-8.06E-04	
6	2.18E-03	8.91E-05
7	-7.39E-04	
8	2.24E-03	5.16E-05
9	-6.99E-04	
10	2.27E-03	3.18E-05
11	-6.73E-04	
12	2.29E-03	2.09E-05
13	-6.56E-04	
14	2.30E-03	1.46E-05
15	-6.44E-04	
16	2.31E-03	1.07E-05
17	-6.34E-04	
18	2.32E-03	8.14E-06
19	-6.27E-04	
20	2.33E-03	6.43E-06

Table A.1. Data table of plastic strain increments for element number 21 node number 54 for the axisymmetric model

Number of cycles	Plastic strains in the hoop direction	Increments Calculated
1	0.0	
2	1.36E-03	
3	-1.02E-03	
4	1.44E-03	7.42E-05
5	-9.61E-04	
6	1.50E-03	2.20E-05
7	-9.19E-04	
8	1.51E-03	1.40E-05
9	-9.05E-04	
10	1.51E-03	1.40E-05
11	-9.05E-04	
12	1.53E-03	1.23E-05
13	-8.93E-04	
14	1.54E-03	1.00E-05
15	-8.85E-04	
16	1.54E-03	7.35E-06
17	-8.78E-04	
18	1.55E-03	5.42E-06
19	-8.73E-04	
20	1.55E-03	4.85E-06

Table A.2. Data table of plastic strain increments for element number 240 node number 26 for the axisymmetric model

Cycles	At shakedown (s.d)	10% above s.d	20% above s.d	40% above s.d
1	2.46E-04	3.02E-04	3.69E-04	5.35E-04
2	8.91E-05	1.30E-04	1.99E-04	4.50E-04
3	5.16E-05	7.99E-04	1.90E-04	4.41E-04
4	5.16E-05	7.99E-04	1.90E-04	4.41E-04
5	3.18E-05	7.91E-04	1.89E-04	4.38E-04
6	3.18E-05	7.91E-04	1.89E-04	4.38E-04

Table A.3. Data table of plastic strain increments for loads near shakedown boundary for the plane strain model

Cycles	At shake-down(s.d)	10% above s.d	20% above s.d	40% above s.d
1	7.5E-05	9.34E-05	1.17E-04	1.88E-04
2	3.96E-05	5.39E-05	8.05E-04	2.27E-04
3	2.25E-05	3.84E-05	8.15E-05	2.52E-04
4	5.16E-05	7.99E-04	1.90E-04	4.41E-04
5	3.18E-05	7.91E-04	1.89E-04	4.38E-04
6	1.43E-05	3.43E-05	1.01E-04	3.52E-04

Table A.4. Data table of plastic strain increments for loads near shakedown boundary for the axisymmetric Model

A.5 Macros for the Non-Cyclic method

```
! set up material table for elements
```

```
! note: highest existing material number = 10
```

```
  /prep7
```

```
*get,nel,elem,0,count
```

```
  *dim,sy,array,nel
```

```
eln=0
```

```
*do,i,1,nel
```

```
eln=elnext(eln)
```

```
*get,matn,elem,eln,attr,mat
```

```
*get,sy(i),biso,matn,,,const,1
```

```
*get,emod,ex,matn,0
```

```
*get,nu,nuxy,matn,0
```

```
tb,biso,10+i
```

```
tbdata,1,sy(i),0
```

```
mp,ex,10+i,emod
```

```
mp,nuxy,10+i,nu
```

```
mpchg,10+i,eln
```

```
*enddo
```

```
fini
```

```
  /eof
```

```
! recalculate material table for elements  
! note: highest existing material number = 10
```

```
    /post1  
set,1  
etab,seq,s,eqv  
    eln=0  
*do,i,1,nel  
    eln=elnnext(eln)  
    *get,seqm,etab,1,elem,eln  
    sy(i)=max(sy(i)-seqm,1000.0)  
*enddo  
fini
```

```
    /prep7  
    eln=0  
*do,i,1,nel  
    tb,biso,10+i  
    tbdata,1,sy(i),0  
*enddo
```

```
    fini  
/eof
```

A.6 Input file for the Bree Problem

```
/PREP7
blc4,0,0,5,1
lesize,4, , ,12
lesize,1, , ,20
!*
et,1,plane82
!*
keyopt,1,3,0
keyopt,1,5,0
keyopt,1,6,0
!*
!*
uimp,1,ex, , ,30e6,
uimp,1,nuxy, , ,0.3,
!uimp,1,nuxy, , ,0.3,
uimp,1,alpx, , ,0.001,
uimp,1,alpy, , ,0,
uimp,1,kxx, , , 0.01,
!*
mshkey,1
amesh,1
mshkey,0
!*
save
```

finish

 /PREP7

ETCHG,STT

FINISH

 /solu

antype,static

 time,1

lsel,s,,1

nsll,s,1

d,all,temp,1.500

lsel,s,,3

nsll,s,1

d,all,temp,-1.500

allsel

solve

 !lsel,s,,4

!nsll,s,1

 time,2

lsel,s,,1

nsll,s,1

d,all,temp,-1.500

```
lsel,s,,3
nssl,s,1
d,all,temp,1.500
allsel
solve
```

```
time,3
```

```
lsel,s,,1
nssl,s,1
d,all,temp,1.500
lsel,s,,3
nssl,s,1
d,all,temp,-1.500
allsel
solve
```

```
time,4
```

```
lsel,s,,1
nssl,s,1
d,all,temp,-1.500
lsel,s,,3
nssl,s,1
d,all,temp,1.500
allsel
solve
```

```
time,5  
lsel,s,,1  
nsl,s,1  
d,all,temp,1.500  
lsel,s,,3  
nsl,s,1  
d,all,temp,-1.500  
allsel  
solve
```

```
time,6  
lsel,s,,1  
nsl,s,1  
d,all,temp,-1.500  
lsel,s,,3  
nsl,s,1  
d,all,temp,1.500  
allsel  
solve
```

```
fini
```

```
/clear  
/inp,smo,a56  
/PREP7  
prs=-6000
```

```
!  
tb,biso,1,1, , ,  
tbtemp,0,  
tbmodif,2,1,30000  
!*  
dl, 4, ,SYMM  
sbetra  
lsel,s,,1  
nsl,s,1  
d,all,uy,0  
  
    lsel,s,,2  
nsl,s,1  
sf,all,pres,prs,  
cp,1,ux,all  
allsel  
save  
finish  
  
    /SOLU  
tref,0  
solcnt,on  
pred,off  
nlgeom,off  
nropt,full  
nsubst,2,5000,2
```

```
kbc,0
solve
nsubst,2,5000,2
*do,i,1,10
ldread,temp,2-mod(i,2),,,,r1,rth
solve
*enddo
fini
```

A.7 Input file for the Three-Bar Problem

```
/PREP7
K,1,0,0,0
K,2,0,5,0
K,3,0,2,0
KDEL,3
K,3,2,0,0
K,4,2,5,0
k,5,6,0,0
kdel,5
k,5,4,0,0
k,6,4,5,0
l,1,2
l,3,4
l,5,6
```

```
ET,1,LINK32
R,1,1
uimp,1,ex, , ,30e6,
uimp,1,nuxy, , ,0.3,
uimp,1,alpx,, ,0.001,
uimp,1,alpy, , ,0.001,
uimp,1,kxx, , , 0.01,
lesize,all,, ,1
lmesh,all,all
save
finish

/solu
antype,static
tref,0
solcmt,on
pred,off
nlgeom,off
nropt,full
nsubst,1,5000,1
kbc,0

time,1
lssel,s,, ,1
nsls,s,1
d,all,temp,1.0
```

allsel

solve

time,2

lsel,s,,1

nsll,s,1

d,all,temp,-1.0

allsel

solve

time,3

lsel,s,,2

nsll,s,1

d,all,temp,1.0

allsel

solve

time,4

lsel,s,,2

nsll,s,1

d,all,temp,-1.0

allsel

solve

time,5

lsel,s,,3

```
nsl,s,1
d,all,temp,1.0
allsel
solve

      time,6
lsl,s,,3
nsl,s,1
d,all,temp,-1.0
allsel solve

      fini

      /clear
      /inp,smod3BAR,a56
      /PREP7
      ETCHG,TTS
      tb,biso,1,1, , ,
      tbtemp,0,
      tbmodif,2,1,30000
      cp,1,uy,1,3,5
      d,2,all
      d,4,all
      d,6,all
      save
      finish
```

```
/solu  
tref,0  
solent,on  
pred,off  
nlgeom,off  
nropt,full  
nsubst,2,5000,2  
kbc,0  
*do,k,1,6,1  
*do,i,1,6,1  
ldread,temp,i,,3bar,rth  
solve  
*enddo  
*enddo  
finish
```

A.8 Input file for the Plane Strain Condition

```
/prep7  
!*  
ET,1,PLANE77  
!*  
MPTEMP,,,,,,,,  
MPTEMP,1,0  
MPDATA,EX,1,,30e6
```

MPDATA,PRXY,1,,0.3
mpdata,alpx,1,,0.001
mpdata,kxx,1,,0.01
TB,BISO,1,1,2,
TBTEMP,0
TBDATA,,30000,0,,,,
KEYOPT,1,1,0
KEYOPT,1,3,0
K,1
K,2,3
K,3,3,3
K,4,,3
CSYS,1
K,5,20 (3.5)
K,6,20,45 (3.5)
K,7,20,90 (3.5)
KGEN,2,5,7,1,0.25
KGEN,2,8,10,1,0.81 (4.74)
L,2,5
*REPEAT,3,1,1
L,5,8
*REPEAT,3,1,1
L,8,11
*REPEAT,3,1,1
CSYS,0
CSYS,1

```
A,2,5,6,3
*REPEAT,3,3,3,3,3
A,3,6,7,4
*REPEAT,3,3,3,3,3
ASEL,S,AREA,,3,6,3
ASEL,ALL
LESIZE,1,,,4,0.5 ! DEFINE LINE SEGMENTS AND DIVISIONS
*REPEAT,3,1
LESIZE,4,,,1.5
*REPEAT,3,1
LESIZE,7,,,9,1.0
*REPEAT,3,1
!*
FLST,2,2,5,ORDE,2
FITEM,2,1
FITEM,2,4
ADELE,P51X
MSHK,1 ! MAPPED AREA MESH
MSHA,0,2D ! USING QUADS
ESIZE,,6
amesh,all

/PREP7
ETCHG,STT
FINISH
```

```
/solu
antype,static

      time,1
lsel,s,,14
nsl,s,1
d,all,temp,2.32
lsel,s,,10
nsl,s,1
d,all,temp,2.32
lsel,s,,17
nsl,s,1
d,all,temp,-2.32
lsel,s,,13
nsl,s,1
d,all,temp,-2.32
allsel
solve

      time,2
lsel,s,,14
nsl,s,1
d,all,temp,-2.32
lsel,s,,10
nsl,s,1
d,all,temp,-2.32
```

```
lsel,s,,17
nsl,s,1
d,all,temp,2.32
lsel,s,,13
nsl,s,1
d,all,temp,2.32
allsel
solve
```

```
    time,3
lsel,s,,14
nsl,s,1
d,all,temp,2.32
lsel,s,,10
nsl,s,1
d,all,temp,2.32
lsel,s,,17
nsl,s,1
d,all,temp,-2.32
lsel,s,,13
nsl,s,1
d,all,temp,-2.32
allsel
solve
```

```
    time,4
```

```
lsel,s,,14
nsl,s,1
d,all,temp,-2.32
lsel,s,,10
nsl,s,1
d,all,temp,-2.32
lsel,s,,17
nsl,s,1
d,all,temp,2.32
lsel,s,,13
nsl,s,1
d,all,temp,2.32
allsel
solve
```

```
time,5
lsel,s,,14
nsl,s,1
d,all,temp,2.32
lsel,s,,10
nsl,s,1
d,all,temp,2.32
lsel,s,,17
nsl,s,1
d,all,temp,-2.32
lsel,s,,13
```

```
nsl,s,1  
d,all,temp,-2.32  
allsel  
solve
```

```
        time,6  
lsl,s,,14  
nsl,s,1  
d,all,temp,-2.32  
lsl,s,,10  
nsl,s,1  
d,all,temp,-2.32  
lsl,s,,17  
nsl,s,1  
d,all,temp,2.32  
lsl,s,,13  
nsl,s,1  
d,all,temp,2.32  
allsel  
solve
```

```
fini
```

```
        /clear  
/inp,asmod,txt  
/PREP7
```

```
ETCHG,TTS  
KEYOPT,1,3,2  
FINISH
```

```
    /PREP7
```

```
prs=413.58  
dl, 6, ,SYMM  
dl, 9, ,SYMM  
dl, 4, ,SYMM  
dl, 7, ,SYMM  
sbctra
```

```
    lsel,s,,14
```

```
nsl,s,1  
sf,all,pres,prs,  
lsel,s,,10  
nsl,s,1  
sf,all,pres,prs,  
allsel  
save  
finish
```

```
    /SOLU
```

```
tref,0  
solcmt,on  
pred,off
```

```
nlgeom,off
nropt,full
nsubst,2,5000,2
kbc,0
solve
nsubst,2,5000,2
*do,i,1,10
ldread,temp,2-mod(i,2),,,,a15,rth
solve
*enddo
fini
```

A.9 Input File for the Clamped Beam Problem

```
/PREP7
blc4,0,0,5,1
lesize,4, , ,12
lesize,1, , ,20
!*
et,1,plane82
!*
keyopt,1,3,0
keyopt,1,5,0
keyopt,1,6,0
!*
```

```
!*  
uimp,1,ex, , ,30e6,  
uimp,1,nuxy, , ,0.3,  
uimp,1,alpx, , ,0.001,  
uimp,1,alpy, , ,0,  
uimp,1,kxx, , , 0.01,
```

```
!*
```

```
mshkey,1
```

```
amesh,1
```

```
mshkey,0
```

```
!*
```

```
save
```

```
finish
```

```
      /PREP7
```

```
ETCHG,STT
```

```
FINISH
```

```
      /solu
```

```
antype,static
```

```
      time,1
```

```
lsel,s,,1
```

```
nsl,s,1
```

```
d,all,temp,1.5
```

```
lsel,s,,3
```

```
nsll,s,1  
d,all,temp,-1.5  
allsel  
solve
```

```
time,2
```

```
lsel,s,,1  
nsll,s,1  
d,all,temp,-1.5  
lsel,s,,3  
nsll,s,1  
d,all,temp,1.5  
allsel  
solve
```

```
time,3
```

```
lsel,s,,1  
nsll,s,1  
d,all,temp,1.5  
lsel,s,,3  
nsll,s,1  
d,all,temp,-1.5  
allsel  
solve
```

```
time,4
```

```
lsel,s,,1  
nsl,s,1  
d,all,temp,-1.5  
lsel,s,,3  
nsl,s,1  
d,all,temp,1.5  
allsel  
solve
```

```
    time,5  
lsel,s,,1  
nsl,s,1  
d,all,temp,1.5  
lsel,s,,3  
nsl,s,1  
d,all,temp,-1.5  
allsel  
solve
```

```
    time,6  
lsel,s,,1  
nsl,s,1  
d,all,temp,-1.5  
lsel,s,,3  
nsl,s,1  
d,all,temp,1.5
```

```
allsel
solve

      fini
/clear
/inp,smod,a56
/PREP7
prs=1000
!
tb,biso,1,1, , ,
tbtemp,0,
tbmodif,2,1,30000
!*
dl, 4, ,ALL !restarin lft and right ends
dl, 2, ,ALL
sbctra

      !lsl,s,,2
!nsl,s,1
!cp,1,ux,all

      !d,all,uy,0

      lsel,s,,3
nsl,s,1
sf,all,pres,prs, ! apply pressur on top surface
```

```
!cp,1,ux,all
```

```
allsel
```

```
save
```

```
finish
```

```
      /SOLU
```

```
tref,0
```

```
solcnt,on
```

```
pred,off
```

```
nlgeom,off
```

```
nropt,full
```

```
nsubst,1,5000,1
```

```
kbc,0
```

```
solve
```

```
nsubst,1,5000,1
```

```
*do,i,1,20
```

```
ldread,temp,2-mod(i,2),,,,s11,rth
```

```
solve
```

```
*enddo
```

```
fini
```

